Applied Materials Today 27 (2022) 101500

Contents lists available at ScienceDirect

Applied Materials Today

journal homepage: www.elsevier.com/locate/apmt

Recent progress of Ag/TiO_2 photocatalyst for wastewater treatment: Doping, co-doping, and green materials functionalization

Devagi Kanakaraju [a,*], Feniellia Diwvya anak Kutiang [a], Ying Chin Lim [b], Pei Sean Goh [c]

[a] Faculty of Resource Science and Technology, Universiti Malaysia Sarawak, 94300 Kota Samarahan, Sarawak, Malaysia
[b] School of Chemistry and Environment, Faculty of Applied Sciences, Universiti Teknologi MARA, 40450 Shah Alam, Selangor, Malaysia
[c] Advanced Technology Membrane Research Centre, School of Chemical and Energy Engineering, Faculty of Engineering, Universiti Teknologi Malaysia, 81310 Skudai, Johor, Malaysia

ARTICLE INFO

Keywords:
Titanium dioxide
Photocatalysis
Silver
Doping
Green materials
Ionic liquid

ABSTRACT

Surface modification via doping or functionalization is one of the most commonly applied approaches for addressing the innate limitations of TiO_2 photocatalysts. Amongst numerous dopants, silver (Ag) has been regarded as an efficient strategy to retard electron holes recombination due to the formation of the Schottky barrier on the TiO_2 interface and extending absorption to the visible region. This review primarily focuses on discussing and evaluating the recent progress in the modification of Ag/TiO_2 via co-doping with non-metals and transition metals, as well as the synthesis strategies that have been applied in engineering the materials. The effects of doping and co-doping on the induced chemical and physical properties, photocatalytic performance, stability, and recyclability aspects have also been highlighted. This review also examines the potential improvement of Ag/TiO_2 through the addition of green materials such as plant-based materials (cellulose-derived composites, chitosan, alginate), ceramic materials (clay, kaolin bentonite), and also ionic liquid green solvent. Recommendations for further research opportunities, limitations, and challenges have also been suggested.

1. Introduction

Nanostructured semiconductors have been regarded as promising materials for environmental remediation due to their high photocatalytic oxidation property when it is activated under ultraviolet (UV) radiation which accounts for only 5% of the solar spectrum. Although physical methods (e.g. adsorption), biological methods, chemical precipitation, and membrane filtration have all been applied for wastewater treatment, they pose various limitations such as membrane fouling, high cost, high energy consumption, production of secondary wastes, mass transfer limitations, and long treatment time [1,2]. As a result, alternative techniques need to be applied to overcome the limitations of conventional methods. From that point of view, semiconductor-mediated photocatalysis would be a feasible approach as it is highly efficient at degrading and mineralizing organic pollutants in wastewater to less toxic products such as CO_2 and H_2O. The photocatalysis technique has received considerable attention for the elimination of pollutants compared to other advanced oxidation processes (AOPs) such as Fenton, chemical oxidation, ozonation, and sonolysis due to its numerous advantages. The photocatalytic oxidation process can be initiated at normal pressure and temperature by highly reactive oxidative species, particularly hydroxyl radicals [3,4]. Amongst various semiconductors applied for environmental remediation, titanium dioxide, TiO_2 is regarded as an important photocatalyst due to its excellent activity under the UV spectrum which makes it an efficient photocatalyst since its oxidation state may change without experiencing decomposition [5]. Other unique properties of TiO_2 nanomaterial which have contributed to its wide application in pollutants remediation include low cost, high refractive index, and high chemical and photostability [6].

Although many studies have applied TiO_2 photocatalysis in wastewater treatment, the shortcomings of TiO_2 such as stability, solar energy, visible light utilization, recovery, and recyclability remain inevitable and demand great attention. As means to improve the

Abbreviations: IL, Ionic liquid; UV, Ultraviolet; AOPs, Advanced Oxidation Processes; LSPR, Localized Surface Plasmon Resonance; MO, Methyl orange; CNFs, Cellulose nanofibers; PEG, Polyethylene glycol; Alg, Alginate; MT, Montmorillonite; CA, Cellulose acetate; SPR, Surface Plasmon Resonance; RTIL, Room temperature ionic liquid; NPs, Nanoparticles.

* Corresponding author.
E-mail address: kdevagi@unimas.my (D. Kanakaraju).

https://doi.org/10.1016/j.apmt.2022.101500
Received 23 January 2022; Received in revised form 10 April 2022; Accepted 25 April 2022
Available online 2 May 2022

photocatalytic performance of TiO_2 photocatalyst, dye sensitization [7], supports, magnetic separation [8,9], and surface modification through doping with non-metals, metals, and transition metals and coupling with other semiconductors [10,11] have been applied. TiO_2 ternary/quaternary-based composites [12,13] and hybrid materials [14] are also making a major trend primarily to achieve higher photonic efficiency by synergistically fine-tuning properties like physical, chemical, and electronic.

Metal oxide/semiconductor coupling and TiO_2 modification via heterojunction have been constantly explored to improve the photocatalytic activity of TiO_2-based materials. In the metal oxide/semiconductor coupling, combinations of semiconductors such as TiO_2, ZnO, CdS, SnO_2, CuO, V_2O_5, WO_3, MoO_3, and Fe_2O_3 with transition metal oxides managed to produce systems with improved photocatalytic activity [15]. For instance, Ag/ZnO/AgO/TiO_2 photocatalyst synthesized via chemical precipitation and hydrothermal method showed 99.3% of rhodamine B degradation at 100 min under UV–vis light irradiation because of the coexistence of Ag, AgO, TiO_2, and ZnO [16]. One potential strategy to overcome low quantum yield or ensure efficient separation or transfer of photogenerated e^-/h^+ pairs of photocatalysis is via the construction of heterojunctions with other semiconductors, metal nanoparticles, and carbon-based nanostructures [17]. Appropriate band gap and band edge alignment are critical because the relative energy level at the interface junction determines charge separation direction and transportation [18]. Monazzam et al. [19] reported that highly efficient Ag/Co/TiO_2 heterojunction supported multi-walled carbon nanotubes on heterojunction was successfully fabricated via the sol-gel method and demonstrated 60.0% removal of 2,4-dichlorophenol under visible light irradiation even after 3 cycles of photocatalytic treatment owing to the presence of cobalt dopant that promoted the separation of photogenerated carriers and extended the absorption range of TiO_2 to the visible region. Typically, the interface configuration of two sections of two different semiconductor materials with differing band gaps is known as a heterojunction [4]. Conventional heterojunctions (Type I, Type II and Type III) and new generation heterojunctions (e.g. p-n, Z-scheme, surface and semiconductor/carbon) are the two main categories of heterojunctions.

TiO_2 surface modification via doping has been commonly explored. Existing literature that covers the surface modification of TiO_2 doped with cations includes rare earth metals [11,20,21], noble metals [22,23], and transition metals [24,25]. In addition, previous reviews have also successfully scrutinized TiO_2 surface doping approaches namely with metals, non-metals, and co-doping [26,27]. Metallic ions-doped TiO_2 typically experience a widening light absorption range, which increases the redox potential of the photogenerated radicals, and enhances the quantum efficiency by inhibiting the recombination of the photogenerated electrons and holes on the conduction and valence bands, respectively [28]. Examples of metallic ions that have been doped with TiO_2 include palladium (Pd) [29–31], cerium (Ce) [32–34], copper (Cu) [35–37], cobalt (Co) [38–40], iron (Fe) [41–43] and gold (Au) [44–46].

Besides those aforementioned, silver (Ag) has been commonly used as TiO_2 doping agent since 1984 based on Scopus search [47–49]. Ag has emerged as a promising dopant candidate due to its advantages in improving the physicochemical properties of TiO_2 for numerous applications like air purification, water purification, antibacterial, and self-cleaning [50–52]. Ag is a noble metal that exhibits a plasmonic effect as well as increased conductivity. For example, a study by Saravanan et al. [53] revealed distinctly high photocatalytic hydrogen production of 2880 μmol/h/g_{cat} and 910 μmol/h/g_{cat} under both UV and simulated solar light, respectively using Ag-doped TiO_2 owing to its enhanced physicochemical properties over undoped TiO_2. Doping of Ag on TiO_2 produced a narrower bandgap (2.77 eV vs 3.1 eV for anatase), smaller total surface area (77 m^2/g vs 239 m^2/g), and Ag surface plasmon resonance (SPR) which increased the materials' ability to harvest visible light. A recent review by Chakhtouna et al. [54] summarized the progress made thus far on Ag-doped TiO_2 based photocatalysts for antibacterial and photocatalytic removal. A search performed on Web of Science (WoS) showed a steady increase in studies related to Ag-doped TiO_2 while Ag-doped TiO_2 and green support have been getting more attention among researchers, particularly in the recent 5 years (Fig. 1).

Despite the extensive research on Ag ion doping on TiO_2, which improves the visible light absorption properties of the material, there are still several limitations in maximizing the full potential of Ag-doped TiO_2 to remediate water pollutants. One of the major issues of Ag-doped TiO_2 (Ag/TiO_2) photocatalyst is associated with the loss of photoactivity during recycling and long-term storage [55] and also the leaching of Ag [56,57]. To resolve these issues, supporting Ag/TiO_2 on high surface area supports particularly green materials can be regarded as an excellent option [58,59].

As far as green materials are concerned, plant-based materials such as cellulose, chitosan, alginate, and ceramic-based support such as clay, kaolin, and bentonite aid in the stability and recyclability of Ag/TiO_2 photocatalyst [60–65]. These materials are efficient since they are biodegradable, and their addition allows the formation of a recyclable photocatalyst. Also, existing research studies have shown that the addition of ionic liquids (ILs) as the template solvent medium can have a significant impact on the activity, crystallinity as well morphology of the photocatalyst particles [66]. The stability of Ag-based photocatalysts can be improved through the addition of IL [67]. For example, Mohaghegh et al. [66] observed improved stability of TiO_2 hybrid composite with Ag_2CO_3 in the presence of IL during the degradation of acid blue 92 dye.

In this review, the recent progress made in the modifications of Ag/TiO_2 via doping and co-doping has been summarized by highlighting their characteristics, recyclability, and photocatalytic performance. Synthesis methods applied for the preparation of co-doped Ag/TiO_2-based materials have been also compared and reported in this review. In addition, emphasis has been given to establishing the application of green materials as support or modifier (e.g. alginate, cellulose, and clay) and IL for the fabrication of Ag/TiO_2-based photocatalysts. To the best of our knowledge, a review of Ag/TiO_2 supported green materials have yet to be established. The conclusions that can be derived from the studies discussed and future prospectives or insights for future work have been presented at the end of this article.

2. Heterogeneous photocatalysis mechanism

The mechanistic pathways of TiO_2 photocatalysis have been elucidated in various related literature [3,4,54]. Fig. 2 illustrates the mechanism of TiO_2 photocatalysis. When TiO_2 is irradiated with UV light (wavelength $\leq$ 388 nm), electrons are excited across the bandgap (3.2 eV anatase or 3.0 eV rutile crystalline phases) into the conduction band (CB), leaving electron holes in the valence band (VB) (Eq (1)). Two oxidation reactions take place as shown in Eq (2) and 3. Firstly, is the electron transfer from adsorbed substrate RX (Eq (2)), and secondly, is the electron transfer from adsorbed solvent molecules (H_2O and HO^-) (Eq (3)). The second reaction is much more important in oxidation processes as a result of the high concentration of H_2O and HO^-adsorbed on the surface of the TiO_2. Hydroxyl radicals produced are the main oxidizing species that are responsible for the photooxidation of organic compounds into water and CO_2 (Eq (4)).

$$TiO_2 + h\nu\ (\lambda \leq 388\ \text{nm}) \rightarrow e^-_{cB} + h^+_{vB} \quad (1)$$

$$TiO_2(h^+) + RX_{ad} \rightarrow TiO_2 + RX_{ad}{}^{\bullet+} \quad (2)$$

$$TiO_2(h^+) + H_2O_{ad} \rightarrow TiO_2 + HO^{\bullet}_{ads} + H^+ \quad (3)$$

$$HO^{\bullet}_{ads} + Pollutant \rightarrow CO_2 + H_2O \quad (4)$$

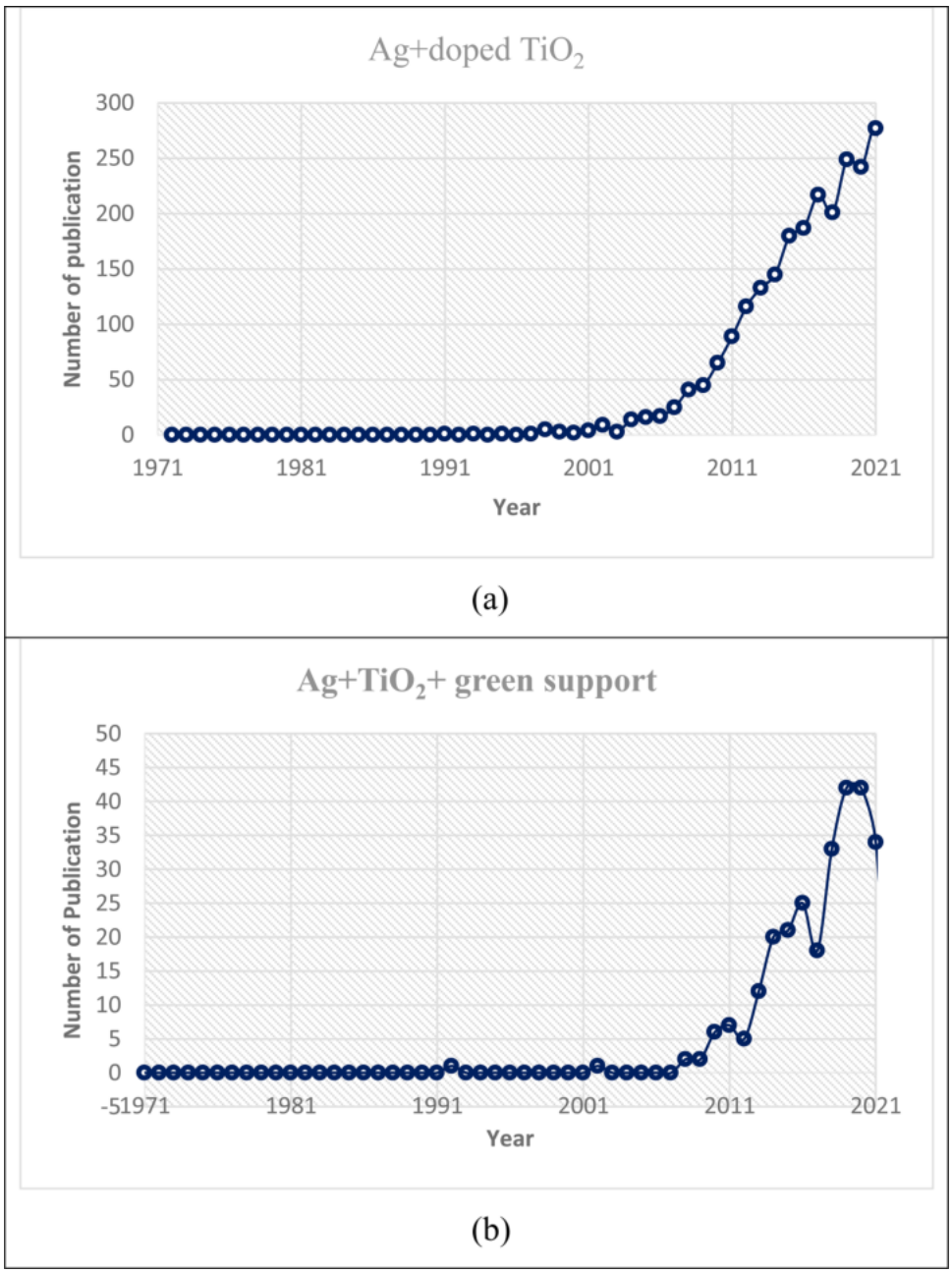

Fig. 1. WoS search (a) Keywords: Ag+doped TiO_2; (b) Ag+TiO_2+green support.

3. Surface modification of TiO_2: doping with metals and non-metals

The recognized limitations of TiO_2 include (i) activation only under UV irradiation with a wavelength lower than 387 nm because of its large bandgap (3.0 − 3.2 eV) [28], (ii) poor efficiency under solar light irradiation as it only absorbs a small fraction of solar light (less than 5% of solar energy is emitted as UV irradiation), (iii) undergo fast recombination of electrons and holes, (iv) experiences slow charge carrier transfer, and (iv) high recycling cost [68,69]. Surface modifications of TiO_2 via doping with metals and non-metals and coupling TiO_2 with other semiconductors such as ZnO, SnO_2, CeO_2, and ZnO [70–72] are performed to conquer these intrinsic issues.

Doping involves the introduction of impurities into a conventional photocatalyst to change its electrical and optical properties as well as the structure of the photocatalyst [73]. It alters the degree of structural metastability and the activation energy in fine crystalline materials by affecting the number and surface site distribution for nucleation as well as its rate of coarsening [74]. In addition, doping results in a bathochromic shift such as a decrease of band gap or induction of intra-band gap states which allow greater absorption under visible light irradiation [11].

3.1. *Defect engineering of TiO_2*

Defects in crystals are prevalent in material science, and this phenomenon is increasingly common as solid materials approach the nanoscale range. Defects are typically regarded as an unfavorable aspect of crystals, and their presence in crystals is generally associated with the disruption of periodic atomic arrangements in the lattice, causing both the geometrical and electronic structures of crystals to be impacted and disordered [75].

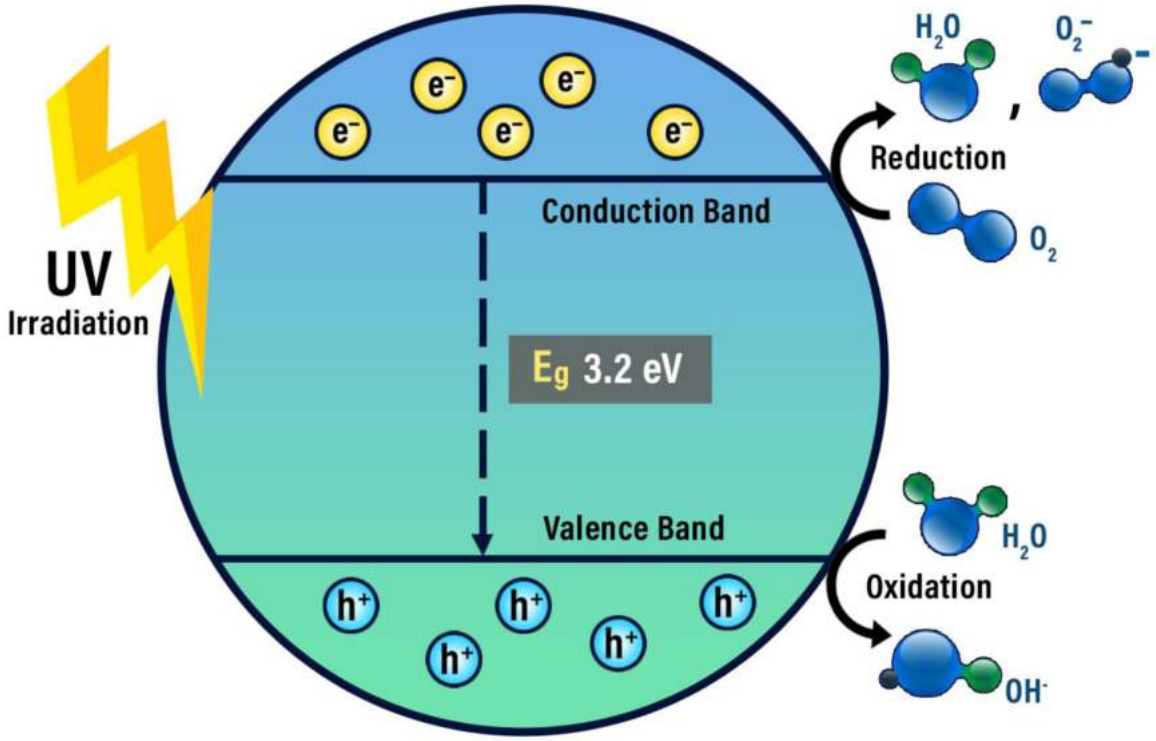

Fig. 2. Schematic illustration of the mechanism of TiO_2 photocatalysis.

However, advances in characterization techniques have enabled and allowed for a deeper knowledge and understanding of the photocatalysis process and revealed the amazing benefits of defects in various catalysis materials and this opens up new possibilities for modifying the catalytic properties of photocatalysts such as in photocatalytic water splitting and reduction of CO_2 into fuels.

Zero-dimensional point defects, such as vacancy and impurity, are the most basic type of defects. In metal oxides such as TiO_2, ZnO, and MoO_3, vacancy is the most widely investigated defect [76–78]. By removing lattice oxygen atoms, oxygen vacancies are created, which usually result in the formation of coordinately unsaturated (CUS) metal atoms and the accumulation of surplus electrons [79,80]. The CUS metal locations are either electron-rich or have a lower valence state than anticipated. On the other hand, cation vacancies such as Ti can also be produced in the lattice. This defect chemistry has been proven to be a useful tool for designing functional properties of TiO_2 such as electronic structure, charge transport, and surface properties [81,82]. For example, Wang et al. [83] has synthesized black TiO_2 nanotubes with improved separation and transmission efficiency of photo-generated charge carriers by synergistic catalytic of NiS and Pt.

In addition to the vacancies induced by defects, impurities are frequently generated by doping foreign atoms such as transition metal, non-metal and noble metal. The doped atoms are inserted into the material lattice either interstitially or substitutionally, resulting in electronic structure modulation. Several extensive reviews have detailed how lattice defects can boost the conductivity, carrier concentration, and bandgap structure, and even drive the transformation from semiconductor to metallicity [84].

3.2. Doping with metal

Doping of TiO_2 with metals usually involves three types of metals namely transition metal, noble metal, and rare earth metal. The addition of transition metals into TiO_2 photocatalyst improves its responses, reduces the recombination rate of photogenerated electron-hole pair, and decreases its bandgap. The changes in the bandgap efficiency cause overlapping of the conduction band because Ti (3d) with transition metals d levels produces a redshift on the band edge of TiO_2. TiO_2 photocatalyst doped with transition metals diminishes the band hole energy through the development of another conductive level between the valence band and conduction band [85].

Transition metals such as Cr, Cu, Fe, Mn, Zn, V, W, Co, and Ru have been reported to greatly affect TiO_2 properties such as bandgap energy, surface area, thermal properties, and particle size which have a direct effect on the photocatalytic performance of the arising material [86,87]. For instance, a study reported the influence of Cr, V, and Co with TiO_2 catalyst synthesized via sol-gel method at different concentrations suppressed the crystallinity of TiO_2 and caused phase transition from anatase to rutile phase [88]. The concentration of transition metal dopant concentration also has a direct influence on the properties of materials [11].

Doping of TiO_2 with noble metals such as Au, Pt, Ag, and Pd has greatly improved the photocatalytic performance of TiO_2 both under UV irradiation and visible light. The increase in absorption towards the visible light region is associated with Ag-doped into TiO_2 where the localized SPR effect of Ag nanoparticles promotes the absorption of Ag/TiO_2 in the visible region [89]. For example, Ag/TiO_2 with 2.7 wt% of Ag demonstrated 98.5% of Orange II Dye degradation under UV irradiation after 2 h as compared to undoped TiO_2 producing only 87.5% of degradation after a prolonged 4 h of irradiation [90]. Rare earth metals which consist of 17 elements including yttrium (Y), scandium (*Sc*), and 15 lanthanoids elements are another type of metals that can be potentially doped with TiO_2 [11]. The incomplete 4f and empty 5d orbitals in these rare earth metals allow its incorporation into the TiO_2 photocatalyst [21]. The degradation of commonly used textile dyes Reactive Blue 21 and Acid Red 114 using rare earth metal Pr^{3+} and Ce^{4+}-doped TiO_2 showed almost complete degradation for both dyes [20].

Although metals greatly improve the photocatalytic performance of TiO_2 limitations on the usage of metals as dopant persists. For example, it was reported that the addition of transition metal in the anatase phase of TiO_2 contributes to the thermal instability of the photocatalyst [11] as well as the low light capability and low quantum efficiency [91]. Doping

with rare earth materials which lead to the formation of rare earth metal -O-Ti bonds on the surface of the photocatalyst causes inhibition of the nanocrystalline size growth [92,93]. Furthermore, rare earth metal-doped TiO_2 is very expensive but it has great potential in the degradation of organic persistent compounds [11].

3.3. Doping with non-metal

Doping with non-metallic elements introduces non-metal elements into the crystal lattice of the catalyst where they react with the oxygen atom and changes the electron cloud density of the oxygen atom [94–96]. As a result, the atomic energy level splitting of the oxygen atom changes and causes an intermediate band gap in the band gap of the catalyst [97]. The intermediate bandgap narrows the band gap of the catalyst and contributes to a wider range of light wavelengths for absorption [98–100]. Non-metallic elements that are mostly used as dopants to improve the performance of TiO_2 photocatalyst include nitrogen (N), carbon (C), sulfur (S), chlorine, (Cl), and fluorine, (F) [11].

Amongst these non-metals, N is the most promising non-metal dopant because of its stability and size of the atom which is comparable to oxygen in TiO_2 [101–104]. N dopant behaves as a center where the photogenerated electrons are trapped and reduces recombination rates of photogenerated species like the electrons and holes [105]. Doping of N into the lattice of TiO_2 causes the construction of a mid-gap energy flat near the valence band and results in a decreased TiO_2 bandgap to 2.5 eV, allowing TiO_2 to become a visible light active catalyst [26]. A study by Selvaraj et al. [106] indicated that the UV–vis reflectance spectra of N doped TiO_2 catalyst showed strong absorption in the visible range indicating a redshift in the bandgap transition from 3.23 eV to 2.89 eV. Another study demonstrated an improved photodegradation rate of phenol (69.3% within 120 min) as a result of N doping which has not only restrained the transformation of TiO_2 from anatase to brookite but also showed reduced average crystal size (8 nm to 6 nm) and reduced optical band gap (3.1 eV to 1.95 eV) [107].

Besides N, C has also been widely used as a dopant in heterogeneous photocatalysis [108,109]. C doped TiO_2 possessed better charge transfer, reduced charge recombination, and larger electron storage capacity [109]. The incorporation of C into the lattice of TiO_2 substitutes lattice O or Ti atom and forms Ti-C or C—O-Ti bond, resulting in a hybrid orbital above the valence band of TiO_2 and allowing absorption in the visible light region [110]. C-doped TiO_2 nanorods prepared via hydrothermal method showed that C-TiO_2 degraded 90.2% of MB within 10 min under visible light irradiation in contrast to undoped P25 TiO_2, which was only 6.4% of degradation after 40 min [111].

In addition, S-doped TiO_2 also showed improved efficiency owing to the good thermal stability of S dopant. S also reduces the bandgap of TiO_2 by changing the crystal and electronic structure of TiO_2 [26]. When thiourea or sulfate was used as S dopant sources [112,113], S^{6+} as a cation in the substitution of Ti^{4+} was reported to be chemically favorable because of its different ionic radius, which formed new states into the conduction band of TiO_2 from S-3 s states just exceeding the valence states of O-2p [112]. In cationic substituted S-doped TiO_2, S acted as electron capturing species, enhanced electrical conductivity of TiO_2 and improved the electron-hole pairs transfer, and also resulted in a greater photocatalytic performance under visible light irradiation [26,114].

Despite studies demonstrating the positive effects of non-metals on TiO_2, issues about non-metals as dopant candidates are inevitable. For example, N-doped TiO_2 photocatalyst has been reported to aggregate and crystallize upon annealing at 500 °C, causing a larger size and a lower number of active sites [115]. Non-metal doped into the lattice of TiO_2 formed oxygen vacancies in the bulk, contributing to greater recombination centres of photo-induced electron-hole pairs [116]. Table 1 provides a summary of the advantages and disadvantages of both metals and non-metal dopants based on the studies reviewed.

Table 1
Advantages and disadvantages of dopants metals and non-metals.

Types of Dopants	Advantages	Disadvantages	Reference
Metal	• Narrows bandgap • Prevents recombination of electron-hole • Improves adsorption of contaminant	• Thermal instability • Dopant concentration dependent • Expensive • Toxic in nature	[11,114, 212]
Non-metal	• Narrows band gap • Improves adsorption of contaminants • Enhances conductivity of TiO_2	• Expensive • Oxygen vacancies formation • Short term efficiency • High temperature needed for preparation • Difficult synthesis routes	[26,105, 107,212]

4. Silver as a dopant of TiO_2

The suitable dopant for TiO_2 varies and all metals and non-metals have their advantages and disadvantages as aforementioned. As can be seen in Fig. 1, many studies have been conducted and reported on Ag-doped with TiO_2. Therefore, it is important to highlight the advantages of doping Ag with TiO_2 semiconductors and to understand the mechanisms involved during the photodegradation of pollutants. As compared to other metals, silver (Ag) is the most stable, low-cost, nontoxic, and shows the highest thermal and electrical conductivity [117]. Other noble metals such as Pt, Pd, Rh, and Au are considered more expensive to be generally used in industries as compared to Ag [118]. Ag has also shown good catalytic activities, large surface area, excellent conductivity, and stability [119] which allow it to provide highly effective and selective organic reactions [120]. Due to its characteristics such as low contact resistance or excellent electron conductivity, it is used as an electron moderator in the Z-scheme photocatalyst structure [25]. Ag nanoparticles may also act as both an electron mediator and a photosensitizer, which then allowed the generation of stable electron-hole pairs using low-energy photons [121].

Doping of Ag nanoparticles with TiO_2 is known to be one of the successful approaches used to reduce the recombination of the electron-hole pairs and extend the light absorption range of TiO_2 photocatalyst toward visible light [122,123]. The presence of Ag improves the photocatalytic activities by two distinct features. Firstly, to act as an electron trap and capture electrons transferred from the conduction band of TiO_2 semiconductor and transfer these electrons to oxygen, converting them into superoxide radicals. Photogenerated holes in the valence band remaining on the TiO_2 react with water molecules and help in the forming of hydroxyl radicals which are then effectively used for pollutants photocatalytic oxidation and bacteria [124]. Secondly, it induces an SPR effect that extends the light absorption to the visible light region and improves TiO_2 photocatalytic efficiency simultaneously [125,126].

Similarly, several studies have also shown that Ag-doped TiO_2 improves its efficiency in three main ways, (1) modification of TiO_2 morphology to give rise to higher affinity for dissolved oxygen [127, 128], (2) reduction of recombination of charge carriers [129,130] and (3) plasmonic effect-electron injection [131,132]. Since photocatalytic efficiency is heavily dependent on the formation of reactive oxygen species produced by photo-excited electrons of TiO_2 and adsorbed O_2, increasing the amount of O_2 on the TiO_2 surface will generate more oxygen species. Ag-doped TiO_2 can improve its affinity for dissolved O_2 by providing it with a higher affinity of O_2 and increasing its surface for adsorption of O_2. Doping of Ag on TiO_2 enhances TiO_2's capacity to attract O_2 from the solution towards its surface [133]. Another study revealed increased O_2 adsorption on Ag-doped TiO_2 photocatalyst with increased concentration of Ag dopant (0.0 wt% to 3.0 wt%) [134]. As

the concentration of O_2 increases on the surface of the photocatalyst, a higher concentration of O_2 and electrons will react, forming more $\bullet O_2^-$ species to enhance the charge carrier separation [135].

Ag dopant improves TiO_2 by forming the Schottky barrier at the Ag/TiO_2 interface [96]. One of the roles of Ag dopant is mediating electron transfer whereby its Fermi energy level influences the charge carrier separation at the interface between TiO_2 and Ag dopant [136,137]. It has been reported that Ag nanoparticles with Fermi level (Ef) located around 0.4 V are good electron acceptors and traps electron efficiently under the irradiation of UV [138]. The Fermi level of Ag is located at an energy level below the conduction band of TiO_2 (Fig. 2), the Schottky barrier formed on Ag/TiO_2 junction leads to the downward bending of the TiO_2 energy bands [135].

The formation of a Schottky barrier at the heterojunction caused an excess in negative charge in Ag and excess in positive charge on TiO_2. The formation of an electron depletion layer between the opposite charges helps in maintaining the charge carrier separation. The negative charge on the noble metal particles is caused by the difference in the Fermi levels of Ag particles and TiO_2 [135]. The gap in the Fermi level promotes electron transfer from material with a higher Fermi level to material with a lower Fermi level [139]. Photo-generated electrons can be trapped in Ag on the surface of TiO_2 and facilitate electron transfer, hence reducing recombination of charge carriers [135]. Fig. 3 illustrates the mechanism of charge transfer in Ag-doped TiO_2 photocatalyst for photocatalytic degradation.

Recently, Basumatary et al. [140] reported a significant synergistic effect between SPR and metal oxide in the fabricated Ag/TiO_2/WO_3 heterojunction photocatalyst which enhanced the visible light response of the material [140]. When light is irradiated on Ag, the electrons in Ag are excited due to its SPR. The electrons then move towards TiO_2 and induce a reduction reaction. It is shown that Ag, due to its plasmonic structure and excellent charge transfer, allows TiO_2 to be more effective in charge transfers. Consequently, Ag-doped TiO_2 has a greater photocatalytic inducing region as compared to undoped TiO_2 [141]. Fig. 4 summarizes the characteristics of Ag and its benefits as a dopant.

Various methods have been used as strategies for doping Ag into the lattice of TiO_2 such as the sol-gel method [142], hydrothermal method [22,143], solvothermal method [144–146], photoreduction method [134,147-150], electrochemical method [90], electrospinning method [118,151], and wet impregnation method [152–154]. These methods are commonly applied in the synthesis of Ag/TiO_2 due to several reasons. For instance, the sol-gel method is eco-friendly, simple as it does not require complicated synthesis conditions or instruments, and known to be an inexpensive technique that can control the purity and homogeneity of the final product, growth, and size of the particles and the flexibility of adding high concentrations of doping agent [54]. Lenzi et al. [155] fabricated Ag-doped TiO_2 via the sol-gel method and demonstrated high adsorption of mercury (II) and 67.0% of reduction under a mercury lamp owing to its porous structure as well as high dispersion of Ag (2 wt%) in the photocatalyst which act as electron-hole recombination centres. The addition of higher concentration Ag in sol-gel synthesis has also shown higher porous structures in Ag-doped TiO_2 films [156]. The porous structure enhanced photocatalytic performance on account of its large surface area [157]. Hence, morphology plays a distinctive function in photocatalytic performance [158,159]. Fig. 5 shows the synthesis of single and co-doped Ag/TiO_2 using the sol-gel method.

Meanwhile, nanocomposite prepared by hydrothermal method showed good crystalline phase, shape, and size [160,161]. The solvothermal technique is almost similar to the hydrothermal method except for the solvent system used. The hydrothermal method uses water as a reaction system while the solvothermal method uses organic solvents, which have a role in controlling the structure, morphology, crystallinity, and shape distribution of Ag-doped TiO_2 photocatalyst [162]. It has been reported that the addition of reducing agent for the reduction of Ag^+ ions to metallic Ag^0 in the hydrothermal synthesis such as ascorbic acid and hydrazine formed striped structures while polyethylene glycol and sodium borohydride formed spherical structures of Ag-doped TiO_2 [22]. Hamed et al. [143] synthesized Ag-doped TiO_2 by hydrothermal method at 150 °C and produced flowerlike rutile phase photocatalyst for the photocatalytic degradation of MB. It was revealed that the flowerlike morphology supplies a high number of active sites meanwhile the presence of rod petals in the structure also provides a direct pathway for the electron in overcoming the recombination between electron and hole in the photocatalytic mechanism. Literature has also shown scattering effect caused by flowerlike morphology aids in the

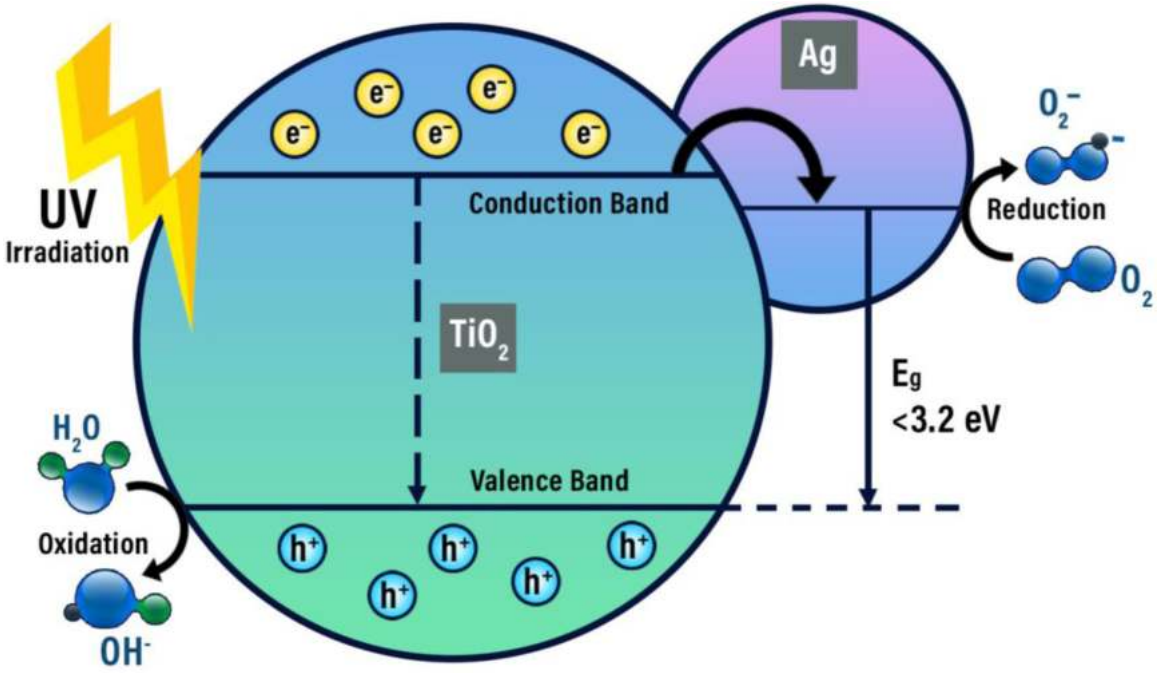

Fig. 3. Schematic illustration of the mechanism of charge transfer in Ag-doped TiO_2 photocatalyst.

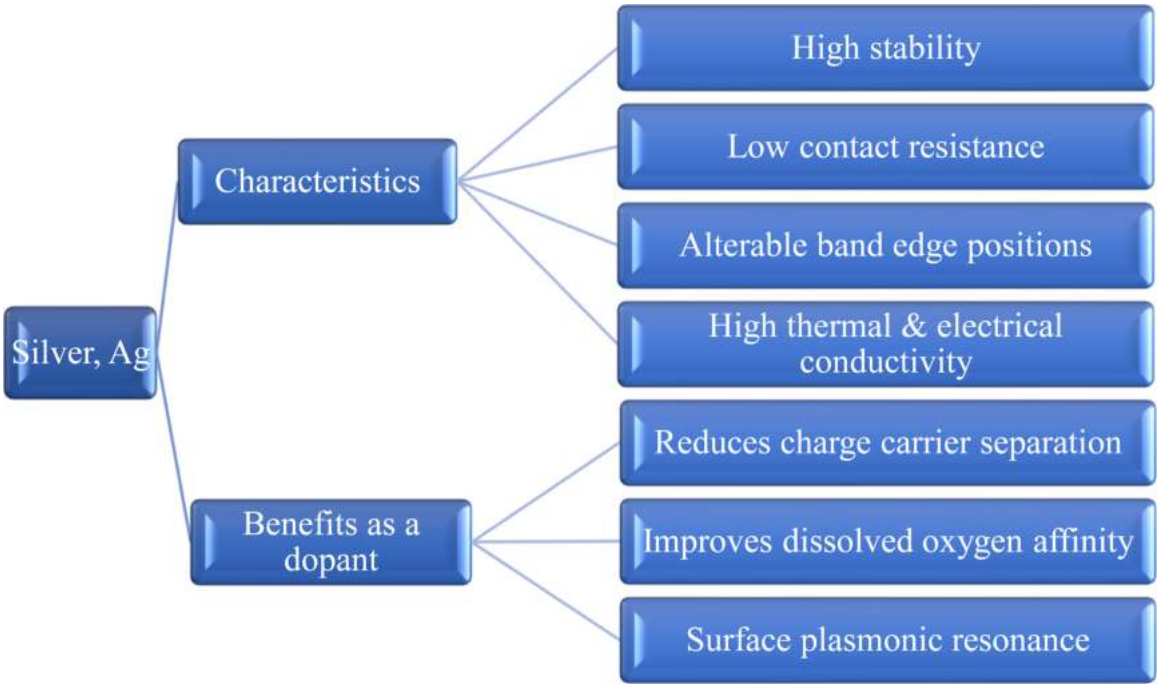

Fig. 4. Characteristics of Ag and its main benefits as a dopant.

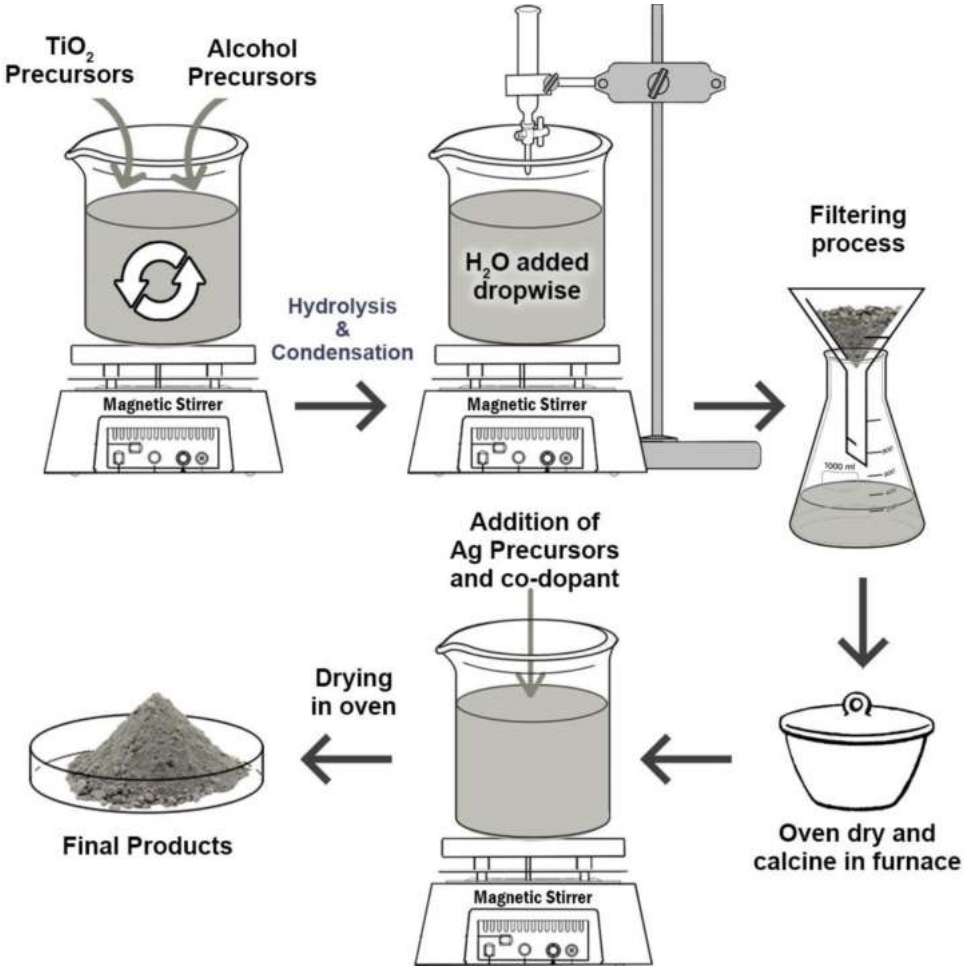

Fig. 5. Schematic diagram of the synthesis of single doped and co-doped Ag/TiO_2 photocatalyst via sol-gel method.

dispersion of photons via the rods and supplies energy for electron excitation in the conduction band [163]. Spherical shape morphology has also been observed by Shojaie et al. [164] in the hydrothermal synthesis of Ag/TiO_2/Fe for the degradation of 4-chlorophenol. The photocatalyst achieved 97.12% photodegradation and its efficiency was maintained even after 5 cycles of operation. This is attributed to the presence of Fe_3O_4 whereby the magnetic core aids in the recovery of the photocatalyst by applying an external magnetic field [164]. Fig. 6 illustrates the general method applied for the recyclability process of a photocatalyst after photocatalytic treatment.

Zhou et al. [145] prepared Ag/TiO_2 nanorods heterostructures via a one-pot solvothermal in-situ synthesis method that uses ethylene glycol as a solvent in the synthesis. The synthesis built a tight contact between the Ag nanorods' core and TiO_2 nanoflakes heterostructures and resulted in the strong plasmonic resonance of Ag nanorods which contributed to enhanced degradation (98.2%) of methyl orange under visible light as compared to bare TiO_2 [145]. Similarly, Wang et al. [152] also reported similar improvement of TiO_2 in the fabrication of Ag/TiO_2 nanofibers via the solvothermal method by using N, N-dimethylformamide (DMF) as solvent. The Ag^+ in DMF solution reacts with the surface hydroxyl groups and oxygen of TiO_2 nanofibers, resulting in the nucleation of Ag atoms through the homogeneous nucleation process on active growth sites provided by the TiO_2 templates and the formation of high crystallinity of Ag particles [152]. The study demonstrated maintained efficiency even after 3 cycles of photodegradation of Rhodamine B, owing to its crystallinity and resistance towards electron migration. Fig. 7 depicts the typical procedures involved in the hydrothermal and solvothermal synthesis of co-doped Ag/TiO_2.

The wet impregnation method has also been commonly employed in the synthesis of Ag-doped TiO_2 due to the formation of high crystallinity of photocatalyst [154]. Zhou et al. [154] successfully synthesized Ag/TiO_2 via the wet impregnation method and showed nearly 80.0% of phenol degradation in 2 h under visible light owing to the formation of small Ag clusters confined in the channels of the mesoporous TiO_2. Literature has reported that poor conductivity, numerous boundaries, and defects in the mesoporous TiO_2 films resulted in reduced transfer efficiency of carriers and caused a decrease in photocatalytic efficiency [165]. Another study has also shown that highly stable Ag-doped TiO_2 was fabricated via the wet-impregnation method allowing Ag nanoparticles to homogeneously cover the surface of TiO_2 nanopillars to form an efficient heterogeneous structure which exhibited nearly complete removal of 2,4-dichlorophenol under visible light and maintained efficiency even after 10 cycles of treatment [166]. A brief wet impregnation synthesis procedure has been illustrated in Fig. 8 while Table 2 highlights some of the commonly used methods for the synthesis of Ag/TiO_2 single-doped and co-doped materials gathered from recent selected studies.

4.1. *Co-doping of Ag/TiO_2*

As single element doping of TiO_2 may limit its photocatalytic enhancement, the co-doping approach using more than two elements can be used to further enhance the properties of the resulting material [97]. For instance, the electronic, chemical, and magnetic properties of the photocatalyst can be effectively altered by doping with two or more metal ions [167]. Co-doping of TiO_2 has improved photocatalytic activity, especially in harvesting visible light as compared to undoped TiO_2 or single-ion doped TiO_2 [135]. Co-doping with non-metal results in a

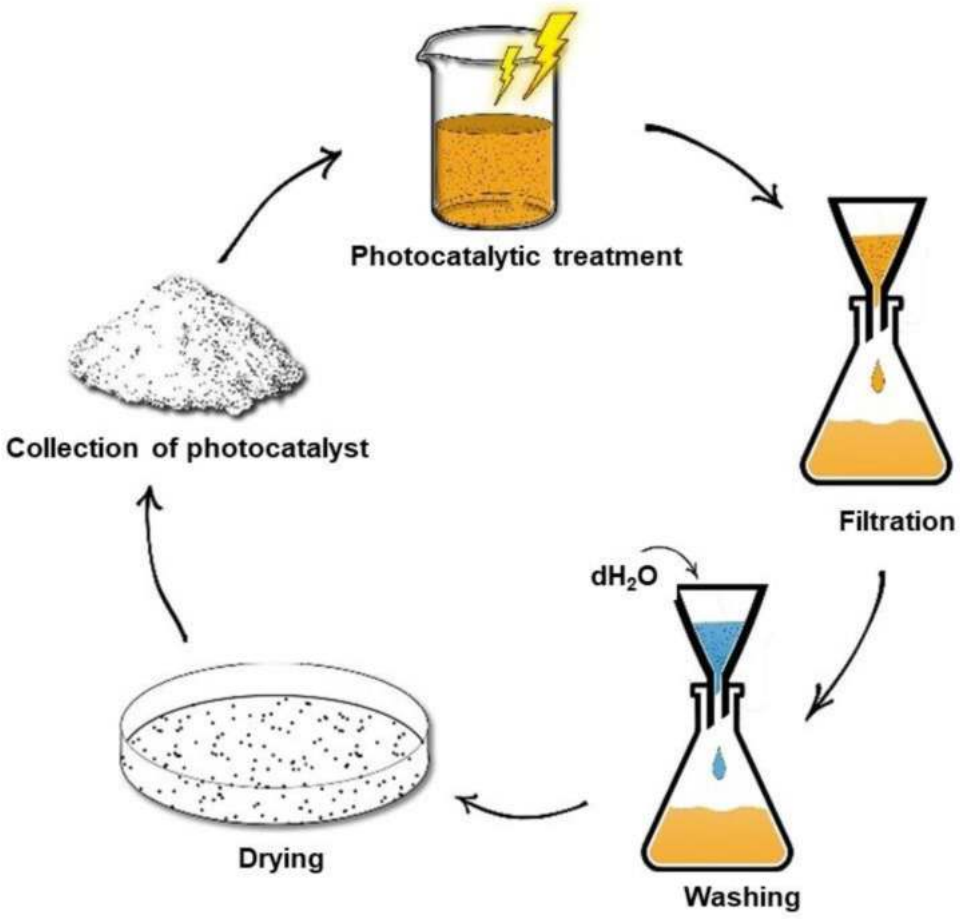

Fig. 6. The schematic illustration of the recyclability process of Ag/TiO_2 photocatalyst.

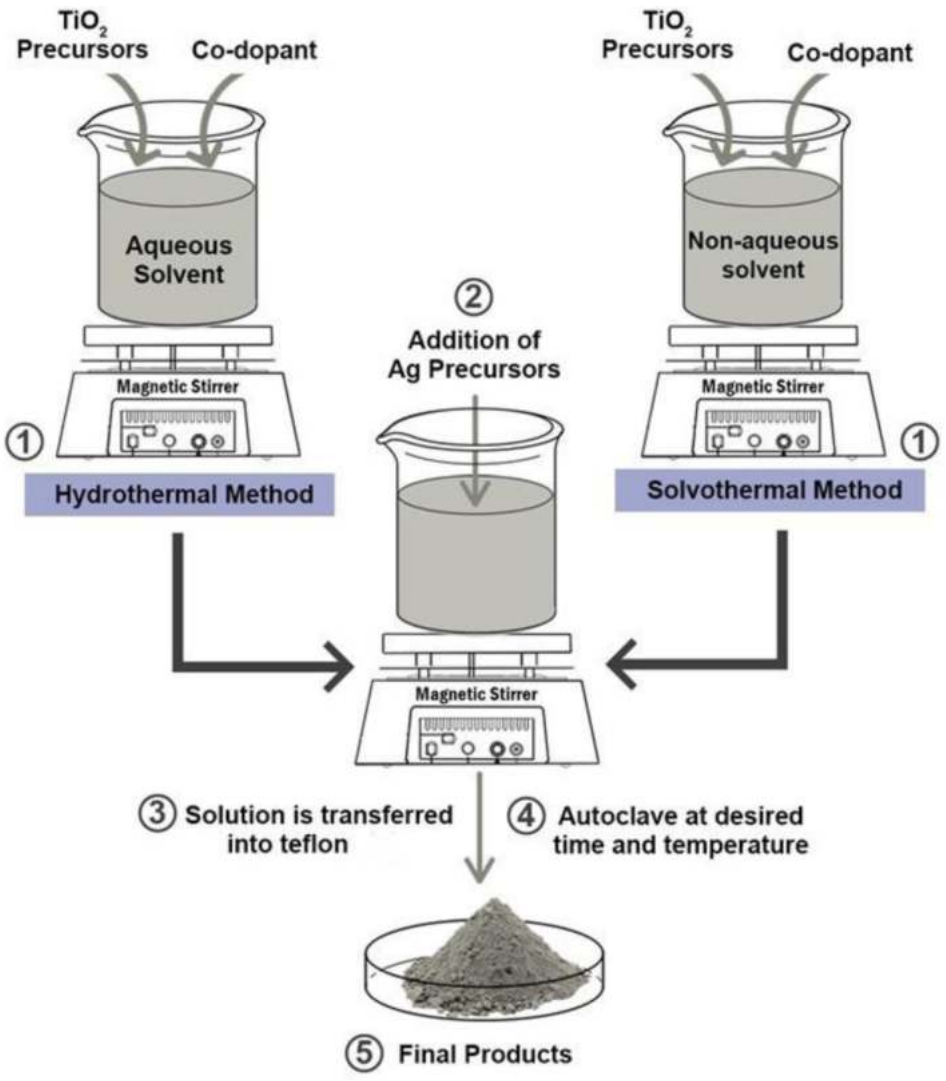

Fig. 7. Schematic illustration of the synthesis of single doped and co-doped Ag/TiO_2 photocatalyst via hydrothermal and solvothermal method.

redshift in the visible region meanwhile co-doping with metal helps in transferring photogenerated charge carriers which then suppresses the recombination [168]. Co-catalyst provides dual advantages: they accelerate the migration of charge carriers by acting as electron trappers and promoting solar energy absorption [169]. The role of co-dopants is not only in narrowing the bandgap, but also contributes to the formation of different heterostructures such as forming different electronic structures with TiO_2 [170]. Studies have shown that co-doping of TiO_2 renders synergistic effects which can further enhance the photocatalytic properties of TiO_2 [97,171]. In addition, choosing compatible co-dopants and the synthesis methods in introducing the dopant are crucial as it affects the doping level [170].

4.1.1. Co-doping of Ag/TiO_2 with non-metals

Co-doping technique with double metal or double non-metal dopants or double metal/non-metal dopants has been greatly scrutinized in research methods due to its synergic effects in improving the visible light absorption efficiency of photocatalysts [172]. Among the effects is restraining the recombination rate of photo-induced carriers [173]. For instance, photocatalysts doped with sulfur, S showed a decrease in the bandgap of the photocatalyst and doping S with TiO_2 resulted in an optical absorption redshift in the composite. A study reported the preparation of Ag-S co-doped TiO_2 via the sol-gel method where the addition of S into the system substitutes oxygen and occupies the interstitial sites of TiO_2 (Table 2). The study showed a reduction in crystallite size from 19 nm to 11 nm and bandgap energy of 3.08 eV to 2.89 eV for pure and co-doped TiO_2 as well as enhanced photocatalytic activity in the degradation of methylene blue under visible light irradiation for co-doped TiO_2 as compared to undoped TiO_2 [171].

Synergistic effects could be observed in the co-doped Ag/TiO_2 system in terms of properties and photo efficiency. Devi et al. [174] showed that Ag/TiO_2/S improved photocatalytic activity under UV and solar light illumination due to the synergistic effect of S dopant, bidentately coordinated surface sulfate sites and Ag particles deposited on TiO_2 surface. Excitation of electrons from the valence band to the S^{6+} dopant energy level occurred and there are three different ways in which the electrons could be trapped: (1) surface modified SO_4^{2-}, (2) Ag particles or (3) surface adsorbed oxygen molecule [175]. The life span of photogenerated electrons increases due to the synergistic effect, and as a result, the electron-hole recombination reduces [174]. The formation of the Schottky junction due to Ag on $TiSO_2$ photocatalyst contributes to an internal electric field close to the TiO_2 interface [176]. The presence of an internal electric field forces electrons and holes to move in different directions, hence reducing the recombination rates [177]. Fig. 9 illustrates the degradation of congo red dye by the photocatalysts in UV light irradiation and solar light illumination.

Another study reported a higher degradation of phenol (92%) by Ag/TiO_2–N synthesized via photoreduction method than single doped TiO_2

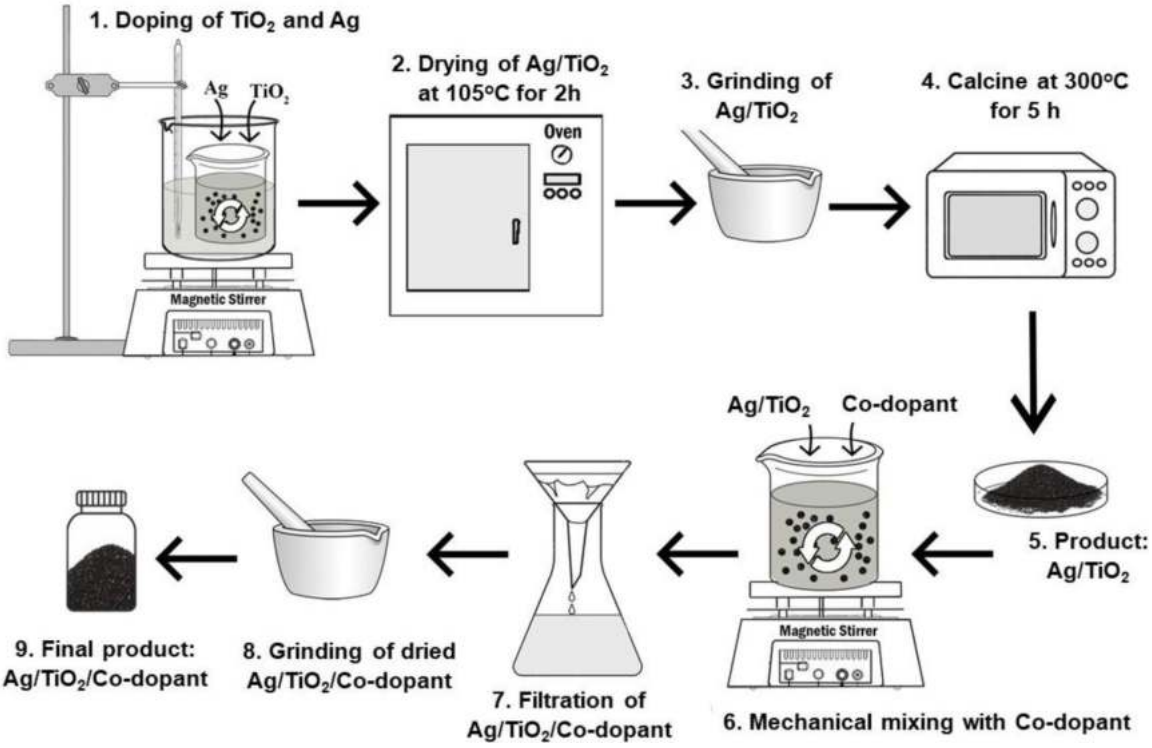

Fig. 8. Schematic illustration of the synthesis of single doped and co-doped Ag/TiO_2 photocatalyst via wet impregnation method.

(46% - 59%) and undoped TiO_2 (38%) due to the excited electrons being trapped in the oxygen vacancies created by N dopant while the holes are trapped by the N dopant level [178]. Furthermore, an easier pathway for the movement of the holes was created as the 2p states of O and N are mixed up [178]. Electrochemically deposited Ag nanoparticles on undoped TiO_2 and TiO_2/N showed improved photocatalytic properties under UV and visible light irradiation for the degradation of orange II dye [179]. It was reported that 0.5% of Ag and N improves the absorbance value and generates shifting of the tail band to the visible domain and the improved photocatalytic activity is attributed to the electron acceptor role of Ag and more holes transported on the surface of TiO_2 [179]. Likewise, the study also revealed significant utilization of visible light in the degradation of phenol when Ag/N was co-doped on TiO_2 with the existence of multiple oxygen vacancies [180]. Since the Fermi levels of Ag and N are lower than TiO_2, the photoexcited electrons are transferred from the conduction band to dopant particles on the surface of TiO_2 as the photogenerated valence band holes remain in TiO_2, thus resulting in reduced electron-hole recombination and increased photocatalytic reactions [179]. The co-doping of different percentages of Ag and N on the photocatalytic properties of titania nanostructures was also investigated and it was found that 2% of N and 5% of Ag calcined at 400 °C showed better photocatalytic properties as compared to other samples [181].

TiO_2 modified with Ag-F nanosheets with exposed (001) facets were prepared via a solvothermal process using different concentrations of $AgNO_3$ and HF solution for the photocatalytic degradation of MB solution. The study showed that the addition of HF in Ag/TiO_2 greatly improved the photocatalytic activities and resulted in higher degradation of methylene blue as compared to TiO_2 and Ag/TiO_2 alone [182]. A strong interaction between Ag and the unsaturated atoms on TiO_2 improves the light response in the UV light region and resulted in higher efficiency in the degradation. Furthermore, the TiO_2 surface with F atoms influenced the surface charge separation and transfer [183]. Due to the high electronegativity of F atoms, a part of the photoelectron is transmitted from O to F via the O-Ti-F links, and the substitution of F atoms on the -OH groups on the TiO_2 surface inhibited the formation of the inactive surface of OH radicals and promoted the production of active free OH radicals, therefore enhancing the photocatalytic activity [182].

4.1.2. *Co-doping of Ag/TiO_2 with transition metals*

The photoresponse of Ag/TiO_2 in the visible region can be improved by co-doping with transition metals. Doping with suitable transition metals such as Fe, Fe, Cr, Sn, Pt, and V can overcome one of the limitations of TiO_2 such as the high electron-hole recombination rate [164]. V, Zn, Mn, Ni, Cr, Co, and Fe were among the transition metals investigated as dopants to improve the properties of Ag/TiO_2. Transition metals ions like Pd^{2+}, Cu^{2+}, Cr^{3+}, V^{5+}, Fe^{3+}, and Ni^{2+} change the electronic structure of TiO_2 by adding a donor and/or acceptor level in the bandgap, causing photons with lower energy to excite a photocatalyst and thus enhancing the photocatalytic activities under visible light [184]. Furthermore, significantly smaller band gaps and improved photocatalytic efficiencies are observed in TiO_2 doped with transition metal ions [185]. Some of the transition metal oxides such as Cu_2O are known as promising and nontoxic p-type semiconductors in solar energy conversion applications [186]. The conduction band and the valence band of Cu_2O are more negative than TiO_2, therefore the formation of Cu_2O-TiO_2 heterojunction results in photoexcited electrons transfer from CB of Cu_2O to TiO_2 [187]. The synergistic effect of the favorable energy level between Cu_2O—Cu-TiO_2 heterojunction enhances its photoelectrochemical properties [187].

Amongst various candidates, Ce appears to be one of the favorite choices as a co-dopant with Ag/TiO_2 due to its oxidation–reduction properties as a result of its readily loss, gain, and storage of surface oxygen [188]. The primary use of Ce in catalysis is driven by its readiness to form oxygen gaps due to the surface reduction [189]. Ce^{3+} or Ce^{4+} allows the formation of cerium oxides such as CeO_2 or Ce_2O_3 and their electronic structures [Ce^{3+} ($4f^1$ $5d^0$) and Ce^{4+} ($4f^0$ $5d^0$)] are the contributing factors towards strong catalytic and optical properties [188]. Enhanced optical properties of TiO_2 in the visible region were observed in a study where TiO_2 was co-doped with Ce and Mn for the degradation of diclofenac [190]. The presence of Ce and Mn as

Table 2
Commonly used methods for the synthesis of Ag/TiO_2 single-doped and co-doped from recent selected studies.

Methods	Doping	Precursors	Characteristics of Products			Pollutant	Photocatalytic performance	Efficiency/ Regeneration (cycles)	Ref.
			Crystal structure (XRD), crystallite size	Morphology (SEM/FESEM)	XPS, TEM, EDX				
Hydrothermal	Single	Titanium (IV) butoxide (Ti $(OBu)_4$), silver nitrate ($AgNO_3$)	Rutile, 33.00 nm to 86.00 nm	Flower-like structure containing a bundle of rods	Concentration of Ti^{3+} and $Ti^{2+} > Ti^{4+}$, fine rods' sizes range from 7 nm to 10 nm, unable to detect the presence of Ag	Methylene blue	75.00% within 5 h under Xenon lamp	N/A	[143]
		TiO_2 (99.8%), Ag powder (99.8%)	Anatase, 17.59 nm - 19.24 nm	Spherical particles bonded together with sponge-like structure, visible white clusters (Ag particles)	N/A	Methylene blue	97.00% in 60 min under visible light	N/A	[213]
		Titanium (IV) isopropoxide Ti $[OCH(CH_3)_2]_4$, $AgNO_3$	Anatase, N/A	Striped and spherical structure	N/A, 20–40 nm, N/A	Indigo blue	75.00% after 150 min under UV light	N/A	[22]
	Co-doping (Fe)	Titanium tetrabutoxide, CH_3COOAg, iron (III) nitrate (Fe $(NO_3)_3 \bullet 9H_2O$	Anatase, 5.32 nm-15.49 nm	Sphere-like shape	N/A, N/A,2.16 wt% of Ag, 0.21 wt% of Fe, 51.36 wt% of Ti, 46.27 wt% O	4-Chlorophenol	97.12% after 165 min under UV irradiation	94% after 165 min under UV irradiation/5	[164]
Photoreduction	Single	Tetrabutyl titanate ($Ti(OC_4H_9)_4$), $AgNO_3$	Anatase, N/A	Irregular block structure	Ag^0 and Ti^{4+} detected, N/A, N/A	Tetrabromobisphenol A	100.00% in 10 min under UV–vis light, 20–27% in 2 h under visible light	~85% in 10 min under UV–Vis light/ 3	[148]
		TiO_2 nanotubes, $AgNO_3$	Anatase, N/A	Ag uniformly dispersed on TiO_2 nanotubes surface	Ti^{3+}, Ti^{4+}, O^{2-}, O^-, Ag^0, Ag^+, Ag^{2+} detected, N/A, N/A	Methylene blue, methyl orange	81.20% (methylene blue) 75.8% (methyl orange) in 150 min under sunlight	N/A	[150]
	Co-doping (C)	Tetrabutyl titanate, $AgNO_3$, Glucose ($C_6H_{12}O_6$)	Mixture of anatase and brookite, 5.83 nm	Uniform black spots could also be seen, indicating that Ag exists uniformly.	Ag^0 detected	Methylene blue	97.82% in 180 min under visible light	94.20% in 180 min under visible light/4	[97]
Electrochemical	Single	TiO_2 nanopowder of 99.5%, 99.999% purity Ag plates	Anatase, 15.6 nm	Spherical shape and exhibit a slight degree of agglomeration	Ag^0 and Ti^{4+} detected, N/A, N/A	Orange II dye	98.50% after 2 h under UV irradiation	N/A	[90]
		TiO_2 nanotube arrays, Ag nanoparticles	Anatase, 13.5 nm	Ag nanoparticles distributed uniformly in the inner structure of TiO_2 nanotube arrays	Ag^0 and Ag^+ detected, N/A, N/A	Methyl orange	70.00% after 2.5 h under Xenon lamp	~64.00% after 2.5 h under Xenon lamp/3	[214]
Electrospinning	Single	Titanium tetraisopropoxide (Ti $(OiPr)_4$), diamminesilver(I), Ag $(NH_3)_2^+$	Anatase, N/A	Continuous fibrous structures	N/A	Rhodamine B	99.00% after 2 h under Xenon lamp	N/A	[118]
		Titanium isopropoxide, $AgNO_3$	Anatase, N/A	Increased roughness on the outer surfaces of nanofibers as the concentration of Ag increases	N/A	Methylene blue	90.50% under UV light	N/A	[215]
	Co-doping (F)	TiO_2, $AgNO_3$, Poly(vinylidene difluoride), PVDF	Mixture of anatase and rutile, N/A	Pristine PVDF membrane & TiO_2/PVDF has round structures and did not contain any ribbon or spider web features, TiO_2 and $AgNO_3$ have a ribbon-like structure	Ag^0 detected, N/A, N/A	Methylene blue	92.30% in 210 min under UV light	N/A	[216]

(*continued on next page*)

Table 2 (*continued*)

Methods	Doping	Precursors	Characteristics of Products			Pollutant	Photocatalytic performance	Efficiency/ Regeneration (cycles)	Ref.
			Crystal structure (XRD), crystallite size	Morphology (SEM/FESEM)	XPS, TEM, EDX				
Solvothermal	Single	Tetrabutyl titanate (97%), $AgNO_3$	Anatase, N/A	TiO_2 nanoflakes, Ag nanorods	Ag^0 and Ti^{4+} detected, 0.20 nm, presence of Ag, Ti and O detected	Methyl orange	98.20% after 50 min under visible light irradiation	~98.20%/5	[145]
		Tetraisopropyl titanate, $AgNO_3$	Anatase, NA	Spherical, rough, and covered with bulges or nanoplates	Ag^0 and Ti^{4+} detected, N/A, 3.02 atomic% of Ag, 26.51 atomic% of Ti, 70.47 atomic% of O	Methyl orange	N/A	N/A	[146]
		Tetrabutyl titanate (TBT), $AgNO_3$	Anatase, N/A	Ag encapsulated on TiO_2 nanofibers	Ag^0 and Ti^{4+} detected, N/A, N/A	Rhodamine B	100.00% degradation after 140 min under UV–vis irradiation	~100.00%/3	[152]
		TiO_2, $AgNO_3$	Anatase, N/A	Regularly arranged tubular structure, Ag nanoparticles are visible on the top as well as inside the tubes	N/A	Methyl orange	89.10% within 70 min under UV light irradiation and 73.20% after 140 min under visible light	83.10%~/5 under UV light	[217]
	Co-doping (F)	Tetrabutyl titanate (TBT), $AgNO_3$, hydrogen fluoride, HF	Anatase, N/A	Truncated octahedral shapes	Ag^0 detected, N/A	Methylene blue	Almost complete degradation in 75 min under UV irradiation	N/A	[182]
Sol-gel	Single	Titanium tetra n-butoxide Ti $(C_4H_9O)_4$, $AgNO_3$	Anatase and brookite, 16 nm	Spherical shape	N/A, 11 nm, N/A	Methylene blue	100% degradation in 35 min under UV light	N/A	[218]
	Single	Titanium (IV) isopropoxide, $(Ti[OCH(CH_3)_2]_4)$	Anatase and brookite, N/A	Porous structure	Ag^0 detected, N/A, N/A	Mercury (II)	67% reduction of Hg^{2+} to Hg^0 in 180 min under UV irradiation	N/A	[155]
	Single	Titanium tetra isopropoxide (TTIP), silver acetate	Anatase, ~9 nm	Dense agglomerates of spherical nanoparticles	Ag^0, Ti^{3+} and Ti^{4+} detected, 4 nm - 6 nm, N/A	Methyl orange	98.9% within 60 min under UV, and 99.3% within 80 min under solar irradiation	~99.3%/3 under solar irradiation	[53]
	Co-doping (C)	Tetrabutyl titanate (TBT), $AgNO_3$, Activated carbon nanotubes (CNT)	Anatase, N/A	Silver-nanoparticles deposited onto the surface of CNT uniformly	Ag^0 and Ti^{4+} detected, N/A, N/A	Methylene blue	80.80% under visible light in 3 h and 99.20% under UV light in 40 min	Slight decrease in efficiency/5	[219]
	Co-doping (S)	Titanium tetra isopropoxide, $AgNO_3$, Thiourea (CH_4N_2S)	Anatase, 11.9 nm	Primary NPs relatively uniformed in size and approximately spherical and many pores were formed with their agglomeration	N/A, N/A, 36.35 atomic% of Ti, 57.67 atomic% of O, 4.44 atomic % of Ag and 2.53 atomic% of S	Methylene blue	~100% degradation under visible light	~90% under visible light/5	[171]
	Co-doping (Cu)	Titanium butoxide, $AgNO_3$	Anatase, 19.32 nm	Spherical particles	Ag^+, Cu^{2+} and Ti^{4+} detected, 39 nm – 60 nm	Methylene blue	43.95% under visible light and 59.64% under UV light	N/A	[208]
	Co-doping (Nb)	Titanium butoxide, $AgNO_3$, Niobium chloride	Mixture of anatase and rutile, 3.1 nm	Regular nanoparticle shape and uniform particle size	Ag^0, Ti^{3+}, $Nb5^+$ detected, 29 nm to 46 nm, O content 27.28%	Methylene blue	95.6% in 2 h under visible light	N/A	[220]
		Titanium isopropoxide, $AgNO_3$, cobalt (II) chloride hexahydrate	Rutile, 18.193 nm		N/A, N/A, 39.03 wt% of Ti, 49.25 wt	2,4-dichlorophenol	60.00% in 180 min under visible light		[19]

(*continued on next page*)

Table 2 (*continued*)

Methods	Doping	Precursors	Characteristics of Products			Pollutant	Photocatalytic performance	Efficiency/ Regeneration (cycles)	Ref.
			Crystal structure (XRD), crystallite size	Morphology (SEM/FESEM)	XPS, TEM, EDX				
	Co-doping (Co)	($CoCl_2$•$_6H_2O$)		Light agglomeration of the samples	% of O, 1.60 wt% of Co, 5.34 wt% of C, 3.44 wt% of Ag, and 1.34 wt% of Cl			~60.00% in 180 min under visible light/3	
Wet impregnation	Single	Tetrabutyl titanate, $AgNO_3$	Anatase, N/A	Ag nanoparticles dispersed uniformly on the surface of TiO_2 nanopillars	N/A, 300.00 – 400.00 nm in diameter and 1.00–3.00 μm, N/A	2,4-dichlorophenol	Nearly 100.00% within 2 h under visible light	~100.00% within 2 h under visible light/10	[166]
		Mesoporous TiO_2, $AgNO_3$	Anatase, N/A	Ag uniformly dispersed on highly crystalline pore walls of mesoporous TiO_2	Ag^0 detected, N/A, N/A	Phenol	Nearly 80.00% in 2 h under visible light	~80.00% in 2 h under visible light/5	[154]
	Co-doping (Fe)	Tetraisopropylorthotitanat (TIP), $AgNO_3$, Fe_3O_4	Anatase, 5.93 nm	TiO_2 nanoparticles attach to multi-walled carbon nanotubes surface and exhibit the decoration surface of TiO_2 and MWCNTs by metallic silver nanoparticles	N/A, N/A, 10.63 wt% of C, 60.52 wt% of Ti, 20.39 wt % of O, 6.67 wt% of Fe and 1.79 wt% of Ag	2,4-dichlorophenol	75% after 180 min irradiation under visible light	~75% after 180 min irradiation under visible light/4	[221]
Photoinduced deposition	Co-doping (S)	$TiCl_4$, $AgNO_3$, H_2SO_4	Anatase, 21.79 nm	Particles appear to be highly spherical	S^{6+}, Ti^{4+}, Ag^0 detected, 38.53 nm, 53.31 atomic% of O, 46.33 atomic% of Ti, 0.19 atomic% of S, and 0.18% atomic% of Ag	Congo red	78.00% under UV light and 80.00% under solar light	78.00% (±0–2%) under UV light and 80.00% (±0–2%) under solar light/3	[174]

*N/A – Not available.

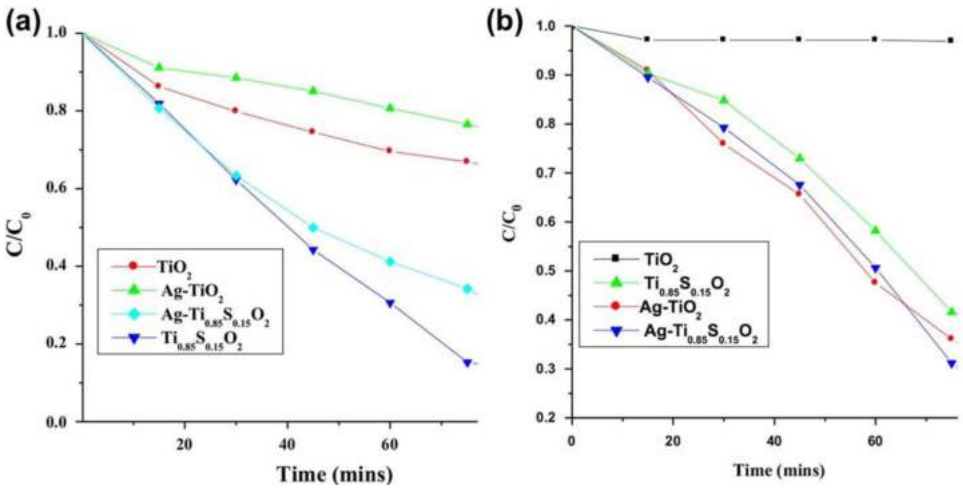

Fig. 9. C/C_0 versus time plot for the photocatalytic degradation of congo red dye under (a) UV light irradiation and (b) solar light illumination using TiO_2, Ag/TiO_2, $Ag/TiO_{0.85}S_{0.15}O_2$ and $TiO_{0.85}S_{0.15}O_2$ [174].

co-dopants in TiO_2 photocatalyst led to 94% of diclofenac degradation after 240 min.

Mesoporous TiO_2 was co-doped with Ag and Ce via two different methods [co-impregnation (Co-IMP) and co-deposition precipitation with urea (Co-DPU)] and investigated for the degradation of ibuprofen under visible light irradiation. The degradation rate of Ce-Ag/TiO_2 (Co-IMP) was 65.5% while Ce-Ag/TiO_2 (Co-DPU) produced 85.0% degradation after 4 h of irradiation which both were higher than that of Ag/TiO_2 and Ce/TiO_2 [188]. The synergistic effects of Ce and Ag on mesoporous TiO_2 were able to significantly reduce the TiO_2 band gap which improve the visible light absorption [188]. A similar finding was also observed in the synthesis of Tin, Sn-doped CeO_2 with Ag nanoparticles. The photocatalytic properties of the nanocomposite were also improved due to a decrease in the bandgap energy as a result of the localized surface plasmon resonance (LSPR) effect from Ag [191].

Lanthanide elements such as La have been employed as co-dopants as well, and it produces complexes with coordination bonding between the f orbitals and lone electron pairs of various Lewis bases [192]. The study decorated TiO_2 nanoparticles with La and Ag elements for the degradation of MO under visible light. Results showed that the addition of La element adheres to degradation products to the surface of TiO_2/La nanoparticles and the presence of Ag transfers the photogenerated electrons on the surface, which efficiently separates the photogenerated electrons and carries the photocatalyst.

Besides that, niobium, Nb was also reported to greatly improve the Lewis acidity of the nanocomposite's surface and the O—H group attached to the catalyst becomes more polarised, this, in turn, increased the adsorption of cationic dye and improves photocatalytic degradation [193,194]. Similar to Wang et al. [192], $Ag/TiO_2/Nb_2O_5$ prepared by Goswami et al. [195] also showed that electron-rich silver nanocluster, TiO_2, and niobium oxide forms a ternary junction, and due to the presence of ternary junction, which strongly electron-hole pair recombination. Therefore, it ascertains that the addition of Ag and Nb_2O_5 helps in the degradation as $Ag/TiO_2/Nb_2O_5$ exhibited nearly complete degradation of malachite green [195].

Co metal is one of the most promising transition metal co-dopants in the case of Ag/TiO_2 [19]. Co^{2+} doping can shift the light absorption of anatase TiO_2 to the visible range, enhancing photocatalytic activities in both the UV as well as visible regions [196]. The photonic efficiency of rutile-type TiO_2 is improved by co-doping with Co and Ag, decorated on multi-walled carbon nanotubes (C) which make electron transfer easier (Fig. 10a), act as electron reservoirs, and decrease charge carriers recombination [19]. The $Ag/Co\text{-}TiO_2/C$ nanocomposite was synthesized using the sol-gel technique and its efficiency was observed by the degradation of 2,4-dichlorophenol (2,4-DCP) solution under visible light. It was observed from (a) that $Ag/Co/TiO_2/C$ photocatalysts possessed a higher surface area in comparison to compared with $Co/TiO_2/C$ and this is attributed to the presence of Ag on $Ag/Co/\text{-}TiO_2/C$. The undoped TiO_2 and $Ag/Co\text{-}TiO_2/C$ photocatalyst resulted in 27% and 60% degradation of 2,4-DCP, respectively after 180 min under visible light irradiation (Fig.10b), in which the improved performance of $Ag/Co\text{-}TiO_2/C$ photocatalyst was attributed to the effect of the SPR of Ag/AgCl, and the presence of Co and C which increases the photonic efficiency and change surface properties to reach sensitivity to visible light [19].

Besides Co and Ce, Fe^{3+} can be also easily incorporated onto TiO_2 crystal lattice and results in a decrease in the recombination of photoelectrons [197–199]. Shojaie et al. [164] fabricated $Fe\text{-}TiO_2$-Ag nanocomposite via the ultrasonic-assisted hydrothermal method and successfully removed 97.12% of 4-chlorophenol 4-CP under UV irradiation and its performance remained consistent up to 5 cycles with an efficiency of 94% owing to the presence of Fe_3O_4 in the photocatalyst. Ahamad et al. [200] fabricated chitosan-based magnetic nanocomposite for tetracycline adsorption and observed the highest adsorption capacity of 215.31 mg/g and 203.41 mg/g of adsorption capacity after 6 cycles. Similarly, the presence of Fe_3O_4 promotes excellent adsorption of the nanocomposite with its superparamagnetic properties that help in the separation and recovering the adsorbent using an external magnet. Literature has shown separation or recovery of adsorbent from aqueous solution is a crucial aspect and it is usually expensive and requires time [201]. By using Fe_3O_4, lower separation cost and shorter time of recovering the adsorbent can be obtained as Fe_3O_4 can be removed easily by using an external magnetic field.

Besides that, Shojaie et al. [164] also showed that doping of Fe and Ag decreases the crystal size of TiO_2 (Degussa P25). Similar findings were observed by other literature, whereby the growth of grains is restrained during the hydrothermal treatment [202]. Sun et al. [12] prepared a heterogeneous structure of Ag/Fe_2O_3 and synthesized $Ag/TiO_2/Fe_2O_3$ via mild hydrolysis hydrothermal method for the degradation of various dyes. The study showed that the photocatalytic activity of $Ag/TiO_2/Fe_2O_3$ is greater than pure TiO_2 and Ag/Fe_2O_3. Literature has reported that the addition of Ag or Fe_2O_3 into TiO_2 enhanced the separation and transfer of photoinduced carriers [203, 204]. In light of the high mineralization degree of dyes and good stability of the composite during a long-term photocatalytic process, it is proven that $Ag/TiO_2/Fe_2O_3$ is a promising photocatalyst in practical applications [12]. Fig. 11 shows the synthesis process of introducing Fe into the Ag-doped photocatalyst system.

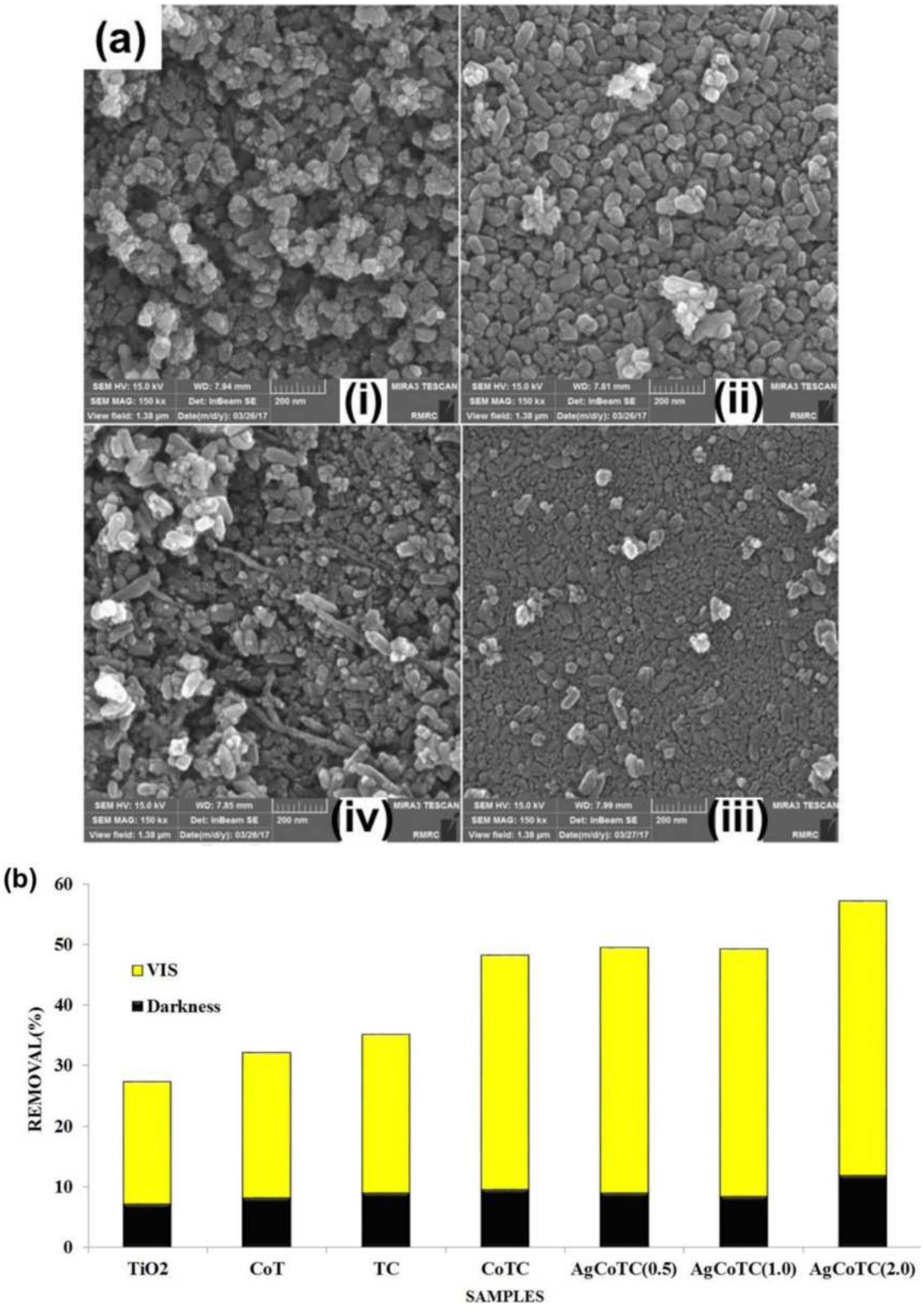

Fig. 10. (a) SEM images of (i) TiO_2, (ii) Co/TiO_2, (iii) $Co/TiO_2/C$ and (iv) $Ag/Co/TiO_2/C$; (b) photodegradation of 2,4-DCP under visible light using all evaluated photocatalysts [19].

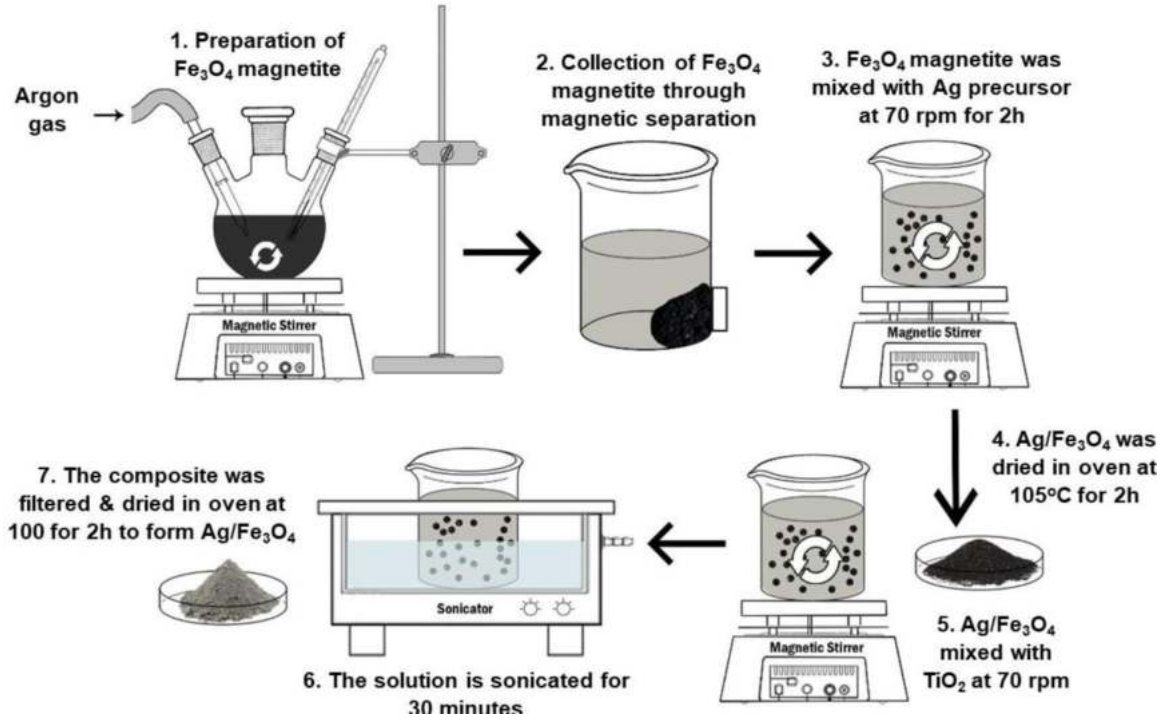

Fig. 11. Schematic illustration of the synthesis of Fe co-doped Ag/TiO_2 photocatalyst.

Literature has also shown that the coupling of TiO_2 with CuO which has a lower bandgap contributed to improved photocatalytic activity [205,206]. The benefits of combining these two compounds include greater optical and photocatalytic properties as compared to single oxide [207]. Ahmadi and Kaleji [208] synthesized the mesoporous structure of TiO_2/CuO composite doped with Ag for the degradation of methylene blue. The addition of CuO to TiO_2 reduced the bandgap energy (3.39 eV to 3.30 eV) and the SPR effect of Cu particles enhance the optical absorption and excites more electron-hole [187]. In addition, it was found that doping of Ag caused the particle size to become finer and increasing the calcination temperature from 550 °C to 650 °C also resulted in increased surface area (52.1 m^2/g to 35.5 m^2/g) of TiO_2/-CuO/Ag, TCA. The highest degradation under visible light was 43.95% by TCA-550 °C and 59.64% under UV light using samples calcined at 650 °C [208]. Behnajady and Eskandarloo [209] also reported similar findings, where the photocatalytic activity of the Ag/TiO_2/Cu catalyst calcined at 550 °C reached a maximum value. As the calcination temperature increased from 350 °C to 550 °C, the crystallite size increased from 11 nm to 20 nm. It was reported that the stability of the anatase phase increased upon co-doping of Ag and Cu to TiO_2 as co-doping suppressed the anatase transformation to rutile phase [209].

Hernández-Gordillo and González [71] fabricated Ag/TiO_2/Cu with 96.0% of anatase phase even after annealing for 4 h at 600 °C, indicating that presence of Cu^{2+} ions delayed the growth process. The synthesized Ag/TiO_2/Cu showed irregular shape and agglomeration of TiO_2 (Fig. 12a) and the presence of Ag nanoparticles on the surface of TiO_2 crystallite has been confirmed by the TEM image (Fig. 12b). Similar to the previous findings, the specific surface area of the Ag/TiO_2/Cu annealed at 400 °C was reported to decrease from 97.83 m^2/g and to 31.44 m^2/g at 600 °C, resulting in the highest intrinsic kinetic value (F) in the degradation of 4-nitrophenol under UV light irradiation [210]. The photoreduction of 4-nitrophenol by TiO_2 alone, TiO_2/Cu-400 °C and Ag/TiO_2/Cu-400 °C is illustrated in Fig. 12c and the comparison rate of 4-nitrophenol for all the evaluated photocatalysts can be observed in Fig. 12d. In addition, it was also revealed that Ag/TiO_2/Cu showed reduced crystallite size (14 nm to 46 nm) when the composite was annealed at 400 °C and 600 °C, indicating that annealing temperature affects the crystallite size of the composite. The previous finding has also shown that increasing Cu dopant in Ag-doped TiO_2–Cu^0 resulted in a decrease in crystallite size and lattice [211].

5. Modification of Ag-doped TiO_2 with green materials

Challenges of Ag/TiO_2 photocatalyst include difficulties in separation after undergoing treatment, issues with leaching or releasing out the particle in continuous flow systems, low stability where it can be easily oxidized, and aggregation, especially at high concentrations [222]. Incomplete recovery of TiO_2 nanoparticles from reaction solution may contribute to secondary pollution. The difficulties in retrieving the photocatalyst after photocatalysis could be associated with the non-uniformity of the pore, low surface area, and formation of colloidal suspension with water [212,223]. Thus far, this problem has been tackled through the addition of supporting matrices such as activated carbon, glass, zeolites, silica, and polymers [212,224,225].

However, green materials may be a better option owing to their copious and sustainable source in nature and can be a renewable chemical source to substitute petroleum-based materials [226,227]. Green materials can be utilized in the fabrication of Ag/TiO_2-based nanomaterials by sustainable pathways. The term “green chemistry” was introduced in 1991 to eliminate or decrease the usage of hazardous substances with the ultimate aim to reduce the negative impact on the environment and humans [228]. The advantages of utilizing green chemistry included reduced/prevention of the formation of unnecessary wastes as most of the solvents used can be recycled, lower hazard chemical reactions, degradable reaction products, and are non-persisting in the environment [228].

Natural materials have properties such as low polar surface, large surface area, and high adsorption capacity for non-polar organic pollutants, making them viable candidates for TiO_2 support [229]. Various green materials such as biomass, biopolymers, plants, animals, and microorganisms have been investigated as support materials to improve the stability and recyclability of TiO_2-based composites. There have been approaches to further improve the properties of Ag/TiO_2 photocatalyst using green materials namely plant and ceramic based materials

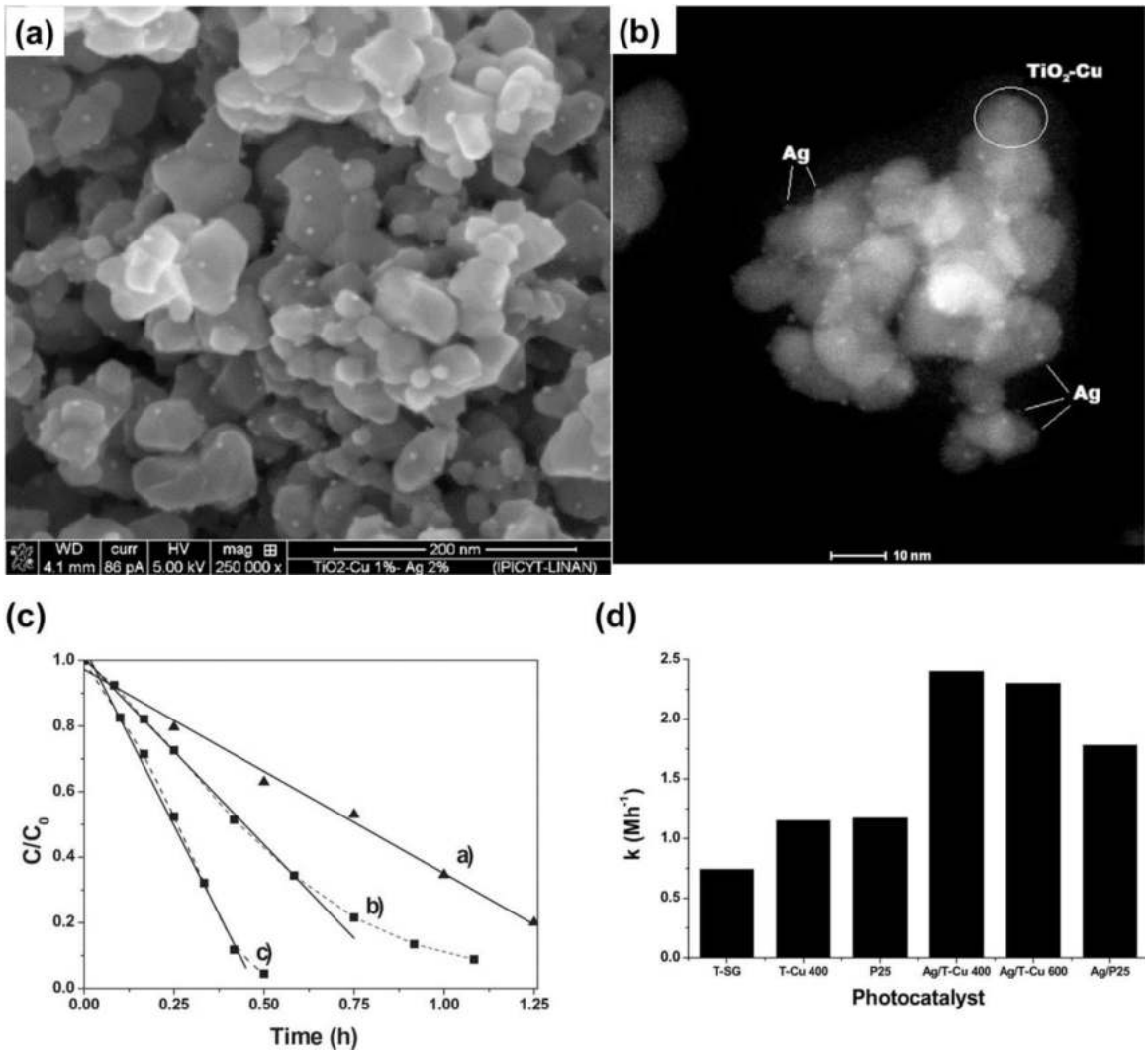

Fig. 12. (a) SEM image of Ag/TiO_2/Cu/−400 °C photocatalyst and (b) TEM image of Ag/TiO_2/Cu/−400 °C photocatalyst (c) C/C_0 versus time plot for the photoreduction of 4-nitrophenol and (d) comparison with: (i) TiO_2; (ii) TiO_2/Cu-400 °C; and (iii) Ag/TiO_2/Cu/−400 °C photocatalyst [210].

and ILs. Green materials that can be introduced as a modifier for Ag/TiO_2 photocatalyst are illustrated in Fig. 13. The commonly used plant-based materials for support include materials such as cellulose, derivatives of cellulose (e.g. cellulose acetate), chitosan, and alginate. Chitosan acts as a stabilizer and reductant in the preparation of Ag nanoparticles on the TiO_2 surface [61].

Besides that, ceramic-based materials such as clay, kaolin, and bentonite have been also incorporated into Ag/TiO_2 photocatalyst. Clay minerals that exist in nature such as alumina, silica, or ferrous materials have been known to be effective absorbents and oxidants in the applications of water purification [230,231]. There are many types of natural clays such as bentonite, kaolinite, and montmorillonite (MT) which have been explored among the naturally abundant adsorbents as an alternative for cheaper but functional adsorbents for the degradation of textile dyes from wastewater [57,232].

The clay materials act as support for TiO_2 by providing high surface area, porosity, and increased surface active sites [233,234]. This prevents TiO_2 from agglomerating, which contributes to a higher percentage of reusability as it may be recovered from the treatment process [235]. The key role of MT behavior lies within the interlayer cations, where it can be easily exchangeable by other cationic molecules via electrostatic interaction or ion exchange [236]. As such, MT has been greatly utilized in the removal of cationic contaminants like trace metals from water and wastewater. Tailoring some modifications on MT helps in increasing its removal of anionic and non-ionic contaminants [237,238]. For instance, a study on the intercalation of Ag/TiO_2 into or on the bentonite interlayers also showed a higher surface area and porosity of the composite which contributed to excellent biological as well as electrochemical properties [239]. However, studies on nanocomposites prepared via ceramic materials, polymer, and carbon are still considered at an early stage and require more studies for further investigation [240].

Besides plant-based and ceramic-based supports, ILs, known as "green solvents" have been used as a replacement for organic solvents because of their remarkable properties [241]. Green chemistry focuses on reducing the number of organic solvents and/or reagents that are toxic within the analysis procedure, to reduce the consumption of energy and wastes, and the reusability of the solvents [242,243]. According to Vekariya [244], the correlation between ILs and green chemistry is understandably linked to the solvent properties of ILs. Some of the properties of ILs include a good solvent for a wide range of inorganic and organic materials, can be highly polar due to the presence of poorly coordinating ions, immiscible with many organic solvents, and can provide a nonaqueous, polar alternative for two-phase systems [244].

ILs are made up of organic cations and strongly induced anions and their properties are manifested through the synergistic effect of the anions and cations [245]. The properties of ILs include high polarity and

Fig. 13. Modifications of Ag/TiO_2 composites using green materials.

thermal stability, high chemical stability and have been greatly used as a solvent, template, and additive [246]. Other excellent properties of ILs includes nonvolatility, thermo-oxidative stability, high ionic conductivity, a wide range of electrochemical window, miscible with organic compounds, and does not react with air and water [247]. The properties of ILs can be altered and the alterations in the structure of ILs may change the polar and dispersive interactions of ILs [248]. These interactions that also exist between IL and TiO_2, influence the surface structure of TiO_2 and result in the change of TiO_2 photoreactivity [249]. The addition of ILs on Ag/TiO_2 also increases the surface area of the photocatalyst and enhances the photocatalytic degradation of pollutants [250] as well as improves its stability and reusability [251]. Table 3 summarizes the applications of some support materials with Ag/TiO_2.

5.1. Addition of plant-based supports

5.1.1. Cellulose-derivatives

Cellulose is a linear polysaccharide with inimitable properties such as biodegradability, chemical stability, high mechanical strength, and has a huge amount of chemical derivations which has drawn much attention [265]. One of the derivatives, cellulose acetate, CA is a biopolymer with excellent biocompatibility, ability to biodegrade, high mechanical strength, hydrophilic, and excellent moisture management properties which resulted in its wide applications in biomedical fields such as tissue engineering and antibacterial applications [255]. CA nanofibers embedded with Ag/TiO_2 nanoparticles showed excellent growth inhibition of Escherichia coli (E. coli) and Staphylococcus aureus (S. aureus) demonstrating good antibacterial properties [62].

Lately, Yang and Luo [266] investigated the role of cellulose-derived carbon beads as a charge carrier for Ag/TiO_2. The study pointed out that the hollow network structure of cellulose-derived carbon beads facilitated the immobilization and, contributed to the uniform distribution of Ag/TiO_2 particles as well as provided more reactive sites [266]. The synthesized catalyst, Ag/TiO_2/C showed stability and reusability up to five cycles during the degradation of ceftriaxone sodium under simulated sunlight. The Ag/TiO_2/C with Ag (0.5 mol%) doping yielded a much higher degradation efficiency (91.92%) of ceftriaxone sodium compared to pure TiO_2 (54.56%) and TiO_2/C (62.7%) after 270 min [266].

Similarly, a study on cellulose nanofibers (CNFs) fabricated with TiO_2 and Ag for the degradation of methylene blue was also able to maintain its efficiency for up to 5 cycles under UV irradiation [267]. It was notable that TiO_2/CNF showed reduced mechanical properties after irradiation as compared to TiO_2–CNF/Ag. The presence of Ag nanoclusters on the matrix allowed the diversion of electrons from the matrix and distribution of the electrons evenly on the MB surface, hence reducing the damage to CNF and extending its recyclability [267]. The Ag nanoclusters were formed on the film surface by UV photoreduction and this process might still be ongoing each time the films were irradiated. The reduction process aided in preserving the CNF matrix and contributed to the extra mechanical strength of the photocatalyst [268, 269].

Despite the lack of studies on the modification of Ag/TiO_2 with cellulose acetate as support for pollutant degradation, studies on TiO_2/cellulose or TiO_2/cellulose acetate alone showed promising properties. For instance, past studies showed that TiO_2/microcrystalline cellulose activated under visible light actively degraded nearly 90% of methylene blue in 4 h [270]. Similarly, TiO_2/cellulose composite films prepared by Zeng et al. [271] showed the regenerated cellulose films contributed to cavities and affinity for the creation and the immobilization of TiO_2 nanoparticles in the cellulose matrix through electrostatic and

Table 3
Applications of support materials with Ag/TiO_2.

Type of Support		Applications
Plant-based support	Cellulose-derived carbon beads, Cellulose/cellulose acetate nanofibers/films/papers/membranes	Microbial [252], water disinfection [253], food packaging [254], tissue engineering [255], lithium ion battery separator [256]
	Chitosan films	Antibacterial and wastewater treatment [60,63], wound dressing [257], food technology [258], antifouling and anti-algal material for marine water systems [259]
Ceramic-based support	Clay, Bentonite	Pollutant removal [260,261] photomineralization of harmful volatile organic compounds [65], drinking water treatment [262], cotton fabric industry [263]
Ionic liquids		Modifiers [251], solvent templates and precursors for photocatalytic treatments [264]

hydrogen-bonding interactions. The study reported high degradation of phenol under weak UV irradiation and the composite films revealed remarkable photostability without a decline in the photocatalytic activity after three cycles of degradation [271].

In addition, the first reported electrospun TiO_2/cellulose acetate composite prepared by Gebru and Das [272] has a smooth morphological structure with relatively high surface area and porosity and was applied for the removal of Pb (II) and Cu (II) ions in wastewater. The highest removal efficiencies of Pb (II) and Cu (II) ions obtained using TiO_2/cellulose acetate with the highest specific surface area (48.47 m^2/g) were 99.7% and 98.9%, respectively [272]. The addition of TiO_2 nanoparticles improved the porosity of cellulose acetate adsorbent as the specific surface area without the addition of TiO_2 was only 30.2 m^2/g whereas upon the addition of TiO_2 it increased to 48.5 m^2/g. Furthermore, introducing TiO_2 within the adsorbent matrix forms a uniform network and it was also believed that the presence of TiO_2 produced spaces within the matrix by separating the cellulose acetate chains, which then contributed to better porosity of the adsorbent (Fig. 14b).

As observed from the FTIR spectra (Fig. 14c), a broad peak at 3490 cm^{-1} and 1750 cm^{-1} indicates the presence of surface hydroxyl stretching and vibrations of OH bonds on the surfaces of the TiO_2 nanoparticles [273]. The broadband observed at 3456 cm^{-1} in pure cellulose acetate is due to OH stretching as a result of strong hydrogen bond of intermolecular and intra-molecular kinds while the band of 2900 cm^{-1} is a result of C—H stretching [274]. The formation of new broadband observed around 600–800 cm^{-1} is attributed to the presence of the Ti-O-Ti band [275]. The FTIR spectra indicate TiO_2 nanoparticles have been successfully incorporated into the cellulose acetate matrix. Meanwhile, the adsorption efficiencies of Pb(II) and Cu(II) ions by TiO_2/cellulose acetate adsorbent showed that the adsorbent could be repeatedly used as it did not show any significant decline in the adsorption efficiencies (Fig. 14d). This indicates that TiO_2/cellulose acetate adsorbent possessed high elimination capacity of Pb(II) and Cu (II) ions. The addition of cellulose with TiO_2 enhances the photodegradation of not only dye pollutants, but heavy metals as well. The application of cellulose in the preparation of material offers a versatile alternative and greener pathway in the fabrication of inexpensive but also highly efficient nanosorbents for the removal of heavy metals from water [276].

5.1.2. Chitosan

The problems associated with the powder forms of TiO_2 in its applications for water treatment such as difficulties in the recovery of the powder and aggregation can be controlled by combining TiO_2 with polymers like chitosan [63]. Likewise, Ag nanoparticles also tend to aggregate due to their high surface energy and causing a reduction in catalytic efficiency, making them unsuitable for large-scale applications in heterogeneous catalysis [277]. Strong metal chelation capability formed during the immobilization of Ag on chitosan could control and address the separation and recovery issues associated with Ag [278].

Literature has shown that chitosan can be an effective biosorbent for the removal of Ag^+ ions and other heavy metals from wastewater [278]. Chitosan is also known as a cationic biopolymer, which is also a deacetylated product of chitin [279,280]. It is a linear bio-based polymer composed of D-glucosamine and N-acetylglucosamine consisting of functional groups such as amine and hydroxyl [63] which play a crucial role in chelation and adsorption [281].

A facile synthesis method was applied for the preparation of Ag nanoparticles on chitosan-TiO_2 composites as recyclable nanocatalysts for the reduction of 4-nitrophenol, 4-NPh [282]. Ag NPs were assembled on the active imprinted sites of chitosan-TiO_2 composite. Complete reduction of 4-NPh to 4-aminophenol, 4-APh by $NaBH_4$ using Ag/TiO_2-chitosan was achieved within 120 min under UV irradiation. One striking observation was in the absence of Ag in the catalyst, chitosan/TiO_2 did not reduce 4-NPh, contrary to complete reduction when

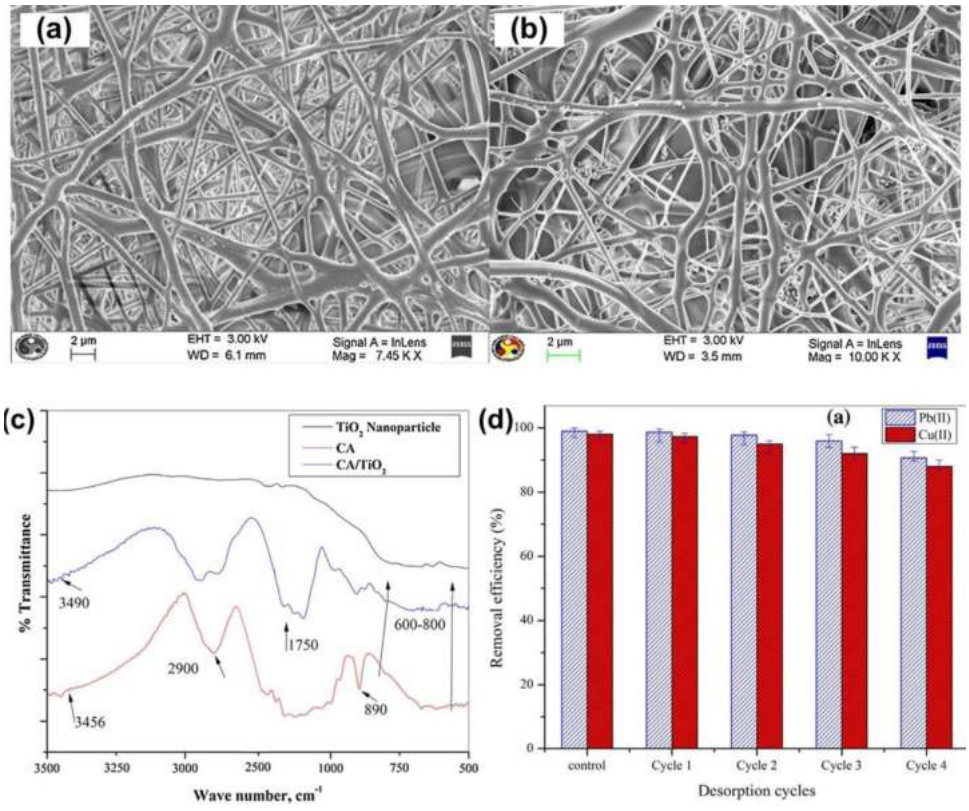

Fig. 14. (a) FESEM image of pure electrospun cellulose acetate, (b) FESEM image of electrospun cellulose acetate, CA with TiO_2 (2.5 wt%), (c) FTIR spectra of CA, TiO_2 and TiO_2/CA, (d) adsorption-desorption cycles of TiO_2/CA on Pb (II) and Cu (II) ions [272].

Ag was present in the catalyst. The incorporation of Ag nanoparticles into the composite system aids the movement of the electrons to the conduction band of TiO_2 due to the excitation of the silver plasmon [63]. The Ag/TiO_2-chitosan also remained stable when it was reused up to 5 times [282].

The synergistic effect of the core-shell composite prepared using quartered chitosan (QCS) hollow microspheres for the growth of TiO_2/N and Ag nanoparticles through electrostatic self-assembly and photodeposition has been reported by Wang et al. [283]. The presence of C_2–NH_2, C_3–OH, and C_6–OH functional groups in chitosan allows it to participate in cross-linking with quaternary ammonium and provides a larger specific surface area for the next assembly of TiO_2, and when TiO_2 is doped with N of the quartered chitosan, the Ag nanoparticles bridges between the complexes for charge transfer. The study revealed that under visible light irradiation, degradation of sodium dodecylbenzene sulfonate reached up to 96.4% within 180 min as a result of highly active sites and adsorption sites on the surface of the quartered chitosan, SPR, and photothermal effect of Ag and effective electron holes separation in N-TiO_2 [283]. Geetha et al. [284] have also prepared Ag/TiO_2 with chitosan and polyethylene glycol, PEG where both chitosan and PEG were employed as reducing agents for the degradation of methylene blue under sunlight. The hydroxyl groups present in the polymers acted as the coordination ligand to TiO_2 ions for homogeneous dispersion of Ag^+ ions with TiO_2 and thus restraining the aggregation of Ag/TiO_2 nanocomposites. In contrast with the previous findings, Geetha et al. [284] revealed that Ag/TiO_2 photocatalyst showed higher degradation of methylene blue under sunlight irradiation as compared to Ag/TiO_2 stabilised with the polymers.

Although previous studies have shown that the immobilizing Ag/TiO_2 on chitosan efficiently enhanced pollutants degradation, some reports have also unveiled the drawbacks of using chitosan in the composite system. For instance, chitosan experiences inadequate mechanical properties, drastic shrinking in its shape, deformation after drying, soluble in acidic conditions, compressibility at high operating pressure, shields and blocks UV irradiation with degradation of textiles and leather [285]. Despite its potential as a biosorbent, chitosan is chemically unstable due to its abundant free amines with a pKa value of approximately 6.5 which can be protonated culminating in hydrosolubility under acidic conditions [286].

5.1.3. Alginate

Alginate, Alg is a nontoxic and anionic compound that naturally exists in bacteria and brown algae [120]. It is a type of linear polymer consisting of 1–4 linked β-D-mannuronic acid (M) and α-L-guloronic acid (G) [287]. The abundance of hydroxyl and carboxyl groups in this macromolecule makes it suitably connected to other compounds as well [120]. As a result, alginate has been greatly employed in aerogel applications and it is inexpensive, renewable, and environmentally friendly. TiO_2 nanoparticles are uniformly dispersed in an alginate matrix to produce a sodium alginate composite aerogel with underwater oleophobic and photocatalytic properties, with methyl orange UV light degradation reaching 97.6% after 150 min [288]. The study also reported its photocatalytic efficiency under the intensive light irradiation remained even after it was reused 6 times, indicating good recyclability and stability [288]. A similar study was also conducted on alginate gel to remove phenanthrene, a type of polycyclic aromatic hydrocarbons, from an aqueous matrix by entrapping crude enzymes on alginate beads combined with TiO_2/C/Ag coated fiberglass. The removal of phenanthrene reported was as high as 94.3 ± 2.0%, in which the pollutant accumulated onto the surface of the alginate beads and coated fiberglass while Ag acted as an active reducing agent in the TiO_2/C/Ag film [289]. Both the alginate gel and TiO_2/C/Ag film were shown to be efficient in removing phenanthrene in the study.

To the best of our knowledge, there is no report on Ag-doped TiO_2 with alginate alone for photocatalytic degradation. However, several studies immobilize Ag nanoparticles on alginate as a recoverable catalyst in the presence of magnetic nanoparticles. The synthesis of Ag on alginate magnetic halloysite combined with magnetic nanoparticles, Fe_3O_4 was applied for the reduction of nitro aromatic compound, nitrobenzene, into target amine derivatives [120]. The nanocatalyst showed good efficacy in reducing nitrobenzene to amine compounds in a short reaction time by using $NaBH_4$ as a mild hydride donor. In addition, the nanocatalyst was able to be recycled up to six times without depletion of its catalytic activity, and the presence of Fe_3O_4 in the system also allows easy separation of the nanocatalyst from the reaction mixture when an external magnetic field is applied [120].

A study by Hasan et al. [290] revealed that incorporating polyacrylonitrile, PAN along with Alg/Ag caused charge carriers to be generated and electron-hole pairs transportation as solar irradiation on the surface of PAN/Alg/Ag leads to excitation of SPR and contributed to higher photocatalytic activities as compared to PAN alone. In addition, XRD data revealed a reduced crystal size of Alg/Ag from 20 nm to 8 nm upon the polymerization of PAN, which formed a well-dispersed, semi-crystalline solid with adequate functional density. Furthermore, the synergistic adsorption properties of PAN and Alg/Ag whereby the copolymerization on the surface caused more charge density to SPR contributed to greater degradation of DNP molecules [291] as Ag helped in preventing the recombination of electron and hole pairs within the photocatalytic process [290].

5.2. Addition of ceramic-based support

5.2.1. Clay

There are various types of nanohybrid materials but among the most promising ones is known to be photocatalyst with the addition of clay because of the wide availability of natural clay minerals and its properties which allows the inclusion of different types of functional molecules on the surface. The extraordinary physicochemical properties of clay included high surface reactivity, high adsorption capability, cation exchange capacity, swelling property, and biocompatibility [292,293]. The structure of clay minerals is made up of tetrahedral (T) silica sheet and an octahedral sheet of either (O) gibbsite ($Al(OH)_3$) or brucite ($Mg(OH)_2$) stacked upon each other [235]. Studies have found that the photocatalytic activity of TiO_2 nanoparticles has been greatly improved with the inclusion of clays. This is due to the physiochemical properties of clays such as high surface area, good adsorption capability, porosity as well as the presence of active sites on TiO_2/clay nanocomposites [294].

Abdel Karim et al. [236] fabricated CA-based membranes incorporated with α-aminophosphonate modified clay and Ag/TiO_2 NPs to obtain a membrane with inherent hydrophilic and high flux. The addition of CA in the membrane induced the formation of the hydrogen-bonded network between CA and the α-aminophosphonate modified clay, which not only improves its mechanical stability but also its performance in terms of flux and trace metal removals [236]. The presence of C–P, $P = O$, and NH_2 bonds in the modified clay plays a great advantage as literature [295] has shown that the C-P bond is very stable due to its high energy and conveys high hydrolytic as well as thermal stability properties while hydrophilic functional groups like $P = O$ and NH_2 improves the hydrophilicity and presence of Ag/TiO_2 act as a bridge for creation of further active sites in the clay of the membrane [236]. Thus, improving the properties of the membrane for the removal of various classes of pollutants.

Recently, Kaur et al. [261] fabricated Ag/Fe/TiO_2 composite by combining fly ash (FA), foundry sand (FS), and clay on Ag-doped TiO_2 whereby this functionalized composite was able to initiate both photo-Fenton and photocatalysis effects under solar light for the degradation and mineralization of ciprofloxacin (CIP). FS and FA have been utilized to provide iron in inducing photo-Fenton for the degradation of non-biodegradable pollutants [260] while natural bentonite clay is applied as inert support to increase the durability [296]. In this study, bentonite clay was used for binding purposes [261]. It was

reported that the degradation and durability were maintained even after 30 cycles. A similar finding was also observed in TiO_2 films synthesized on ceramisite substrates (a mixture of clay, coal gangue, and quicklime) for the degradation of hydroquinone and the removal under UV irradiation which remained at about 84% after 40 cycles indicating the ceramisite substrate possessed good regeneration ability [297].

In the case of Ag/TiO_2/bentonite composite, mixing of Ti and Ag precursors with bentonite first initiated the ion exchange process in a water medium (Na^+ ions were replaced by Ag^0, Ti^{4+} ions), then conversion to intermediate Ag/$Ti(OH)_4$ and finally conversion to Ag/TiO_2 via calcination (Eq (5)) [239]. The Ag/TiO_2 intercalation process that took place within the layers of Na-bentonite was confirmed by various characterization analyses performed. Fig. 15 shows the schematic structure of Ag/TiO_2 nanoparticles intercalation into bentonite clay. The surface area of Ag/TiO_2/bentonite composite possessed a much larger surface area of 80 m^2/g than that of the pristine bentonite with only 40 m^2/g indicating efficient transfer of electrons and ions.

$$AgNO_3 + Ti(OC_3H_7)_4 + Na - \text{bent clay} + nH_2O \; Ag/TiO_2/\text{bent} + Na{+}NO_3^- + (C_3H_7O)_4^- + nH_2O \quad (5)$$

The photocatalytic study was done on TiO_2-coated Tunisian clay (TiO_2-clay) prepared via the common impregnation method completely removed reactive blue 19 (RB 19) after 20 min [64]. The study showed that the specific surface area of TiO_2 increased from 36.6 m^2/g to 116.7 m^2/g with the addition of clay and the total pore volume increased from 0.13 to 0.26 cm^3/g, indicating the successful pillaring of TiO_2 species onto the silicate layers of the clay and hence increased surface area greatly improves the photocatalytic activity of TiO_2-clay [64].

5.2.2. Kaolin

Clay materials such as kaolinite have recently shown great importance mostly because of their abundance, inexpensive, and can be obtained easily. Metal ions have been added or eliminated via kaolinite clay through ion exchange and adsorption mechanisms respectively [298]. Kaolinite is made up of a two-layered structure that consists of silicon-oxygen tetrahedral sheet linked to alumina octahedral sheet through the hydrogen bonding of -Al-O-H—O-Si-, making it known as a 1:1 dioctahedral clay mineral [232]. Kaolinite clays have abundant hydroxyl groups on the surface which allows them to be modified easily and also have the potential in anchoring TiO_2 nanoparticles to improve their photocatalytic activities [299].

A study on the degradation of antibiotics using clays/TiO_2 found that kaolinite nanoflakes with TiO_2 degraded 98% after 60 min, owing to two-dimensional morphology, stronger surface absorptivity, greater loading efficiency, smaller particle size, and intimate interfacial contact [299]. In another study, kaolinite ceramic adsorbents in Ag/TiO_2 were used for photodegradation and removal of Cu^{2+} and Co^{2+} from high concentration aqueous solution. The data from the study was fitted better by the Langmuir isotherm than by Freundlich models, and the study concluded that photocatalytic kaolinite clay adsorbents showed enhanced removal of Cu^{2+} and Co^{2+} ions from relatively high concentrated aqueous solutions [298].

5.2.3. Bentonite

One of the impure montmorillonite (2:1 clay with two tetrahedral silica sheets and one octahedral gibbsite sheet) is bentonite which contains quartz, cristobalite, feldspar, pyrites, carbonates, mica, and illite exists naturally in the Earth's crust [300]. TiO_2-Ag/bentonite composite displayed high reactivity in both chlorobenzene and benzaldehyde degradation under visible and UV light because of its high exciton lifetime (2.60 ns) that successfully induced highly oxidative superoxide and hydroxyl radicals which improves photocatalytic activity [235]. The Fermi level position of Ag, which is near to conduction band of TiO_2, increased the transfer of electrons between AgNPs and TiO_2, contributing to the high exciton lifetime in Ag/TiO_2/bentonite [235].

Bentonite was used as a support in Ag/TiO_2/bentonite, in which Ag/TiO_2 was added to a bentonite suspension for the degradation of phenol [301]. The addition of bentonite to the system as support influenced the phase transformation of TiO_2 and the distribution of Ag, as there were no peaks observed in the XRD pattern for the rutile phase and Ag (0) on Ag-TiO_2/bentonite [301]. This observation showed that the material dispersion on bentonite support prevents the anatase-rutile phase transformation, leading to improved photocatalytic activity under solar radiation up to 31.14%. The significantly reduced TiO_2 particle size also resulted in increased surface area and active centres for the photocatalyst to degrade the pollutant [239,301]. Compared to TiO_2/-bentonite, Ag/TiO_2/bentonite exhibited higher photocatalytic activity under solar irradiation. The findings of this study corroborated with the one observed by Mishra et al. [65] for the mineralization of chlorobenzene under UV irradiation.

The TiO_2/bentonite nanocomposite was found to be highly porous with a uniform pore size distribution, with a surface area of 97 m^2/g and a pore volume of 0.3315 cm^3/g, whereas the addition of Ag (3 wt%) reduced the surface area and pore volume to 69 m^2/g and 0.2007 cm^3/g, respectively. It was concluded that bentonite plays an important role in terms of stability, porosity and hydrophobicity, which allows it to be separable and improves the recyclability of the nanocomposite making it a promising photocatalyst for a larger scale of air or water treatment processes [65,239].

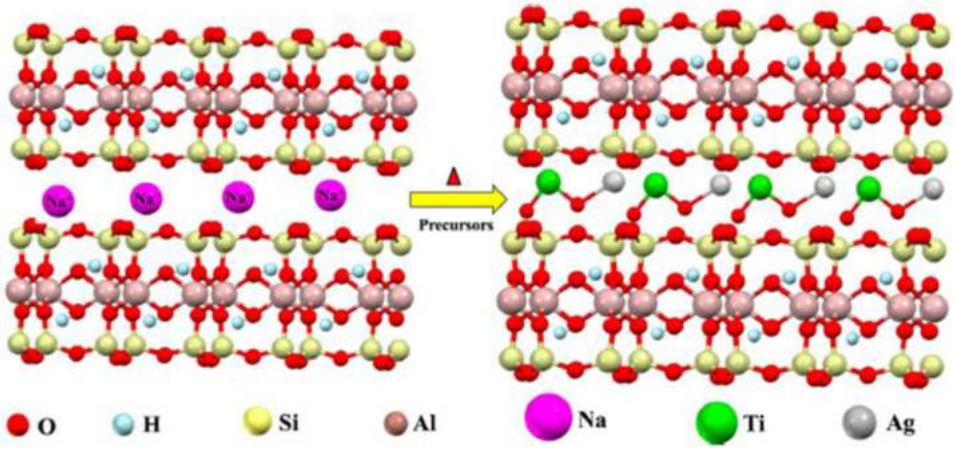

Fig. 15. Schematic illustration of the reaction mechanism of Ag/TiO_2 nanoparticles and their intercalation processes into the bentonite clay [239].

5.3. Addition of ionic liquid

The addition of IL in the synthesis of the photocatalysts affects the catalyst formation through electrostatic action, viscosity, steric hindrance, and amphiphilicity, altering the morphology and structure of the product [302–304]. The first study to demonstrate the stabilizing effect of room temperature ILs on metal particle size control on nanocomposite was done by Zhang and Chen [305] whereby a one-pot method was used to synthesize Ag/TiO_2 nanocomposite powders. It was found that the IL, 1-butyl-3-methylimidazolium hexafluorophosphate ([bmim]PF_6) plays an indispensable role in controlling the cluster size of Ag and allowing good dispersion on the TiO_2 surface, leading to its superior bactericidal [305]. Since then, many studies have been conducted and confirmed the capacity of ILs in controlling the properties of TiO_2-based photocatalysts [306–308].

The fabrication of mesostructured CeO_2-TiO_2 nanoparticles via (1-hexadecane3-methylimidazolium bromide, [C_{16}MIM]Br), an IL as a template for the hydrothermal synthesis produced nanoparticles with large specific surface area (198.3 m^2/g) and uniform particle sizes (15 ± 5 nm) [309]. Likewise, Ag-doped SiO_2-TiO_2 aerogels synthesized using 1-butyl-3-methylimidazolium bromide, (Bmim)Br as a co-solvent and aging agent, also showed a high surface area of the materials (385.2 m^2/g), and microcrystalline anatase of 6.2 nm. Photocatalytic degradation of 99.7% was achieved for the reactive blue solution and the study also revealed that increasing the concentration of Ag enhanced the photocatalytic abilities of aerogels [250].

Yoo et al. [209] prepared Ag/TiO_2 using various ILs (1-Butyl-3-methylimidazolium trifluoromethanesulfonate, [Bmim][CF_3SO_3], 1-Methyl-3-octyl-imidazolium-hexafluorophosphate, [Omim][PF_6], 1-Butyl-3-methylimidazolium hexafluorophosphate, [Bmim][PF_6], 1-Methyl-3-octyl-imidazolium-tetrafluoroborate [Omim][BF_4], 1-Hexyl-3-methyl-imidazolium-hexafluorophosphate, [Hmim][PF_6], 1-Butyl-3-methylimi dazolium tetrafluoroborate [Bmim][BF_4], 1-Ethyl-3-methylimidazolium tetrafluoroborate, [Emim][BF_4] and 1-Hexyl-3-methyl-imidazolium-tetrafluoroborate, [Hmim][BF_4]) as a support to improve its photocatalytic activity and the samples were examined by cyclic voltammetry to investigate the optimum sample in water electrolysis. It was revealed that the surface area of TiO_2-IL/Ag (147 m^2/g) samples was 3 times greater higher than that of Ag/TiO_2 samples and Ag/TiO_2 with BCF_3-IL possessed flowerlike structure provided the highest electrocatalytic activity as compared to Ag/TiO_2 with BPF_6-IL which has rough aggregation of spherical particles [264].

Similarly, Paszkiewicz et al. [303] have also studied the effect of ionic liquid structure (chain length in the imidazolium cation) and its concentration in the solvothermal synthesis of TiO_2 particles. Unlike Yoo et al. [264], the study used only 2 types of ILs (1-butyl-3-methylimidazolium chloride [BMIM][Cl] and 1-decyl-3-methylimidazolium chloride [DMIM][Cl]) to investigate the effect of IL on the morphology and photoactivity of TiO_2 particles. The highest photocatalytic degradation of phenol (85%) was achieved using TiO_2 particles synthesized in the presence of [BMIM][Cl] while 84.2% degradation took place in the presence of [DMIM][Cl] [303].

Lin et al. [251] indicated that the highest Rhodamine B removal of 72.97% was attained with Ag/TiO_2 synthesized with 1-butyl-3-methylimidazolium chloride, (Bmim)Cl compared to TiO_2, TiO_2/(BMIM)Cl, Ag^+/TiO_2 which only resulted in 2.71%, 41.11%, and 49.11%, respectively. The improved photocatalytic performance of Ag/TiO_2(BMIM)Cl is associated with the formation of AgCl, which is known as a photosensitive material [310]. In addition, it was reported that the addition of (BMIM)Cl contributed to high stability and recyclability of the photocatalyst as there was no significant loss of activity after 5 cycles of usage [251]. The stability of the photocatalyst is attributed to the addition of 1-butyl-3-methylimidazole group as ligands, which is further supported by its high absolute value of Zeta potential (18.57 mV) in comparison to TiO_2 (−11.41 mV) and Ag^+/TiO_2 (−6.60 mV) [251].

Mohaghegh et al. [66] synthesized TiO_2 nanoparticles via sol-gel method using room temperature IL (RTIL), 2-hydroxylethylammonium formate as a template solvent and coupled with a visible light semiconductor photocatalyst, sensitive silver carbonate, Ag_2CO_3. The findings from this study showed that pure TiO_2 has only a rutile phase while the addition of IL resulted in the anatase phase. The increase in the anatase phase in TiO_2-IL is attributed not only to the addition of IL but also to the presence of Ag_2CO_3 addition which retarded the transformation of anatase to rutile phase. The study showed an average crystal size of 122 nm, 85 nm, and 50 nm for pure TiO_2, TiO_2/RTIL, and Ag_2CO_3/TiO_2/RTIL, respectively. It is observed that the particle sizes reduced in TiO_2/RTIL and Ag_2CO_3/TiO_2/RTIL as compared to pure TiO_2 and Ag_2CO_3/TiO_2/RTIL showed a much higher photodegradation rate of the pollutant as opposed to pure TiO_2 (Fig. 16a-c). Due to its high polarity, RTIL has low interface tensions which contributed to a high nucleation rate and forms particles of a smaller size that aids in the formation of the anatase phase [66]. The addition of ionic liquid increases the weight fraction of anatase in the TiO_2 sample from 30.8% to 42.2–60.5%, as a result, the photocatalyst has a higher specific surface area and contributed to higher photocatalytic activity (Fig. 16d-f) as compared to pure TiO_2 [311].

Past studies have shown that ILs are good at mediating the formation of specific structures such as forming mesoporous structures, forming structures with high crystallinity and thermal stability as well as producing particles with homogeneous size distribution [312]. However, some literature has also mentioned that ILs are considered green chemicals but certain types can be highly hazardous [313]. There are several issues pertaining to the application of ILs. For instance, the life cycle assessments of ILs showed that ILs are toxic and nonbiodegradable [312]. Furthermore, the chemicals and solvents involved in the preparation of ILs may also contribute negative impacts on human beings and the environment [314]. Therefore, these limitations should be taken into account when choosing and applying ILs in the preparation of TiO_2-based photocatalysts. Table 4 summarizes the effect of green supports on the performance of Ag/TiO_2 photocatalysts.

6. Conclusion and outlook

TiO_2 has been extensively studied as a promising photocatalyst in a variety of applications particularly photocatalytic-mediated processes for wastewater treatment. Despite their widespread utilization, TiO_2 nanoparticles suffer from a few major drawbacks which include inefficient exploitation of visible light, low adsorption capacity for hydrophobic contaminants, low quantum efficiency, aggregation, and difficulty to be recovered after water treatment. TiO_2 surface modification via doping (e.g. metal doping, non-metal doping, and co-doping) has been opted to enhance its absorption in visible light and overcome the aforementioned limitations. Various types of metals, non-metals, and co-dopants have been investigated as potential modifiers for TiO_2. The outcomes in term of morphology and optical and electronic properties greatly varies with the type of dopant(s) applied in the modification. Ag has been regarded as an excellent dopant of TiO_2 photocatalyst due to its striking advantages when compared to other noble metals. Studies have concluded that Ag-doped TiO_2 successfully results in excellent charge transfer and the synergistic effect between SPR and metal oxides or heterojunctions enhances the resulting materials' visible light responsiveness. Various synthetic methods such as sol-gel, hydrothermal, solvothermal, wet impregnation, and photoreduction have been applied for the preparation of Ag-doped TiO_2 photocatalysts. The choice of methods dictates the photocatalytic performance and physicochemical properties (e.g. crystallinity, morphology, and surface area) of the engineered Ag-doped TiO_2-based photocatalysts. However, one open question still exists is that there was no consensus on the most effective synthetic method for Ag-doped TiO_2. Green materials namely plant and ceramic-based materials and ILs have been emerging as interesting candidates for the modification of Ag/TiO_2 as they are sustainable and renewable materials and reduce the unwanted release of

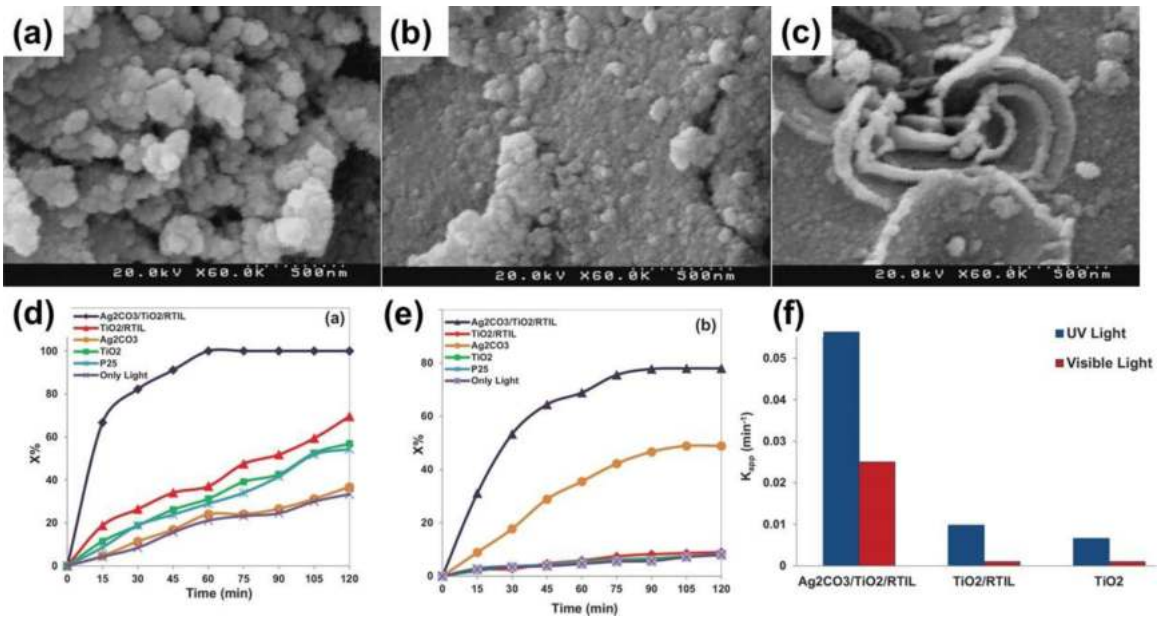

Fig. 16. SEM images of (a) pure TiO_2, (b) TiO_2/RTIL and (c) Ag_2CO_3/TiO_2/RTIL, Photocatalytic degradation of AB92 by all evaluated samples under (d) UV light irradiation; (e) visible light irradiation; (f) Degradation rate constant of synthesized photocatalysts under UV and visible light irradiation [66].

Table 4
Effect of addition of green supports on the performance of Ag/TiO_2 photocatalysts.

Type of Support	Advantage(s) of support	Pollutant	Efficiency	Efficiency/ Regeneration (cycles)	Reference
Plant-based support					
Cellulose-derived carbon beads	1. Facilitates immobilization and uniform distribution of TiO_2/Ag particles 2. Provides more reactive sites	Ceftriaxone sodium	91.92% in 270 min under sunlight	73.96%/5	[266]
Cellulose nanofibers	1. Provides extra mechanical strength	Methylene blue	75% in 60 min under sunlight	<75%/4	[267]
Chitosan	1. Preparation of TiO_2/Ag without any additional chemicals (such as $NaBH_4$) or irradiation. 2. Provides even distribution of Ag on TiO_2	Salicylic acid	20% more than pure TiO_2 under solar irradiation	N/A	[61]
			83% after 8 h under visible light		[63]
		o-toluidine	> 95% after 2 h under visible light	80%/3	
		4-aminomethyl benzoic acid	68% after 8 h under visible light	N/A	
		4-nitrophenol	100% after 120 min	~100%/5	[282]
		Sodium dodecylbenzene sulfonate	96.4% within 180 min under visible light	~96.4%/4	[283]
Ceramic-based support					
Clay	1. Improves mechanical stability	Ciprofloxacin	94.4% in 60 min under solar irradiation	81.6%/30	[261]
Bentonite Ionic Liquid	1. Bentonite support prevents anatase-rutile phase transformation	Methylene blue	98.94% in 60 min	N/A	[301]
Bmim(Cl)	1. Bmim(Cl) provides chloride ions for the formation of photosensitive AgCl2. Provides ligand (1-butyl-3-methylimidazole group) which stabilizes the photocatalyst	Rhodamine B	72.97% in 120 min under visible light	~70%/5	[251]
Bmim(Br)	1. Forms microcrystalline anatase photocatalyst	Methyl orange	Up to 99.7%	>85%/6	[288]

chemical wastes into the environment. Plant-based supports were more mechanically stable, while chitosan and alginate are both excellent biosorbents. However, inconsistent and mixed results were obtained from several studies that demonstrated few limitations in utilizing chitosan as support such as poor mechanical properties, deformations after application, and instability in acidic solutions. Ceramic materials, on the other hand, displayed excellent characteristics and properties as substrates for immobilization of TiO_2, as well as producing high levels of pollutant degradation. Nevertheless, the most robust, versatile, and essential support for Ag-doped TiO_2 remains a debate.

The insights gained from this review have led to the identification of gaps that can be further explored by future studies. Firstly, studies on Ag/TiO_2 with cellulose acetate, alginate, and ceramic materials are still scarce, similar to the exploration of ILs in the preparation of Ag/TiO_2 and Ag/TiO_2-based photocatalysts. Although studies have shown that the separation of TiO_2 particles from wastewater treatment can be achieved through immobilization of TiO_2 onto support structures and the addition of green materials, numerous other aspects such as

mechanism or mechanistic pathways and knowledge or understanding of structural bonding of Ag/TiO_2 with green materials are still lacking. Secondly, studies should also explore the mineralization ability and degradation products formed from the synthesized Ag/TiO_2 photocatalysts to ensure that no toxic products are formed during the photocatalytic treatment besides focusing on the photocatalytic efficiency of the Ag/TiO_2 photocatalysts or composites. Another trend observed is the inclination of researchers towards determining the performance efficiency of the synthesized photocatalysts using a single pollutant rather than mixed pollutants and real wastewaters. A greater emphasis on the performance efficiency of fabricated photocatalysts on mixed pollutants (e.g. dyes, heavy metals, pharmaceuticals, and pesticides) and real wastewaters (e.g. industrial, textiles, agriculture, and pharmaceutical) would be more environmentally relevant and could shed more light on their effectiveness and establish the links between their properties and photocatalytic ability. Further studies into the choice or types of ILs would be worthwhile, as the surface morphology of TiO_2 is known to be affected by the types of IL used. The photocatalytic activity of the materials is also influenced by their morphological structure. Therefore, not only it is important to choose a suitable IL candidate which can enhance the photocatalytic activity of Ag/TiO_2, but it is also important to weigh the effects of ILs possess on the environment particularly in satisfying green chemistry synthesis methods as some of the ILs can be toxic to the environment. Another main challenge lies in finding suitable green materials support that will enhance the capabilities of Ag/TiO_2 photocatalyst while maintaining its properties towards green chemistry and remaining economically viable. Overall, we believe that Ag-doped TiO_2, with unique optical, electrical, and structural properties, is a promising material in practical applications associated with wastewater treatment and other energy and environmental remediation. Nevertheless, further experimental works and efforts are required to better understand the nature of Ag-doped TiO_2 as well as to exploit the efficient approach to improve its performance.

Data availability

Data supporting this study are not applicable as this is a review paper.

CRediT authorship contribution statement

Devagi Kanakaraju: Conceptualization, Writing – original draft, Resources, Supervision, Writing – review & editing. **Feniellia Diwvya anak Kutiang:** Writing – original draft, Resources. **Ying Chin Lim:** Writing – review & editing. **Pei Sean Goh:** Writing – review & editing.

Declaration of Competing Interest

The authors declare that they have no competing interests.

Acknowledgement

This study was supported by the Ministry of Higher Education, Malaysia under the Fundamental Research Grant Scheme [FRGS/1/2019/STG07/UNIMAS/02/3]. The authors would like to express their gratitude to Mohamad Azim Bin Abdullah for his assistance in the creation of some of the figures.

References

[1] D. Kanakaraju, B.D. Glass, M. Oelgemöller, Advanced oxidation process-mediated removal of pharmaceuticals from water: a review, J. Environ. Manag. 219 (2018) 189–207, https://doi.org/10.1016/j.jenvman.2018.04.103.

[2] P.M. Rajaitha, S. Hajra, M. Sahu, K. Mistewicz, B. Toroń, R. Abolhassani, S. Panda, Y. Mishra, H.J. Kim, Unraveling highly efficient nanomaterial photocatalyst for pollutant removal: a comprehensive review and future progress, Mater. Today Chem. 23 (2022), 100692, https://doi.org/10.1016/j.mtchem.2021.100692.

[3] K. Sharma, V. Dutta, S. Sharma, P. Raizada, A. Hosseini-Bandegharaei, P. Thakur, P. Singh, Recent advances in enhanced photocatalytic activity of bismuth oxyhalides for efficient photocatalysis of organic pollutants in water: a review, J. Ind. Eng. Chem 78 (2019) 1–20, https://doi.org/10.1016/j.jiec.2019.06.022.

[4] V. Dutta, S. Sharma, P. Raizada, A. Hosseini-Bandegharaei, V.K. Gupta, P. Singh, Review on augmentation in photocatalytic activity of $CoFe_2O_4$ via heterojunction formation for photocatalysis of organic pollutants in water, J. Saudi Chem. Soc. 23 (8) (2019) 1119–1136, https://doi.org/10.1016/j.jscs.2019.07.003.

[5] K.P. Gopinath, N.V. Madhav, A. Krishnan, R. Malolan, G. Rangarajan, Present applications of titanium dioxide for the photocatalytic removal of pollutants from water: a review, J. Environ. Manag. 270 (2020), 110906, https://doi.org/10.1016/j.jenvman.2020.110906.

[6] V. Ferreira, P. Santos, C. Silva, M. Azenha, Latest developments on TiO_2-based photocatalysis: a special focus on selectivity and hollowness for enhanced photonic efficiency, Appl. Catal. A 623 (2021), 118243, https://doi.org/10.1016/j.apcata.2021.118243.

[7] Z. Li, Y. Fang, X. Zhan, S. Xu, Facile preparation of squarylium dye sensitized TiO_2 nanoparticles and their enhanced visible-light photocatalytic activity, J. Alloys Compd. 564 (2013) 138–142, https://doi.org/10.1016/j.jallcom.2013.03.002.

[8] T.A. Gad-Allah, S. Kato, S. Satokawa, T. Kojima, Role of core diameter and silica content in photocatalytic activity of $TiO_2/SiO_2/Fe_3O_4$ composite, Solid State Sci. 9 (8) (2007) 737–743, https://doi.org/10.1016/j.solidstatesciences.2007.05.012.

[9] Y. Tang, G. Zhang, C. Liu, S. Luo, X. Xu, L. Chen, B. Wang, Magnetic TiO_2-graphene composite as a high-performance and recyclable platform for efficient photocatalytic removal of herbicides from water, J. Hazard. Mater. 252 (2013) 115–122, https://doi.org/10.1016/j.jhazmat.2013.02.053.

[10] X. Zhao, G. Zhang, Z. Zhang, TiO_2-based catalysts for photocatalytic reduction of aqueous oxyanions: state-of-the-art and future prospects, Environ. Int. 136 (2020), 105453, https://doi.org/10.1016/j.envint.2019.105453.

[11] M. Al-Mamun, S. Kader, M. Islam, M. Khan, Photocatalytic activity improvement and application of UV-TiO_2 photocatalysis in textile wastewater treatment: a review, J. Environ. Chem. Eng. 7 (5) (2019), 103248, https://doi.org/10.1016/j.jece.2019.103248.

[12] Q. Sun, P. Hou, S. Wu, L. Yu, L. Dong, The enhanced photocatalytic activity of Ag-Fe_2O_3-TiO_2 performed in Z-scheme route associated with localized surface plasmon resonance effect, Colloids Surf. A 628 (2021), 127304, https://doi.org/10.1016/j.colsurfa.2021.127304.

[13] K. Xu, Z. Liu, S. Qi, Z. Yin, S. Deng, M. Zhang, Z. Sun, The quaternary system of Ag_2S/ZnS co-modified ZnO/TiO_2 nanotree arrays: excellent photocatalysis and photoelectrochemistry performance, Appl. Surf. Sci. 538 (2021), 148044, https://doi.org/10.1016/j.apsusc.2020.148044.

[14] Y. Zhao, L. Nie, H. Yang, K. Song, H. Hou, Tailored Fabrication of TiO_2/In_2O_3 Hybrid Mesoporous Nanofibers towards Enhanced Photocatalytic Performance, Colloids Surf. A 629 (2021), 127455, https://doi.org/10.1016/j.colsurfa.2021.127455.

[15] C.B. Anucha, I. Altin, E. Bacaksiz, V.N. Stathopoulos, Titanium Dioxide (TiO_2)-based photocatalyst materials activity enhancement for contaminants of emerging concern (CECs) degradation: in the light of modification strategies, Chem. Eng. J. Adv. 10 (2022), 100262, https://doi.org/10.1016/j.ceja.2022.100262.

[16] H. Bian, Z. Zhang, X. Xu, Y. Gao, T. Wang, Photocatalytic activity of Ag/ZnO/AgO/TiO_2 composite, Phys. E 124 (2020), 114236, https://doi.org/10.1016/j.physe.2020.114236.

[17] K. Li, C. Teng, S. Wang, Q. Min, Recent advances in TiO_2-based heterojunctions for photocatalytic CO_2 reduction with water oxidation: a review, Front. Chem. 9 (2021), https://doi.org/10.3389/fchem.2021.637501.

[18] M. Humayun, F. Raziq, A. Khan, W. Luo, Modification strategies of TiO_2 for potential applications in photocatalysis: a critical review, Green Chem. Lett. Rev. 11 (2) (2018) 86–102, https://doi.org/10.1080/17518253.2018.1440324.

[19] P. Monazzam, A.E. Pirbazari, Z. Khodaee, Enhancement of visible light photoactivity of rutile-type TiO_2 by deposition of silver onto Co-TiO_2/MWCNTs nanocomposite for degradation of 2, 4-dichlorophenol, Mater. Chem. Phys. 228 (2019) 263–271, https://doi.org/10.1016/j.matchemphys.2019.02.067.

[20] S. Goyal, Sonochemical decolourisation of reactive blue 21 and acid red 114 in the presence of TiO_2 and rare earths, Mater. Sci. Forum 734 (2013) 237–246, https://doi.org/10.4028/www.scientific.net/MSF.734.237.

[21] C.M. Teh, A.R. Mohamed, Roles of titanium dioxide and ion-doped titanium dioxide on photocatalytic degradation of organic pollutants (phenolic compounds and dyes) in aqueous solutions: a review, J. Alloys Compd. 509 (5) (2011) 1648–1660, https://doi.org/10.1016/j.jallcom.2010.10.181.

[22] O. Avciata, Y. Benli, S. Gorduk, O. Koyun, Ag doped TiO_2 nanoparticles prepared by hydrothermal method and coating of the nanoparticles on the ceramic pellets for photocatalytic study: surface properties and photoactivity, J. Eng. Technol. Appl. Sci. 1 (1) (2016) 34–50, https://doi.org/10.30931/jetas.281381.

[23] S.T. Kochuveedu, D.-.P. Kim, D.H. Kim, Surface-plasmon-induced visible light photocatalytic activity of TiO_2 nanospheres decorated by Au nanoparticles with controlled configuration, J. Phys. Chem. C 116 (3) (2012) 2500–2506, https://doi.org/10.1021/jp209520m.

[24] A. Amorós-Pérez, L. Cano-Casanova, A. Castillo-Deltell, M.Á. Lillo-Ródenas, M.d. C. Román-Martínez, TiO_2 Modification with transition metallic species (Cr, Co, Ni, and Cu) for photocatalytic abatement of acetic acid in liquid phase and propene in gas phase, Materials (Basel) 12 (1) (2019) 40, https://doi.org/10.3390/ma12010040.

[25] M.M. Nesfchi, A.E. Pirbazari, F.E.K. Saraei, F. Rojaee, F. Mahdavi, S.A. Fa'al Rastegar, Fabrication of plasmonic nanoparticles/cobalt doped TiO_2 nanosheets for degradation of tetracycline and modeling the process by artificial intelligence techniques, Mater. Sci. Semicond. Process. 122 (2021), 105465, https://doi.org/10.1016/j.mssp.2020.105465.

[26] P.S. Basavarajappa, S.B. Patil, N. Ganganagappa, K.R. Reddy, A.V. Raghu, C. V. Reddy, Recent progress in metal-doped TiO_2, non-metal doped/codoped TiO_2 and TiO_2 nanostructured hybrids for enhanced photocatalysis, Int. J. Hydrog. Energy 45 (13) (2020) 7764–7778, https://doi.org/10.1016/j.ijhydene.2019.07.241.

[27] D. Chen, Y. Cheng, N. Zhou, P. Chen, Y. Wang, K. Li, S. Huo, P. Cheng, P. Peng, R. Zhang, Photocatalytic degradation of organic pollutants using TiO_2-based photocatalysts: a review, J. Clean. Prod. 268 (2020), 121725, https://doi.org/10.1016/j.jclepro.2020.121725.

[28] R. Daghrir, P. Drogui, D. Robert, Modified TiO_2 for environmental photocatalytic applications: a review, Ind. Eng. Chem. Res. 52 (10) (2013) 3581–3599, https://doi.org/10.1021/ie303468t.

[29] C.H. Nguyen, C.-C. Fu, R.-S. Juang, Degradation of methylene blue and methyl orange by palladium-doped TiO_2 photocatalysis for water reuse: efficiency and degradation pathways, J. Clean. Prod. 202 (2018) 413–427, https://doi.org/10.1016/j.jclepro.2018.08.110.

[30] M.H. Engelhard, D.R. Baer, L. Chen, X-ray photoelectron spectroscopy data from lightly Pd doped TiO_2 anatase nanoparticles, Surf. Sci. Spectra. 27 (2) (2020), 024011, https://doi.org/10.1116/6.0000407.

[31] Y. Li, C. Zhang, H. He, J. Zhang, M. Chen, Influence of alkali metals on Pd/TiO_2 catalysts for catalytic oxidation of formaldehyde at room temperature, Catal. Sci. Technol. 6 (7) (2016) 2289–2295, https://doi.org/10.1039/C5CY01521A.

[32] M. Tsega, F. Dejene, Structural and optical properties of Ce-doped TiO_2 nanoparticles using the sol-gel process, ECS J. Solid State Sci. Technol. 5 (2) (2015) R17, https://doi.org/10.1149/2.0341602jss.

[33] G. Bahmanrokh, C. Cazorla, S.S. Mofarah, R. Shahmiri, Y. Yao, I. Ismail, W.-F. Chen, P. Koshy, C.C. Sorrell, Band gap engineering of Ce-doped anatase TiO_2 through solid solubility mechanisms and new defect equilibria formalism, Nanoscale 12 (8) (2020) 4916–4934, https://doi.org/10.1039/C9NR08604H.

[34] J.Y. Lee, J.-H. Choi, Sonochemical synthesis of Ce-doped TiO_2 nanostructure: a visible-light-driven photocatalyst for degradation of toluene and O-xylene, Materials 12 (8) (2019) 1265, https://doi.org/10.3390/ma12081265.

[35] A. Garzon-Roman, C. Zuñiga-Islas, E. Quiroga-González, Immobilization of doped TiO_2 nanostructures with Cu or In inside of macroporous silicon using the solvothermal method: morphological, structural, optical and functional properties, Ceram. Int. 46 (1) (2020) 1137–1147, https://doi.org/10.1016/j.ceramint.2019.09.082.

[36] A.M. Alotaibi, B.A. Williamson, S. Sathasivam, A. Kafizas, M. Alqahtani, C. Sotelo-Vazquez, J. Buckeridge, J. Wu, S.P. Nair, D.O. Scanlon, Enhanced photocatalytic and antibacterial ability of Cu-doped anatase TiO_2 thin films: theory and experiment, ACS Appl. Mater. Interfaces. 12 (13) (2020) 15348–15361, https://doi.org/10.1021/acsami.9b22056.

[37] C. Byrne, L. Moran, D. Hermosilla, N. Merayo, Á. Blanco, S. Rhatigan, S. Hinder, P. Ganguly, M. Nolan, S.C. Pillai, Effect of Cu doping on the anatase-to-rutile phase transition in TiO_2 photocatalysts: theory and experiments, Appl. Catal. B 246 (2019) 266–276, https://doi.org/10.1016/j.apcatb.2019.01.058.

[38] T.M.H. Nguyen, C.W. Bark, Synthesis of cobalt-doped TiO_2 based on metal–organic frameworks as an effective electron transport material in perovskite solar cells, ACS Omega 5 (5) (2020) 2280–2286, https://doi.org/10.1021/acsomega.9b03507.

[39] G. Ren, Z. Li, W. Wu, S. Han, C. Liu, Z. Li, M. Dong, W. Guo, Performance improvement of planar perovskite solar cells with cobalt-doped interface layer, Appl. Surf. Sci. 507 (2020), 145081, https://doi.org/10.1016/j.apsusc.2019.145081.

[40] W.-F. Chen, H. Chen, P. Koshy, A. Nakaruk, C.C. Sorrell, Effect of doping on the properties and photocatalytic performance of titania thin films on glass substrates: single-ion doping with Cobalt or Molybdenum, Mater. Chem. Phys. 205 (2018) 334–346, https://doi.org/10.1016/j.matchemphys.2017.11.021.

[41] G. Li, L. Yi, J. Wang, Y. Song, Hydrodynamic cavitation degradation of Rhodamine B assisted by Fe^{3+}-doped TiO_2: mechanisms, geometric and operation parameters, Ultrason. Sonochemistry. 60 (2020), 104806, https://doi.org/10.1016/j.ultsonch.2019.104806.

[42] G. Han, J.Y. Kim, K.-J. Kim, H. Lee, Y.-M. Kim, Controlling surface oxygen vacancies in Fe-doped TiO_2 anatase nanoparticles for superior photocatalytic activities, Appl. Surf. Sci. 507 (2020), 144916, https://doi.org/10.1016/j.apsusc.2019.144916.

[43] M. Valero-Romero, J. Santaclara, L. Oar-Arteta, L. Van Koppen, D. Osadchii, J. Gascon, F. Kapteijn, Photocatalytic properties of TiO_2 and Fe-doped TiO_2 prepared by metal organic framework-mediated synthesis, Chem. Eng. J. 360 (2019) 75–88, https://doi.org/10.1016/j.cej.2018.11.132.

[44] D. Hariharan, A.J. Christy, S. Pitchaiya, S. Sagadevan, P. Thangamuniyandi, U. Devan, L. Nehru, Green hydrothermal synthesis of gold and palladium doped titanium dioxide nanoparticles for multifunctional performance, J. Mater. Sci. 30 (13) (2019) 12812–12819, https://doi.org/10.1007/s10854-019-01647-9.

[45] J. Shi, X. Zhao, L. Zhang, X. Xue, Z. Guo, Y. Gao, S. Li, An oxidized magnetic Au single atom on doped TiO_2 (110) becomes a high performance CO oxidation catalyst due to the charge effect, J. Mater. Chem. A. 5 (36) (2017) 19316–19322, https://doi.org/10.1039/C7TA05483A.

[46] D. Tiwari, A. Tiwari, A. Shukla, D.-J. Kim, Y.-Y. Yoon, S.-M. Lee, Facile synthesis and characterization of nanocomposite Au0 (NPs)/titanium dioxide: photocatalytic degradation of Alizarin Yellow, J. Ind. Eng. Chem. 82 (2020) 153–163, https://doi.org/10.1016/j.jiec.2019.10.008.

[47] S.R. Seyedmonir, D.E. Strohmayer, G.L. Geoffroy, M.A. Vannice, H.W. Young, J. W. Linowski, Characterization of supported silver catalysts: I. Adsorption of O_2, H_2, N_2O, and the H_2-titration of adsorbed oxygen on well-dispersed Ag on TiO_2, J. Catal. 87 (2) (1984) 424–436, https://doi.org/10.1016/0021-9517(84)90202-1.

[48] K. Fujimoto, H. Kawai, H. Okamoto, Y. Hamakawa, Improvement in the efficiency of amorphous silicon solar cells utilizing the optical confinement effect by means of a TiO_2/Ag/SUS back-surface reflector, Sol. Cells 11 (4) (1984) 357–366, https://doi.org/10.1016/0379-6787(84)90099-1.

[49] T. Sakata, T. Kawai, K. Hashimoto, Heterogeneous photocatalytic reactions of organic acids and water. New reaction paths besides the photo-Kolbe reaction, J. Phys. Chem. 88 (11) (1984) 2344–2350, https://doi.org/10.1021/j150655a032.

[50] S.-J. Wang, X.-Y. Zhang, D. Su, Y.-F. Wang, C.-M. Qian, X.-R. Zhou, Y.-Z. Li, T. Zhang, Electrospinning Ag-TiO_2 nanorod-loaded air treatment filters and their applications in air purification, Molecules 25 (15) (2020) 3369, https://doi.org/10.3390/molecules25153369.

[51] L. Wang, J. Ali, C. Zhang, G. Mailhot, G. Pan, Simultaneously enhanced photocatalytic and antibacterial activities of TiO_2/Ag composite nanofibers for wastewater purification, J. Environ. Chem. Eng. 8 (1) (2020), 102104, https://doi.org/10.1016/j.jece.2017.12.057.

[52] S. Nazhirah, S. Ghoshal, R. Arifin, K. Hamzah, Effects of bimetallic nanoparticles Ag and TiO_2 embedment on tellurite zinc–silicate glass: self-cleaning characteristics, Surf. Interfaces 25 (2021), 101236, https://doi.org/10.1016/j.surfin.2021.101236.

[53] R. Saravanan, D. Manoj, J. Qin, M. Naushad, F. Gracia, A.F. Lee, M.M. Khan, M. Gracia-Pinilla, Mechanothermal synthesis of Ag/TiO_2 for photocatalytic methyl orange degradation and hydrogen production, Process Saf. Environ. Prot. 120 (2018) 339–347, https://doi.org/10.1016/j.psep.2018.09.015.

[54] H. Chakhtouna, H. Benzeid, N. Zari, R. Bouhfid, Recent progress on Ag/TiO_2 photocatalysts: photocatalytic and bactericidal behaviors, Environ. Sci. Pollut. Res. 28 (2021) 44638–44666, https://doi.org/10.1007/s11356-021-14996-y.

[55] S.N.A. Sulaiman, M.Z. Noh, N.N. Adnan, N. Bidin, S.N. Ab Razak, Effects of photocatalytic activity of metal and non-metal doped TiO_2 for hydrogen production enhancement-a review, J. Phys. 1027 (2018), 012006, https://doi.org/10.1088/1742-6596/1027/1/012006.

[56] T.H.M. Wint, M.F. Smith, N. Chanlek, F. Chen, T.Z. Oo, P. Songsiriritthigul, Physical origin of diminishing photocatalytic efficiency for recycled TiO_2 nanotubes and Ag-loaded TiO_2 nanotubes in organic aqueous solution, Catalysts 10 (7) (2020) 737, https://doi.org/10.3390/catal10070737.

[57] T.-S. Wu, K.-X. Wang, G.-D. Li, S.-Y. Sun, J. Sun, J.-S. Chen, Montmorillonite-supported Ag/TiO_2 nanoparticles: an efficient visible-light bacteria photodegradation material, ACS Appl. Mater. Interfaces. 2 (2) (2010) 544–550, https://doi.org/10.1021/am900743d.

[58] A.Y. Shan, T.I.M. Ghazi, S.A. Rashid, Immobilisation of titanium dioxide onto supporting materials in heterogeneous photocatalysis: a review, Appl. Catal. A 389 (1–2) (2010) 1–8, https://doi.org/10.1016/j.apcata.2010.08.053.

[59] X. Collard, A. Comès, C. Aprile, Mesoporous metal oxide/silica composites with photocatalytic activity and magnetic response, Catal. Today 241 (2015) 33–39, https://doi.org/10.1016/j.cattod.2014.03.057.

[60] E. Farshchi, S. Pirsa, L. Roufegarinejad, M. Alizadeh, M. Rezazad, Photocatalytic/biodegradable film based on carboxymethyl cellulose, modified by gelatin and TiO_2-Ag nanoparticles, Carbohydr. Polym. 216 (2019) 189–196, https://doi.org/10.1016/j.carbpol.2019.03.094.

[61] I. Grčić, A. Gajović, M. Plodinec, K. Šimunković, H. Ivanković, M.-G. Willinger, Enhanced visible-light driven photocatalytic activity of Ag@ TiO_2 photocatalyst prepared in chitosan matrix, Catalysts 10 (7) (2020) 763, https://doi.org/10.3390/catal10070763.

[62] A.W. Jatoi, I.S. Kim, Q.-Q. Ni, Cellulose acetate nanofibers embedded with AgNPs anchored TiO_2 nanoparticles for long term excellent antibacterial applications, Carbohydr. Polym. 207 (2019) 640–649, https://doi.org/10.1016/j.carbpol.2018.12.029.

[63] A. Jbeli, Z. Hamden, S. Bouattour, A. Ferraria, D. Conceição, L.V. Ferreira, M. Chehimi, A.B. do Rego, M.R. Vilar, S. Boufi, Chitosan-Ag-TiO_2 films: an effective photocatalyst under visible light, Carbohydr. Polym. 199 (2018) 31–40, https://doi.org/10.1016/j.carbpol.2018.06.122.

[64] H.B. Hadjltaief, M.E. Gálvez, M.B. Zina, P.Da Costa, TiO_2/clay as a heterogeneous catalyst in photocatalytic/photochemical oxidation of anionic reactive blue 19, Arab. J. Chem. 12 (7) (2019) 1454–1462, https://doi.org/10.1016/j.arabjc.2014.11.006.

[65] A. Mishra, A. Mehta, M. Sharma, S. Basu, Impact of Ag nanoparticles on photomineralization of chlorobenzene by TiO_2/bentonite nanocomposite, J. Environ. Chem. Eng. 5 (1) (2017) 644–651, https://doi.org/10.1016/j.jece.2016.12.042.

[66] N. Mohaghegh, B. Eshaghi, E. Rahimi, M. Gholami, Ag_2CO_3 sensitized TiO_2 nanoparticles prepared in ionic liquid medium: a new Ag_2CO_3/TiO_2/RTIL heterostructure with highly efficient photocatalytic activity, J. Mol. Catal. A 406 (2015) 152–158, https://doi.org/10.1016/j.molcata.2015.06.004.

[67] H. Dong, G. Chen, J. Sun, C. Li, Y. Yu, D. Chen, A novel high-efficiency visible-light sensitive Ag_2CO_3 photocatalyst with universal photodegradation performances: simple synthesis, reaction mechanism and first-principles study, Appl. Catal. B. 134 (2013) 46–54, https://doi.org/10.1016/j.apcatb.2012.12.041.

[68] Z. Wu, Y. Wang, L. Sun, Y. Mao, M. Wang, C. Lin, An ultrasound-assisted deposition of NiO nanoparticles on TiO_2 nanotube arrays for enhanced photocatalytic activity, J. Mater. Chem. A. 2 (22) (2014) 8223–8229, https://doi.org/10.1039/C4TA00850B.

[69] M. Ge, C. Cao, S. Li, S. Zhang, S. Deng, J. Huang, Q. Li, K. Zhang, S.S. Al-Deyab, Y. Lai, Enhanced photocatalytic performances of n-TiO_2 nanotubes by uniform creation of p–n heterojunctions with p-Bi_2O_3 quantum dots, Nanoscale 7 (27) (2015) 11552–11560, https://doi.org/10.1039/C5NR02468D.

[70] R. Candal, A. Martínez-de la Cruz, New visible-light active semiconductors. Photocatalytic Semiconductors, Springer, Cham, 2015.

[71] A. Hernández-Ramírez, I. Medina-Ramírez, Photocatalytic Semiconductors, Springer, 2016.

[72] R. Vinu, G. Madras, Renewable energy via photocatalysis, Curr. Org. Chem. 17 (21) (2013) 2538–2558.

[73] M.R. Panigrahi, M. Devi, Variation of optical and electrical properties of Zr Doped TiO_2 thin films with different annealing temperatures, J. Phys. Conf. Ser. (2019), 012046, https://doi.org/10.1088/1742-6596/1172/1/012046.

[74] J. Schneider, M. Matsuoka, M. Takeuchi, J. Zhang, Y. Horiuchi, M. Anpo, D. W. Bahnemann, Understanding TiO_2 photocatalysis: mechanisms and materials, Chem. Rev. 114 (19) (2014) 9919–9986, https://doi.org/10.1021/cr5001892.

[75] N. Zhang, C. Gao, Y. Xiong, Defect engineering: a versatile tool for tuning the activation of key molecules in photocatalytic reactions, J. Energy Chem. 37 (2019) 43–57, https://doi.org/10.1016/j.jechem.2018.09.010.

[76] S.K. Cushing, F. Meng, J. Zhang, B. Ding, C.K. Chen, C.-.J. Chen, R.-.S. Liu, A. D. Bristow, J. Bright, P. Zheng, Effects of defects on photocatalytic activity of hydrogen-treated titanium oxide nanobelts, ACS Catal 7 (3) (2017) 1742–1748, https://doi.org/10.1021/acscatal.6b02177.

[77] J. Wang, Y. Xia, Y. Dong, R. Chen, L. Xiang, S. Komarneni, Defect-rich ZnO nanosheets of high surface area as an efficient visible-light photocatalyst, Appl. Catal. B 192 (2016) 8–16, https://doi.org/10.1016/j.apcatb.2016.03.040.

[78] M. Chen, C. Friend, E. Kaxiras, The chemical nature of surface point defects on MoO_3 (010): adsorption of hydrogen and methyl, J. Am. Chem. Soc. 123 (10) (2001) 2224–2230, https://doi.org/10.1021/ja994376s.

[79] Y.-.F. Li, U. Aschauer, J. Chen, A. Selloni, Adsorption and reactions of O_2 on anatase TiO_2, Acc. Chem. Res. 47 (11) (2014) 3361–3368, https://doi.org/10.1021/ar400312t.

[80] S. Wendt, P.T. Sprunger, E. Lira, G.K. Madsen, Z. Li, J.Ø. Hansen, J. Matthiesen, A. Blekinge-Rasmussen, E. Lægsgaard, B. Hammer, The role of interstitial sites in the Ti 3d defect state in the band gap of titania, Science 320 (5884) (2008) 1755–1759, https://doi.org/10.1126/science.1159846.

[81] W. Zhou, W. Li, J.-.Q. Wang, Y. Qu, Y. Yang, Y. Xie, K. Zhang, L. Wang, H. Fu, D. Zhao, Ordered mesoporous black TiO_2 as highly efficient hydrogen evolution photocatalyst, J. Am. Chem. Soc. 136 (26) (2014) 9280–9283, https://doi.org/10.1021/ja504802q.

[82] Z. Li, H. Li, S. Wang, F. Yang, W. Zhou, Mesoporous black TiO_2/MoS_2/Cu_2S hierarchical tandem heterojunctions toward optimized photothermal-photocatalytic fuel production, Chem. Eng. J. 427 (2022), 131830, https://doi.org/10.1016/j.cej.2021.131830.

[83] S. Wang, H. Sun, P. Qiao, Z. Li, Y. Xie, W. Zhou, NiS/Pt nanoparticles co-decorated black mesoporous TiO_2 hollow nanotube assemblies as efficient hydrogen evolution photocatalysts, Appl. Mater. Today. 22 (2021), 100977, https://doi.org/10.1016/j.apmt.2021.100977.

[84] Z. Li, S. Wang, J. Wu, W. Zhou, Recent progress in defective TiO_2 photocatalysts for energy and environmental applications, Renew. Sustain. Energy Rev. 156 (2022), 111980, https://doi.org/10.1016/j.rser.2021.111980.

[85] T. Aguilar, J. Navas, R. Alcántara, C. Fernández-Lorenzo, J. Gallardo, G. Blanco, J. Martín-Calleja, A route for the synthesis of Cu-doped TiO_2 nanoparticles with a very low band gap, Chem. Phys. Lett. 571 (2013) 49–53, https://doi.org/10.1016/j.cplett.2013.04.007.

[86] S.I. Mogal, M. Mishra, V.G. Gandhi, R.J. Tayade, Metal doped titanium dioxide: synthesis and effect of metal ions on physico-chemical and photocatalytic properties, Mater. Sci. Forum. 734 (2013) 364–378, https://doi.org/10.4028/www.scientific.net/MSF.734.364.

[87] A. Saleem, M. Imran, A. Shahzadi, M. Junaid, H. Majeed, A. Rafiq, I. Shahzadi, M. Ikram, M. Naz, S. Ali, Drastic improvement in catalytic, optical and visible-light photocatalytic behavior of cobalt and nickel doped TiO_2 nanopowder, Mater. Res. Express 6 (1) (2018), 015003, https://doi.org/10.4028/www.scientific.net/MSF.734.364.

[88] P. Koh, L. Yuliati, S. Lee, Effect of transition metal oxide doping (Cr, Co, V) in the photocatalytic activity of TiO_2 for congo red degradation under visible light, J. Teknol. 69 (5) (2014), https://doi.org/10.11113/jt.v69.3203.

[89] C. Liao, Y. Li, S.C. Tjong, Visible-light active titanium dioxide nanomaterials with bactericidal properties, Nanomaterials 10 (1) (2020) 124, https://doi.org/10.3390/nano10010124.

[90] A. Petica, A. Florea, C. Gaidau, D. Balan, L. Anicai, Synthesis and characterization of silver-titania nanocomposites prepared by electrochemical method with enhanced photocatalytic characteristics, antifungal and antimicrobial activity, J. Mater. Res. Technol. 8 (1) (2019) 41–53, https://doi.org/10.1016/j.jmrt.2017.09.009.

[91] J. Wang, W. Zhu, Y. Zhang, S. Liu, An efficient two-step technique for nitrogen-doped titanium dioxide synthesizing: visible-light-induced photodecomposition of methylene blue, J. Phys. Chem. C. 111 (2) (2007) 1010–1014, https://doi.org/10.1021/jp066156o.

[92] J.W. Shi, J.T. Zheng, P. Wu, Preparation, characterization and photocatalytic activities of holmium-doped titanium dioxide nanoparticles, J. Hazard. Mater. 161 (1) (2009) 416–422, https://doi.org/10.1016/j.jhazmat.2008.03.114.

[93] T. Tong, J. Zhang, B. Tian, F. Chen, D. He, M. Anpo, Preparation of Ce–TiO_2 catalysts by controlled hydrolysis of titanium alkoxide based on esterification reaction and study on its photocatalytic activity, J. Colloid Interface Sci. 315 (1) (2007) 382–388, https://doi.org/10.1016/j.jcis.2007.06.051.

[94] W. Qian, P.A. Greaney, S. Fowler, S.-.K. Chiu, A.M. Goforth, J. Jiao, Low-temperature nitrogen doping in ammonia solution for production of N-doped TiO_2-hybridized graphene as a highly efficient photocatalyst for water treatment, ACS Sustain. Chem. Eng. 2 (7) (2014) 1802–1810, https://doi.org/10.1021/sc5001176.

[95] M. Nadeem, H. Idriss, Photo-thermal reactions of ethanol over Ag/TiO_2 catalysts. The role of silver plasmon resonance in the reaction kinetics, Chem. Commun. 54 (41) (2018) 5197–5200, https://doi.org/10.1039/C8CC01814F.

[96] X. Liu, Z. Xing, Y. Zhang, Z. Li, X. Wu, S. Tan, X. Yu, Q. Zhu, W. Zhou, Fabrication of 3D flower-like black N-TiO_2-x@ MoS_2 for unprecedented-high visible-light-driven photocatalytic performance, Appl. Catal. B 201 (2017) 119–127, https://doi.org/10.1016/j.apcatb.2016.08.031.

[97] W. Wang, H. Zhao, P. Pan, K. Xue, Z. Zhang, J. Duan, Enhanced the photocatalytic activity of B–C–N–TiO_2 under visible light: synergistic effect of element doping and Z-scheme interface heterojunction constructed with Ag nanoparticles, Ceram. Int. 47 (5) (2021) 6094–6104, https://doi.org/10.1016/j.ceramint.2020.10.188.

[98] T.A. Saleh, G. Fadillah, Recent trends in the design of chemical sensors based on graphene–metal oxide nanocomposites for the analysis of toxic species and biomolecules, TrAC, Trends Anal. Chem. 120 (2019), 115660, https://doi.org/10.1016/j.trac.2019.115660.

[99] A.M. Alansi, M. Al-Qunaibit, I.O. Alade, T.F. Qahtan, T.A. Saleh, Visible-light responsive BiOBr nanoparticles loaded on reduced graphene oxide for photocatalytic degradation of dye, J. Mol. Liq. 253 (2018) 297–304, https://doi.org/10.1016/j.molliq.2018.01.034.

[100] G. Fadillah, T.A. Saleh, S. Wahyuningsih, E.N.K. Putri, S. Febrianastuti, Electrochemical removal of methylene blue using alginate-modified graphene adsorbents, Chem. Eng. J. 378 (2019), 122140, https://doi.org/10.1016/j.cej.2019.122140.

[101] X. Fang, Z. Zhang, Q. Chen, H. Ji, X. Gao, Dependence of nitrogen doping on TiO_2 precursor annealed under NH_3 flow, J. Solid State Chem. 180 (4) (2007) 1325–1332, https://doi.org/10.1016/j.jssc.2007.02.010.

[102] A. Fujishima, X. Zhang, D.A. Tryk, TiO_2 photocatalysis and related surface phenomena, Surf. Sci. Rep. 63 (12) (2008) 515–582, https://doi.org/10.1016/j.surfrep.2008.10.001.

[103] J. Ananpattarachai, S. Seraphin, P. Kajitvichyanukul, Formation of hydroxyl radicals and kinetic study of 2-chlorophenol photocatalytic oxidation using C-doped TiO_2, N-doped TiO_2, and C, N Co-doped TiO_2 under visible light, Environ. Sci. Pollut. Res. 23 (4) (2016) 3884–3896, https://doi.org/10.1007/s11356-015-5570-8.

[104] M. Pelaez, N.T. Nolan, S.C. Pillai, M.K. Seery, P. Falaras, A.G. Kontos, P.S. Dunlop, J.W. Hamilton, J.A. Byrne, K. O'shea, A. review on the visible light active titanium dioxide photocatalysts for environmental applications, Appl. Catal. B 125 (2012) 331–349, https://doi.org/10.1016/j.apcatb.2012.05.036.

[105] S.A. Ansari, M.M. Khan, M.O. Ansari, M.H. Cho, Nitrogen-doped titanium dioxide (N-doped TiO_2) for visible light photocatalysis, New J. Chem. 40 (4) (2016) 3000–3009, https://doi.org/10.1039/C5NJ03478G.

[106] A. Selvaraj, R. Parimiladevi, K. Rajesh, Synthesis of nitrogen doped titanium dioxide (TiO_2) and its photocatalytic performance for the degradation of indigo carmine dye, J. Environ. Nanotechnol. 2 (1) (2013) 35–41, https://doi.org/10.13074/jent.2013.02.121026.

[107] X. Cheng, X. Yu, Z. Xing, J. Wan, Enhanced photocatalytic activity of nitrogen doped TiO_2 anatase nano-particle under simulated sunlight irradiation, Energy Procedia 16 (2012) 598–605, https://doi.org/10.1016/j.egypro.2012.01.096.

[108] J. Payormhorm, R. Idem, Synthesis of C-doped TiO_2 by sol-microwave method for photocatalytic conversion of glycerol to value-added chemicals under visible light, Appl. Catal. A 590 (2020), 117362, https://doi.org/10.1016/j.apcata.2019.117362.

[109] L. Ji, Y. Zhang, S. Miao, M. Gong, X. Liu, In situ synthesis of carbon doped TiO_2 nanotubes with an enhanced photocatalytic performance under UV and visible light, Carbon N Y 125 (2017) 544–550, https://doi.org/10.1016/j.carbon.2017.09.094.

[110] L. Hua, Z. Yin, S. Cao, Recent advances in synthesis and applications of carbon-doped TiO_2 nanomaterials, Catalysts 10 (12) (2020) 1431, https://doi.org/10.3390/catal10121431.

[111] J. Shao, W. Sheng, M. Wang, S. Li, J. Chen, Y. Zhang, S. Cao, In situ synthesis of carbon-doped TiO_2 single-crystal nanorods with a remarkably photocatalytic efficiency, Appl. Catal. B 209 (2017) 311–319, https://doi.org/10.1016/j.apcatb.2017.03.008.

[112] T. Ohno, M. Akiyoshi, T. Umebayashi, K. Asai, T. Mitsui, M. Matsumura, Preparation of S-doped TiO_2 photocatalysts and their photocatalytic activities under visible light, Appl. Catal. A 265 (1) (2004) 115–121, https://doi.org/10.1016/j.apcata.2004.01.007.

[113] T. Sano, N. Mera, Y. Kanai, C. Nishimoto, S. Tsutsui, T. Hirakawa, N. Negishi, Origin of visible-light activity of N-doped TiO_2 photocatalyst: behaviors of N and S atoms in a wet N-doping process, Appl. Catal. B 128 (2012) 77–83, https://doi.org/10.1016/j.apcatb.2012.06.034.

[114] S.A. Bakar, C. Ribeiro, A comparative run for visible-light-driven photocatalytic activity of anionic and cationic S-doped TiO_2 photocatalysts: a case study of possible sulfur doping through chemical protocol, J. Mol. Catal. A 421 (2016) 1–15, https://doi.org/10.1016/j.molcata.2016.05.003.

[115] M. Anas, D.S. Han, K. Mahmoud, H. Park, A. Abdel-Wahab, Photocatalytic degradation of organic dye using titanium dioxide modified with metal and non-

metal deposition, Mater. Sci. Semicond. Process. 41 (2016) 209–218, https://doi.org/10.1016/j.mssp.2015.08.041.
[116] F. Dong, S. Guo, H. Wang, X. Li, Z. Wu, Enhancement of the visible light photocatalytic activity of C-doped TiO_2 nanomaterials prepared by a green synthetic approach, J. Phys. Chem. C. 115 (27) (2011) 13285–13292, https://doi.org/10.1021/jp111916q.
[117] R.M. Kakhki, R. Tayebee, F. Ahsani, New and highly efficient Ag doped ZnO visible nano photocatalyst for removing of methylene blue, J. Mater. Sci. Mater. Electron. 28 (8) (2017) 5941–5952, https://doi.org/10.1007/s10854-016-6268-5.
[118] H. Guan, X. Wang, Y. Guo, C. Shao, X. Zhang, Y. Liu, R.-.F. Louh, Controlled synthesis of Ag-coated TiO_2 nanofibers and their enhanced effect in photocatalytic applications, Appl. Surf. Sci. 280 (2013) 720–725, https://doi.org/10.1016/j.apsusc.2013.05.050.
[119] A. Rostami-Vartooni, M. Nasrollahzadeh, M. Alizadeh, Green synthesis of seashell supported silver nanoparticles using Bunium persicum seeds extract: application of the particles for catalytic reduction of organic dyes, J. Colloid Interface Sci. 470 (2016) 268–275, https://doi.org/10.1016/j.jcis.2016.02.060.
[120] P. Mohammadi, M. Heravi, M. Daraie, Ag nanoparticles immobilized on new magnetic alginate halloysite as a recoverable catalyst for reduction of nitroaromatics in aqueous media, Sci. Rep. 11 (1) (2021) 1–10, https://doi.org/10.1038/s41598-021-96421-5.
[121] D.O. Adenuga, S.M. Tichapondwa, E.M. Chirwa, Facile synthesis of a Ag/AgCl/BiOCl composite photocatalyst for visible–light–driven pollutant removal, J. Photochem. Photobiol. A 401 (2020), 112747, https://doi.org/10.1016/j.jphotochem.2020.112747.
[122] M. Harikishore, M. Sandhyarani, K. Venkateswarlu, T. Nellaippan, N. Rameshbabu, Effect of Ag doping on antibacterial and photocatalytic activity of nanocrystalline TiO_2, Procedia Manuf 6 (2014) 557–566, https://doi.org/10.1016/j.mspro.2014.07.071.
[123] Z. Noreen, N. Khalid, R. Abbasi, S. Javed, I. Ahmad, H. Bokhari, Visible light sensitive Ag/TiO_2/graphene composite as a potential coating material for control of Campylobacter jejuni, Mater. Sci. Eng. C 98 (2019) 125–133, https://doi.org/10.1016/j.msec.2018.12.087.
[124] M.I. Din, R. Khalid, Z. Hussain, Minireview: silver-doped titanium dioxide and silver-doped zinc oxide photocatalysts, Anal. Lett. 51 (6) (2018) 892–907, https://doi.org/10.1080/00032719.2017.1363770.
[125] M.R. Khan, T.W. Chuan, A. Yousuf, M. Chowdhury, C.K. Cheng, Schottky barrier and surface plasmonic resonance phenomena towards the photocatalytic reaction: study of their mechanisms to enhance photocatalytic activity, Catal. Sci. Technol. 5 (5) (2015) 2522–2531, https://doi.org/10.1039/C4CY01545B.
[126] A. Furube, S. Hashimoto, Insight into plasmonic hot-electron transfer and plasmon molecular drive: new dimensions in energy conversion and nanofabrication, NPG Asia Mater 9 (12) (2017), https://doi.org/10.1038/am.2017.191 e454-e454.
[127] J. Murcia, E. Ávila-Martínez, H. Rojas, J.A. Navío, M. Hidalgo, Study of the E. coli elimination from urban wastewater over photocatalysts based on metallized TiO_2, Appl. Catal. B 200 (2017) 469–476, https://doi.org/10.1016/j.apcatb.2016.07.045.
[128] R.P. Suri, H.M. Thornton, M. Muruganandham, Disinfection of water using Pt-and Ag-doped TiO_2 photocatalysts, Environ. Technol. 33 (14) (2012) 1651–1659, https://doi.org/10.1080/09593330.2011.641590.
[129] Z. Cao, C. Liu, D. Chen, J. Liu, Preparation of an Au-TiO_2 photocatalyst and its performance in removing phycocyanin, Sci. Total Environ. 692 (2019) 572–581, https://doi.org/10.1016/j.scitotenv.2019.07.117.
[130] P. Ribao, J. Corredor, M.J. Rivero, I. Ortiz, Role of reactive oxygen species on the activity of noble metal-doped TiO_2 photocatalysts, J. Hazard. Mater. 372 (2019) 45–51, https://doi.org/10.1016/j.jhazmat.2018.05.026.
[131] P. Dong, F. Yang, X. Cheng, Z. Huang, X. Nie, Y. Xiao, X. Zhang, Plasmon enhanced photocatalytic and antimicrobial activities of Ag-TiO_2 nanocomposites under visible light irradiation prepared by DBD cold plasma treatment, Mater. Sci. Eng. C. 96 (2019) 197–204, https://doi.org/10.1016/j.msec.2018.11.005.
[132] W. Xu, M. Qi, X. Li, X. Liu, L. Wang, W. Yu, M. Liu, A. Lan, Y. Zhou, Y. Song, TiO_2 nanotubes modified with Au nanoparticles for visible-light enhanced antibacterial and anti-inflammatory capabilities, J. Electroanal. Chem. 842 (2019) 66–73, https://doi.org/10.1016/j.jelechem.2019.04.062.
[133] V.V. Torbina, A.A. Vodyankin, S. Ten, G.V. Mamontov, M.A. Salaev, V.I. Sobolev, O.V. Vodyankina, Ag-based catalysts in heterogeneous selective oxidation of alcohols: a review, Catalysts 8 (10) (2018) 447, https://doi.org/10.3390/catal8100447.
[134] Z. Xiong, J. Ma, W.J. Ng, T.D. Waite, X. Zhao, Silver-modified mesoporous TiO_2 photocatalyst for water purification, Water Res 45 (5) (2011) 2095–2103, https://doi.org/10.1016/j.watres.2010.12.019.
[135] J. He, A. Kumar, M. Khan, I.M. Lo, Critical Review of photocatalytic disinfection of bacteria: from noble metals-and carbon nanomaterials-TiO_2 composites to challenges of water characteristics and strategic solutions, Sci. Total Environ. (2020), 143953, https://doi.org/10.1016/j.scitotenv.2020.143953.
[136] A. Takai, P.V. Kamat, Capture, store, and discharge. Shuttling photogenerated electrons across TiO_2–silver interface, ACS Nano 5 (9) (2011) 7369–7376, https://doi.org/10.1021/nn202294b.
[137] S. Shen, L. Guo, X. Chen, F. Ren, C.X. Kronawitter, S.S. Mao, Effect of noble metal in CdS/M/TiO_2 for photocatalytic degradation of methylene blue under visible light, Int. J. Green Nanotechnol. Mater. Sci. Technol. 1 (2) (2010) M94–M104, https://doi.org/10.1080/19430841003684823.
[138] T. Hirakawa, P.V. Kamat, Charge separation and catalytic activity of Ag@TiO_2 core− shell composite clusters under UV− irradiation, J. Am. Chem. Soc. 127 (11) (2005) 3928–3934, https://doi.org/10.1021/ja042925a.
[139] L.G. Devi, R. Kavitha, A review on plasmonic metal TiO_2 composite for generation, trapping, storing and dynamic vectorial transfer of photogenerated electrons across the Schottky junction in a photocatalytic system, Appl. Surf. Sci. 360 (2016) 601–622, https://doi.org/10.1016/j.apsusc.2015.11.016.
[140] B. Basumatary, R. Basumatary, A. Ramchiary, D. Konwar, Evaluation of Ag@TiO_2/WO_3 heterojunction photocatalyst for enhanced photocatalytic activity towards methylene blue degradation, Chemosphere 286 (2022), 131848, https://doi.org/10.1016/j.chemosphere.2021.131848.
[141] S. Linic, P. Christopher, D.B. Ingram, Plasmonic-metal nanostructures for efficient conversion of solar to chemical energy, Nat. Mater. 10 (12) (2011) 911–921, https://doi.org/10.1038/nmat3151.
[142] M. Sharma, M. Pathak, P.N. Kapoor, The sol-gel method: pathway to ultrapure and homogeneous mixed metal oxide nanoparticles, Asian J. Chem 30 (7) (2018) 1405–1412, https://doi.org/10.14233/ajchem.2018.20845.
[143] N. Hamed, M. Ahmad, N. Hairom, A. Faridah, M. Mamat, A. Mohamed, A. Suriani, N. Nafarizal, F. Fazli, S. Mokhtar, Dependence of photocatalysis on electron trapping in Ag-doped flowerlike rutile-phase TiO_2 film by facile hydrothermal method, Appl. Surf. Sci. 534 (2020), 147571, https://doi.org/10.1016/j.apsusc.2020.147571.
[144] W. Wei, D. Yu, Q. Huang, Preparation of Ag/TiO_2 nanocomposites with controlled crystallization and properties as a multifunctional material for SERS and photocatalytic applications, Spectrochim. Spectrochim. Acta A 243 (2020), 118793, https://doi.org/10.1016/j.apsusc.2020.147571.
[145] X. Zhou, B. Jin, J. Luo, X. Ning, L. Zhan, X. Xu, X. Fan, F. Yang, S. Zhang, One-pot solvothermal synthesis of 1D plasmonic TiO_2@ Ag nanorods with enhanced visible-light photocatalytic performance, Int. J. Hydrog. Energy 44 (21) (2019) 10585–10592, https://doi.org/10.1016/j.ijhydene.2019.02.234.
[146] X. Yu, L. Shang, D. Wang, L. An, Z. Li, J. Liu, J. Shen, Plasmon-resonance-enhanced visible-light photocatalytic activity of Ag quantum dots/TiO_2 microspheres for methyl orange degradation, Solid State Sci 80 (2018) 1–5, https://doi.org/10.1016/j.solidstatesciences.2018.03.014.
[147] C. Díaz-Uribe, J. Viloria, L. Cervantes, W. Vallejo, K. Navarro, E. Romero, C. Quiñones, Photocatalytic activity of Ag-TiO_2 composites deposited by photoreduction under UV irradiation, Int. J. Photoenergy 2018 (2018), https://doi.org/10.1155/2018/6080432.
[148] Y. Zhang, S. Zhou, X. Su, J. Xu, G. Nie, Y. Zhang, Y. He, S. Yu, Synthesis and characterization of Ag-loaded p-type TiO_2 for adsorption and photocatalytic degradation of tetrabromobisphenol A, Water Environ. Res. 92 (5) (2020) 713–721, https://doi.org/10.1002/wer.1264.
[149] Y. Gao, W. Zhang, P. Liu, Enhanced photocatalytic efficiency of TiO_2 membrane decorated with Ag and Au nanoparticles, Appl. Sci. 8 (6) (2018) 945, https://doi.org/10.3390/app8060945.
[150] P. Van Viet, B.T. Phan, D. Mott, S. Maenosono, T.T. Sang, C.M. Thi, Silver nanoparticle loaded TiO_2 nanotubes with high photocatalytic and antibacterial activity synthesized by photoreduction method, J. Photochem. Photobiol. A 352 (2018) 106–112, https://doi.org/10.1016/j.jphotochem.2017.10.051.
[151] M.J. Nalbandian, M. Zhang, J. Sanchez, S. Kim, Y.-.H. Choa, D.M. Cwiertny, N. V. Myung, Synthesis and optimization of Ag–TiO_2 composite nanofibers for photocatalytic treatment of impaired water sources, J. Hazard. Mater. 299 (2015) 141–148, https://doi.org/10.1016/j.jhazmat.2015.05.053.
[152] Y. Wang, L. Yan, X. He, J. Li, D. Wang, Controlled fabrication of Ag/TiO_2 nanofibers with enhanced stability of photocatalytic activity, J. Mater. Sci. 27 (5) (2016) 5190–5196, https://doi.org/10.1007/s10854-016-4412-x.
[153] J.M. Freire, M.A. Matos, D.S. Abreu, H. Becker, I.C. Diogenes, A. Valentini, E. Longhinotti, Nitrate photocatalytic reduction on TiO_2: metal loaded, synthesis and anions effect, J. Environ. Chem. Eng. 8 (4) (2020), 103844, https://doi.org/10.1016/j.jece.2020.103844.
[154] W. Zhou, T. Li, J. Wang, Y. Qu, K. Pan, Y. Xie, G. Tian, L. Wang, Z. Ren, B. Jiang, Composites of small Ag clusters confined in the channels of well-ordered mesoporous anatase TiO_2 and their excellent solar-light-driven photocatalytic performance, Nano Res 7 (5) (2014) 731–742, https://doi.org/10.1007/s12274-014-0434-y.
[155] G. Lenzi, C. Fávero, L. Colpini, H. Bernabe, M. Baesso, S. Specchia, O. Santos, Photocatalytic reduction of Hg (II) on TiO_2 and Ag/TiO_2 prepared by the sol–gel and impregnation methods, Desalination 270 (1–3) (2011) 241–247, https://doi.org/10.1016/j.desal.2010.11.051.
[156] D.S.C. Halin, N. Mahmed, M.A.A. Mohd Salleh, A. Mohd Sakeri, K.A. Razak, Synthesis and characterization of Ag/TiO_2 thin film via sol-gel method, Solid State Phenom 273 (2018) 140–145, https://doi.org/10.4028/www.scientific.net/SSP.273.140.
[157] A. Shokuhfar, M. Alzamani, E. Eghdam, M. Karimi, S. Mastali, SiO_2-TiO_2 nanostructure films on windshields prepared by sol-gel dip-coating technique for self-cleaning and photocatalytic applications, Nanosci. Nanotechnol 2 (1) (2012) 16–21, https://doi.org/10.5923/j.nn.20120201.04.
[158] L. Wei, C. Yu, Q. Zhang, H. Liu, Y. Wang, TiO_2-based heterojunction photocatalysts for photocatalytic reduction of CO_2 into solar fuels, J. Mater. Chem. A 6 (45) (2018) 22411–22436, https://doi.org/10.1039/C8TA08879A.
[159] W. Zhou, F. Sun, K. Pan, G. Tian, B. Jiang, Z. Ren, C. Tian, H. Fu, Well-ordered large-pore mesoporous anatase TiO_2 with remarkably high thermal stability and improved crystallinity: preparation, characterization, and photocatalytic performance, Adv. Funct. Mater. 21 (10) (2011) 1922–1930, https://doi.org/10.1002/adfm.201002535.

[160] S. Singh, S.L. Lo, V.C. Srivastava, A.D. Hiwarkar, Comparative study of electrochemical oxidation for dye degradation: parametric optimization and mechanism identification, J. Environ. Chem. Eng. 4 (3) (2016) 2911–2921, https://doi.org/10.1016/j.jece.2016.05.036.

[161] V.K. Saharan, D.V. Pinjari, P.R. Gogate, A.B. Pandit, Advanced Oxidation Technologies For Wastewater treatment: an Overview, Elsevier, Butterworth, Heinemann, UK, 2014.

[162] J. Li, Q. Wu, J. Wu, Synthesis of Nanoparticles via Solvothermal and Hydrothermal Methods 12 (2016), https://doi.org/10.1007/978-3-319-15338-4_17.

[163] H. Li, C. Liu, G. Li, Q. Guo, H. Luo, A start strategy for synchronized connection of MMCs to an AC system, Int. J. Electr. Power Energy Syst. 69 (2015) 380–390, https://doi.org/10.1016/j.ijepes.2015.01.016.

[164] A. Shojaie, M. Fattahi, S. Jorfi, B. Ghasemi, Hydrothermal synthesis of Fe-TiO_2-Ag nano-sphere for photocatalytic degradation of 4-chlorophenol (4-CP): investigating the effect of hydrothermal temperature and time as well as calcination temperature, J. Environ. Chem. Eng. 5 (5) (2017) 4564–4572, https://doi.org/10.1016/j.jece.2017.07.024.

[165] Q. Wang, J. Qiao, X. Cui, J. Zhong, Y. Xu, S. Zhang, Q. Zhang, P. Chang, M. Li, C. Zhang, Preparation of mesoporous Ag-containing TiO_2 heterojunction film and its photocatalytic property, J. Nanoparticle Res. 17 (3) (2015) 1–8, https://doi.org/10.1007/s11051-015-2941-5.

[166] L. Jiang, G. Zhou, J. Mi, Z. Wu, Fabrication of visible-light-driven one-dimensional anatase TiO_2/Ag heterojunction plasmonic photocatalyst, Catal. Commun. 24 (2012) 48–51, https://doi.org/10.1016/j.catcom.2012.03.017.

[167] V. Soni, P. Raizada, A. Kumar, V. Hasija, S. Singal, P. Singh, A. Hosseini-Bandegharaei, V.K. Thakur, V.-.H. Nguyen, Indium sulfide-based photocatalysts for hydrogen production and water cleaning: a review, Environ. Chem. Lett. 19 (2) (2021) 1065–1095, https://doi.org/10.1007/s10311-020-01148-w.

[168] O. Ola, M.M. Maroto-Valer, Review of material design and reactor engineering on TiO_2 photocatalysis for CO_2 reduction, J. Photochem. Photobiol. C 24 (2015) 16–42, https://doi.org/10.1016/j.jphotochemrev.2015.06.001.

[169] V. Hasija, A. Kumar, A. Sudhaik, P. Raizada, P. Singh, Q. Van Le, T.T. Le, V.-.H. Nguyen, Step-scheme heterojunction photocatalysts for solar energy, water splitting, CO_2 conversion, and bacterial inactivation: a review, Environ. Chem. Lett. 19 (4) (2021) 2941–2966, https://doi.org/10.1007/s10311-021-01231-w.

[170] V. Jeyalakshmi, R. Mahalakshmy, K. Krishnamurthy, B. Viswanathan, Photocatalytic reduction of carbon dioxide by water: a step towards sustainable fuels and chemicals, Mater. Sci. Forum 734 (2013) 1–62, https://doi.org/10.4028/www.scientific.net/MSF.734.1.

[171] M. Kunnamareddy, B. Diravidamani, R. Rajendran, B. Singaram, K. Varadharajan, Synthesis of silver and sulphur codoped TiO_2 nanoparticles for photocatalytic degradation of methylene blue, J. Mater. Sci. 29 (21) (2018) 18111–18119, https://doi.org/10.1007/s10854-018-9922-2.

[172] A.G. Akerdi, S.H. Bahrami, Application of heterogeneous nano-semiconductors for photocatalytic advanced oxidation of organic compounds: a review, J. Environ. Chem. Eng. 7 (5) (2019), 103283, https://doi.org/10.1016/j.jece.2019.103283.

[173] S. Thota, S.R. Tirukkovalluri, S. Bojja, Effective catalytic performance of manganese and phosphorus co-doped titania nanocatalyst for Orange-II dye degradation under visible light irradiation, J. Environ. Chem. Eng. 2 (3) (2014) 1506–1513, https://doi.org/10.1016/j.jece.2014.06.021.

[174] L.G. Devi, R. Kavitha, B. Nagaraj, Bulk and surface modification of TiO_2 with sulfur and silver: synergetic effects of dual surface modification in the enhancement of photocatalytic activity Mater, Sci. Semicond. Process. 40 (2015) 832–839, https://doi.org/10.1016/j.mssp.2015.07.070.

[175] L.G. Devi, R. Kavitha, Enhanced photocatalytic activity of sulfur doped TiO_2 for the decomposition of phenol: a new insight into the bulk and surface modification, Mater. Chem. Phys. 143 (3) (2014) 1300–1308, https://doi.org/10.1016/j.matchemphys.2013.11.038.

[176] A. Bumajdad, M. Madkour, Understanding the superior photocatalytic activity of noble metals modified titania under UV and visible light irradiation, Phys. Chem. Chem. Phys. 16 (16) (2014) 7146–7158, https://doi.org/10.1039/C3CP54411G.

[177] A. Bumajdad, M. Madkour, Y. Abdel-Moneam, M. El-Kemary, Nanostructured mesoporous Au/TiO_2 for photocatalytic degradation of a textile dye: the effect of size similarity of the deposited Au with that of TiO_2 pores, J. Mater. Sci. 49 (4) (2014) 1743–1754, https://doi.org/10.1007/s10853-013-7861-0.

[178] L.G. Devi, B. Nagaraj, K.E. Rajashekhar, Synergistic effect of Ag deposition and nitrogen doping in TiO_2 for the degradation of phenol under solar irradiation in presence of electron acceptor, Chem. Eng. J. 181 (2012) 259–266, https://doi.org/10.1016/j.cej.2011.11.076.

[179] C. Gaidau, A. Petica, M. Ignat, O. Iordache, L.-.M. Ditu, M. Ionescu, Enhanced photocatalysts based on Ag- TiO_2 and Ag-N- TiO_2 nanoparticles for multifunctional leather surface coating, Open Chem 14 (1) (2016) 383–392, https://doi.org/10.1515/chem-2016-0040.

[180] H. Zhang, Y. Jiang, B. Zhou, Z. Wei, Z. Zhu, L. Han, P. Zhang, Y. Hu, Preparation and photocatalytic performance of silver-modified and nitrogen-doped TiO_2 nanomaterials with oxygen vacancies, New J. Chem. 45 (10) (2021) 4694–4704, https://doi.org/10.1039/D0NJ04755D.

[181] Q. Chen, Y. Zhang, D. Zhang, Y. Yang, Ag and N co-doped TiO_2 nanostructured photocatalyst for printing and dyeing wastewater, J. Water Process Eng. 16 (2017) 14–20, https://doi.org/10.1016/j.jwpe.2016.11.007.

[182] Y. Luo, S. Yu, B. Li, L. Dong, F. Wang, M. Fan, F. Zhang, Synthesis of (Ag, F)-modified anatase TiO_2 nanosheets and their enhanced photocatalytic activity, New J. Chem. 40 (3) (2016) 2135–2144, https://doi.org/10.1039/C5NJ02544C.

[183] M.V. Dozzi, E. Selli, Doping TiO_2 with p-block elements: effects on photocatalytic activity, J. Photochem. Photobiol. C 14 (2013) 13–28, https://doi.org/10.1016/j.jphotochemrev.2012.09.002.

[184] L. Pan, J.-.J. Zou, X. Zhang, L. Wang, Photoisomerization of norbornadiene to quadricyclane using transition metal doped TiO_2, Ind. Eng. Chem. Res. 49 (18) (2010) 8526–8531, https://doi.org/10.1021/ie100841w.

[185] N. Arora, A. Mehta, A. Mishra, S. Basu, 4-Nitrophenol reduction catalysed by Au-Ag bimetallic nanoparticles supported on LDH: homogeneous vs. heterogeneous catalysis, Appl. Clay Sci. 151 (2018) 1–9, https://doi.org/10.1016/j.clay.2017.10.015.

[186] S. Sun, Recent advances in hybrid Cu_2O-based heterogeneous nanostructures, Nanoscale 7 (25) (2015) 10850–10882, https://doi.org/10.1039/C5NR02178B.

[187] L. Yang, W. Wang, H. Zhang, S. Wang, M. Zhang, G. He, J. Lv, K. Zhu, Z. Sun, Electrodeposited Cu_2O on the {101} facets of TiO_2 nanosheet arrays and their enhanced photoelectrochemical performance, Sol. Energy Mater. Sol. Cells 165 (2017) 27–35, https://doi.org/10.1016/j.solmat.2017.02.026.

[188] H. Chaker, S. Fourmentin, L. Chérif-Aouali, Efficient photocatalytic degradation of ibuprofen under visible light irradiation using silver and cerium co-doped mesoporous TiO_2, ChemistrySelect 5 (38) (2020) 11787–11796, https://doi.org/10.1002/slct.202002730.

[189] Z. Shayegan, F. Haghighat, C.-.S. Lee, Surface fluorinated Ce-doped TiO_2 nanostructure photocatalyst: a trap and remove strategy to enhance the VOC removal from indoor air environment, Chem. Eng. J. 401 (2020), 125932, https://doi.org/10.1016/j.cej.2020.125932.

[190] I. Tbessi, M. Benito, E. Molins, J. LIorca, A. Touati, S. Sayadi, W. Najjar, Effect of Ce and Mn co-doping on photocatalytic performance of sol-gel TiO_2, Solid State Sci 88 (2019) 20–28, https://doi.org/10.1016/j.solidstatesciences.2018.12.004.

[191] M. Kazazi, B. Moradi, M.D. Chermahini, Enhanced photocatalytic degradation of methyl orange using Ag/Sn-doped CeO_2 nanocomposite, J. Mater. Sci. 30 (6) (2019) 6116–6126, https://doi.org/10.1007/s10854-019-00913-0.

[192] Q. Wang, X. Gao, R. Zhang, B. Shen, Z. Tan, Z. Li, S. Yu, Decorated TiO_2 nanoparticles with La and Ag elements to improve photocatalytic activity under visible light for the degradation of Mo, J. Nanosci. Nanotechnol. 16 (4) (2016) 3587–3591, https://doi.org/10.1166/jnn.2016.11794.

[193] M. Liu, X. Qiu, K. Hashimoto, M. Miyauchi, Cu (II) nanocluster-grafted, Nb-doped TiO_2 as an efficient visible-light-sensitive photocatalyst based on energy-level matching between surface and bulk states, J. Mater. Chem. A 2 (33) (2014) 13571–13579, https://doi.org/10.1039/C4TA02211D.

[194] M. Tanaka, H. Shima, T. Yokoi, T. Tatsumi, J.N. Kondo, Changes in surface property and catalysis of mesoporous Nb_2O_5 from amorphous to crystalline pore walls, Catal. Lett. 141 (2) (2011) 283–292, https://doi.org/10.1007/s10562-010-0458-1.

[195] T. Goswami, K.M. Reddy, A. Bheemaraju, Silver Nanocluster Anchored TiO_2/Nb_2O5 Hybrid Nanocomposite as Highly Efficient and Selective Visible-Light Sensitive Photocatalyst, ChemistrySelect 4 (22) (2019) 6790–6799, https://doi.org/10.1002/slct.201901097.

[196] P. Monazzam, B.F. Kisomi, Co/TiO_2 nanoparticles: preparation, characterization and its application for photocatalytic degradation of methylene blue, Desalin. Water Treat. 63 (2017) 283–292, https://doi.org/10.5004/dwt.2017.20205.

[197] S. Sood, A. Umar, S.K. Mehta, S.K. Kansal, Highly effective Fe-doped TiO_2 nanoparticles photocatalysts for visible-light driven photocatalytic degradation of toxic organic compounds, J. Colloid Interface Sci. 450 (2015) 213–223, https://doi.org/10.1016/j.jcis.2015.03.018.

[198] V.M. Vasconcelos, F.L. Migliorini, J.R. Steter, M.R. Baldan, N.G. Ferreira, M.R. de Vasconcelos Lanza, Electrochemical oxidation of RB-19 dye using a highly BDD/Ti: proposed pathway and toxicity, J. Environ. Chem. Eng. 4 (4) (2016) 3900–3909, https://doi.org/10.1016/j.jece.2016.08.029.

[199] Y. Zhao, C. Tao, G. Xiao, G. Wei, L. Li, C. Liu, H. Su, Controlled synthesis and photocatalysis of sea urchin-like Fe_3O_4@TiO_2@Ag nanocomposites, Nanoscale 8 (9) (2016) 5313–5326, https://doi.org/10.1039/C5NR08624H.

[200] T. Ahamad, M. Naushad, T. Al-Shahrani, N. Al-Hokbany, S.M. Alshehri, Preparation of chitosan based magnetic nanocomposite for tetracycline adsorption: kinetic and thermodynamic studies, Int. J. Biol. Macromol. 147 (2020) 258–267, https://doi.org/10.1016/j.ijbiomac.2020.01.025.

[201] T. Ahamad, M. Naushad, A.N. Alhabarah, S.M. Alshehri, N/S doped highly porous magnetic carbon aerogel derived from sugarcane bagasse cellulose for the removal of bisphenol-A, Int. J. Biol. Macromol. 132 (2019) 1031–1038, https://doi.org/10.1016/j.ijbiomac.2019.04.004.

[202] H. Hamad, W. Sadik, M. Abd El-latif, A. Kashyout, M. Feteha, Photocatalytic parameters and kinetic study for degradation of dichlorophenol-indophenol (DCPIP) dye using highly active mesoporous TiO_2 nanoparticles, J. Environ. Sci. 43 (2016) 26–39, https://doi.org/10.1016/j.jes.2015.05.033.

[203] Y. Duan, M. Zhang, L. Wang, F. Wang, L. Yang, X. Li, C. Wang, Plasmonic Ag-TiO_2-x nanocomposites for the photocatalytic removal of NO under visible light with high selectivity: the role of oxygen vacancies, Appl. Catal. B 204 (2017) 67–77, https://doi.org/10.1016/j.apcatb.2016.11.023.

[204] M. Li, Z. Xing, J. Jiang, Z. Li, J. Yin, J. Kuang, S. Tan, Q. Zhu, W. Zhou, Surface plasmon resonance-enhanced visible-light-driven photocatalysis by Ag nanoparticles decorated S-TiO_2-x nanorods, J. Taiwan Inst. Chem. Eng. 82 (2018) 198–204, https://doi.org/10.1016/j.jtice.2017.11.023.

[205] S. Iqbal, M. Javed, A. Bahadur, M.A. Qamar, M. Ahmad, M. Shoaib, M. Raheel, N. Ahmad, M.B. Akbar, H. Li, Controlled synthesis of Ag-doped CuO nanoparticles as a core with poly (acrylic acid) microgel shell for efficient removal of methylene blue under visible light, J. Mater. Sci. 31 (11) (2020) 8423–8435, https://doi.org/10.1007/s10854-020-03377-9.

[206] X. Tian, Q. Wang, Q. Zhao, L. Qiu, X. Zhang, S. Gao, SILAR deposition of CuO nanosheets on the TiO_2 nanotube arrays for the high performance solar cells and photocatalysts, Sep. Purif. Technol. 209 (2019) 368–374, https://doi.org/10.1016/j.seppur.2018.07.057.
[207] J.F. de Brito, M.V.B. Zanoni, On the application of Ti/TiO_2/CuO np junction semiconductor: a case study of electrolyte, temperature and potential influence on CO_2 reduction, Chem. Eng. J. 318 (2017) 264–271, https://doi.org/10.1016/j.cej.2016.08.033.
[208] M. Ahmadi, B.K. Kaleji, TCA (Ag doped TiO_2-CuO) mesoporous composite nanoparticles: optical, XPS and morphological characterization, J. Mater. Sci. 32 (10) (2021) 13450–13461, https://doi.org/10.1007/s10854-021-05923-5.
[209] M.A. Behnajady, H. Eskandarloo, Characterization and photocatalytic activity of Ag–Cu/TiO_2 nanoparticles prepared by sol–gel method, J. Nanosci. Nanotechnol. 13 (1) (2013) 548–553, https://doi.org/10.1166/jnn.2013.6859.
[210] A. Hernández-Gordillo, V.R. González, Silver nanoparticles loaded on Cu-doped TiO_2 for the effective reduction of nitro-aromatic contaminants, Chem. Eng. J. 261 (2015) 53–59, https://doi.org/10.1016/j.cej.2014.05.148.
[211] J. Jalali, M. Mozammel, M. OjaghiIlkhchi, Photodegradation of organic dye using co-doped Ag/Cu TiO_2 nanoparticles: synthesis and characterization, J. Mater. Sci. 28 (22) (2017) 16776–16787, https://doi.org/10.1007/s10854-017-7592-0.
[212] H. Dong, G. Zeng, L. Tang, C. Fan, C. Zhang, X. He, Y. He, An overview on limitations of TiO_2-based particles for photocatalytic degradation of organic pollutants and the corresponding countermeasures, Water Res 79 (2015) 128–146, https://doi.org/10.1016/j.watres.2015.04.038.
[213] O. Ibukun, H.K. Jeong, Tailoring titanium dioxide by silver particles for photocatalysis, Curr. Appl. Phys. 20 (1) (2020) 23–28, https://doi.org/10.1016/j.cap.2019.10.009.
[214] Q. Wang, J. Qiao, X. Cui, J. Zhong, Y. Xu, S. Zhang, Q. Zhang, P. Chang, M. Li, C. Zhang, Preparation of mesoporous Ag-containing TiO_2 heterojunction film and its photocatalytic property, J. Nanoparticle Res. 17 (3) (2015) 1–8, https://doi.org/10.1007/s11051-015-2941-5.
[215] M. Raffi, Z. Batool, M. Ahmad, M. Zakria, R.I. Shakoor, M.A. Mirza, A. Mahmood, Synthesis of Ag-loaded TiO_2 electrospun nanofibers for photocatalytic decolorization of methylene blue, Fibers Polym 19 (9) (2018) 1930–1939, https://doi.org/10.1007/s12221-018-8227-7.
[216] T. He, A. Bahi, W. Zhou, F. Ko, Electrospun nanofibrous Ag–TiO_2/Poly (vinylidene fluoride)(PVDF) membranes with enhanced photocatalytic activity, J. Nanosci. Nanotechnol. 16 (7) (2016) 7388–7394, https://doi.org/10.1166/jnn.2016.11120.
[217] J. Zhong, Q. Wang, Y. Yu, Solvothermal preparation of Ag nanoparticles sensitized TiO_2 nanotube arrays with enhanced photoelectrochemical performance, J. Alloys Compd. 620 (2015) 168–171, https://doi.org/10.1016/j.jallcom.2014.08.205.
[218] S. Abbad, K. Guergouri, S. Gazaout, S. Djebabra, A. Zertal, R. Barille, M. Zaabat, Effect of silver doping on the photocatalytic activity of TiO_2 nanopowders synthesized by the sol-gel route, J. Environ. Chem. Eng. 8 (3) (2020), 103718, https://doi.org/10.1016/j.jece.2020.103718.
[219] C. Zhao, J. Guo, C. Yu, Z. Zhang, Z. Sun, X. Piao, Fabrication of CNTs-Ag-TiO_2 ternary structure for enhancing visible light photocatalytic degradation of organic dye pollutant, Mater. Chem. Phys. 248 (2020), 122873, https://doi.org/10.1016/j.matchemphys.2020.122873.
[220] M. Gorgani, B.K. Kaleji, Structural, photocatalytic and surface analysis of Nb/Ag codoped TiO_2 mesoporous nanoparticles, J. Sol-Gel Sci. Technol. 96 (3) (2020) 728–741, https://doi.org/10.1007/s10971-020-05403-y.
[221] S. Pakdaman, A.E. Pirbazari, N. Gilani, Deposition of Ag nanoparticles onto TiO_2/Fe_3O_4/MWCNTs quaternary nanocomposite: a visible-light-driven plasmonic photocatalyst for degradation of 2, 4-dichlorophenol, Desalin. Water Treat. 102 (2018) 241–252, https://doi.org/10.5004/dwt.2018.21901.
[222] Z.-.R. Tóth, K. Hernadi, L. Baia, G. Kovács, Z. Pap, Controlled formation of Ag-AgxO nanoparticles on the surface of commercial TiO_2 based composites for enhanced photocatalytic degradation of oxalic acid and phenol, Catal. Today (2020), https://doi.org/10.1016/j.cattod.2020.06.051.
[223] X. Wang, R. Yu, K. Wang, G. Yang, H. Yu, Facile template-induced synthesis of Ag-modified TiO_2 hollow octahedra with high photocatalytic activity, Chin, J. Catal. 36 (12) (2015) 1211–2218, https://doi.org/10.1016/S1872-2067(15)60978-0.
[224] D. Kanakaraju, J. Kockler, C.A. Motti, B.D. Glass, M. Oelgemöller, Titanium dioxide/zeolite integrated photocatalytic adsorbents for the degradation of amoxicillin, Appl. Catal. B 166 (2015) 45–55, https://doi.org/10.1016/j.apcatb.2014.11.001.
[225] E. Bet-Moushoul, Y. Mansourpanah, K. Farhadi, M. Tabatabaei, TiO_2 nanocomposite based polymeric membranes: a review on performance improvement for various applications in chemical engineering processes, Chem. Eng. J. 283 (2016) 29–46, https://doi.org/10.1016/j.cej.2015.06.124.
[226] H. Ma, B. Zhou, H.-.S. Li, Y.-.Q. Li, S.-.Y. Ou, Green composite films composed of nanocrystalline cellulose and a cellulose matrix regenerated from functionalized ionic liquid solution, Carbohydr. Polym. 84 (1) (2011) 383–389, https://doi.org/10.1016/j.carbpol.2010.11.050.
[227] M. Soheilmoghaddam, M.U. Wahit, N.I. Akos, Regenerated cellulose/epoxidized natural rubber blend film, Mater. Lett. 111 (2013) 221–224, https://doi.org/10.1016/j.matlet.2013.08.109.
[228] O.V. Kharissova, B.I. Kharisov, C.M. Oliva González, Y.P. Méndez, I. López, Greener synthesis of chemical compounds and materials, R. Soc. open sci. 6 (11) (2019), 191378, https://doi.org/10.1098/rsos.191378.
[229] M. Borges, M. Sierra, E. Cuevas, R. García, P. Esparza, Photocatalysis with solar energy: sunlight-responsive photocatalyst based on TiO_2 loaded on a natural material for wastewater treatment, Sol. Energy 135 (2016) 527–535, https://doi.org/10.1016/j.solener.2016.06.022.
[230] K. Morotti, A.A. Ramirez, J.P. Jones, M. Heitz, Analysis and comparison of biotreatment of air polluted with ethanol using biofiltration and biotrickling filtration, Environ. Technol. 32 (16) (2011) 1967–1973, https://doi.org/10.1080/09593330.2011.562550.
[231] T.N. König, S. Shulami, G. Rytwo, Brine wastewater pretreatment using clay minerals and organoclays as flocculants, Appl. Clay Sci. 67 (2012) 119–124, https://doi.org/10.1016/j.clay.2012.05.009.
[232] T.A. Khan, S. Dahiya, I. Ali, Use of kaolinite as adsorbent: equilibrium, dynamics and thermodynamic studies on the adsorption of Rhodamine B from aqueous solution, Appl. Clay Sci. 69 (2012) 58–66, https://doi.org/10.1016/j.clay.2012.09.001.
[233] J. Pérez-Carvajal, P. Aranda, S. Obregón, G. Colón, E. Ruiz-Hitzky, TiO_2-clay based nanoarchitectures for enhanced photocatalytic hydrogen production, Microporous Mesoporous Mater 222 (2016) 120–127, https://doi.org/10.1016/j.micromeso.2015.10.007.
[234] J.-.H. Yang, H. Piao, A. Vinu, A.A. Elzatahry, S.-.M. Paek, J.-.H. Choy, TiO_2-pillared clays with well-ordered porous structure and excellent photocatalytic activity, RSC Adv 5 (11) (2015) 8210–8215, https://doi.org/10.1039/C4RA12880J.
[235] A. Mishra, A. Mehta, S. Basu, Clay supported TiO_2 nanoparticles for photocatalytic degradation of environmental pollutants: a review, J. Environ. Chem. Eng. 6 (5) (2018) 6088–6107, https://doi.org/10.1016/j.jece.2018.09.029.
[236] A. Abdel-Karim, M.E. El-Naggar, E. Radwan, I.M. Mohamed, M. Azaam, E.-.R. Kenawy, High-performance mixed-matrix membranes enabled by organically/inorganic modified montmorillonite for the treatment of hazardous textile wastewater, Chem. Eng. J. 405 (2021), 126964, https://doi.org/10.1016/j.cej.2020.126964.
[237] Y.Y. Yilmaz, E.E. Yalcinkaya, D.O. Demirkol, S. Timur, 4-aminothiophenol-intercalated montmorillonite: organic-inorganic hybrid material as an immobilization support for biosensors, Sens. Actuators B 307 (2020), 127665, https://doi.org/10.1016/j.snb.2020.127665.
[238] S. Liu, M. Chen, X. Cao, G. Li, D. Zhang, M. Li, N. Meng, J. Yin, B. Yan, Chromium (VI) removal from water using cetylpyridinium chloride (CPC)-modified montmorillonite, Sep. Purif. Technol. 241 (2020), 116732, https://doi.org/10.1016/j.seppur.2020.116732.
[239] B. Krishnan, S. Mahalingam, Ag/TiO_2/bentonite nanocomposite for biological applications: synthesis, characterization, antibacterial and cytotoxic investigations, Adv. Powder Technol. 28 (9) (2017) 2265–2280, https://doi.org/10.1016/j.apt.2017.06.007.
[240] S. Yaqoob, F. Ullah, S. Mehmood, T. Mahmood, M. Ullah, A. Khattak, M.A. Zeb, Effect of waste water treated with TiO_2 nanoparticles on early seedling growth of Zea mays L, J. Water Reuse Desalin. 8 (3) (2018) 424–431, https://doi.org/10.2166/wrd.2017.163.
[241] F. Ren, J. Wang, F. Xie, K. Zan, S. Wang, S. Wang, Applications of ionic liquids in starch chemistry: a review, Green Chem 22 (7) (2020) 2162–2183, https://doi.org/10.1039/C9GC03738A.
[242] I. Pacheco-Fernández, V. Pino, Green solvents in analytical chemistry, Curr. Opin. Green Sustain. Chem. 18 (2019) 42–50, https://doi.org/10.1016/j.cogsc.2018.12.010.
[243] A.I. Olives, V. Gonzalez-Ruiz, M.A. Martín, Sustainable and eco-friendly alternatives for liquid chromatographic analysis, Acs Sustain. Chem. Eng. 5 (7) (2017) 5618–5634, https://doi.org/10.1021/acssuschemeng.7b01012.
[244] R.L. Vekariya, A review of ionic liquids: applications towards catalytic organic transformations, J. Mol. Liq. 227 (2017) 44–60, https://doi.org/10.1016/j.molliq.2016.11.123.
[245] A. Bielicka–Giełdoń, P. Wilczewska, A. Malankowska, K. Szczodrowski, J. Ryl, A. Zielińska-Jurek, E.M. Siedlecka, Morphology, surface properties and photocatalytic activity of the bismuth oxyhalides semiconductors prepared by ionic liquid assisted solvothermal method, Sep. Purif. Technol. 217 (2019) 164–173, https://doi.org/10.1016/j.seppur.2019.02.031.
[246] Z. Wei, R. Li, R. Wang, Enhanced visible light photocatalytic activity of BiOBr by in situ reactable ionic liquid modification for pollutant degradation, RSC Adv 8 (15) (2018) 7956–7962, https://doi.org/10.1039/C7RA13779F.
[247] J. Singh, T. Dutta, K.-.H. Kim, M. Rawat, P. Samddar, P. Kumar, Green'synthesis of metals and their oxide nanoparticles: applications for environmental remediation, J. Nanobiotechnology 16 (1) (2018) 1–24, https://doi.org/10.1186/s12951-018-0408-4.
[248] I.M. Gindri, C.P. Frizzo, C.R. Bender, A.Z. Tier, M.A. Martins, M.A. Villetti, G. Machado, L.C. Rodriguez, D.C. Rodrigues, Preparation of TiO_2 nanoparticles coated with ionic liquids: a supramolecular approach, ACS Appl. Mater. Interfaces 6 (14) (2014) 11536–11543, https://doi.org/10.1021/am5022107.
[249] M. Paszkiewicz-Gawron, S. Makurat, J. Rak, M. Zdrowowicz, W. Lisowski, A. Zaleska-Medynska, E. Kowalska, P. Mazierski, J. Łuczak, Theoretical and experimental studies on the visible light activity of TiO_2 modified with halide-based ionic liquids, Catalysts 10 (4) (2020) 371, https://doi.org/10.3390/catal10040371.
[250] H. Dai, Z. Jun, Y. Yin, G. Shao, C. Yu, Synthesis of Ag doped SiO_2-TiO_2 aerogels with nano-sized microcrystalline anatase structure through IL control, IOP Conf. Ser. 587 (2019), 012016, https://doi.org/10.1088/1757-899X/587/1/012016.
[251] X. Lin, Y. Li, Preparation of TiO_2/Ag [BMIM] Cl composites and their visible light photocatalytic properties for the degradation of rhodamine B, Catalysts 11 (6) (2021) 661, https://doi.org/10.3390/catal11060661.

[252] S. Sreeja, V. Shetty, Microbial disinfection of water with endotoxin degradation by photocatalysis using Ag@TiO_2 core shell nanoparticles, Environ. Sci. Pollut. Res. 23 (18) (2016) 18154, https://doi.org/10.1007/s11356-016-6841-8.
[253] S. Sreeja, V. Shetty, Photocatalytic water disinfection under solar irradiation by Ag@TiO_2 core-shell structured nanoparticles, Sol. Energy 157 (2017) 236–243, https://doi.org/10.1016/j.solener.2017.07.057.
[254] A.M. Youssef, S.M. El-Sayed, Bionanocomposites materials for food packaging applications: concepts and future outlook, Carbohydr. Polym. 193 (2018) 19–27, https://doi.org/10.1016/j.carbpol.2018.03.088.
[255] R. Ashraf, H.S. Sofi, T. Akram, H.A. Rather, A. Abdal-hay, N. Shabir, R. Vasita, S. H. Alrokayan, H.A. Khan, F.A. Sheikh, Fabrication of multifunctional cellulose/TiO_2/Ag composite nanofibers scaffold with antibacterial and bioactivity properties for future tissue engineering applications, J. Biomed. Mater. Res. A 108 (4) (2020) 947–962, https://doi.org/10.1002/jbm.a.36872.
[256] M.V. Bhute, S.B. Kondawar, Electrospun poly (vinylidene fluoride)/cellulose acetate/AgTiO_2 nanofibers polymer electrolyte membrane for lithium ion battery, Solid State Ion 333 (2019) 38–44, https://doi.org/10.1016/j.ssi.2019.01.019.
[257] V.K.H. Bui, D. Park, Y.-.C. Lee, Chitosan combined with ZnO, TiO_2 and Ag nanoparticles for antimicrobial wound healing applications: a mini review of the research trends, Polymers (Basel) 9 (1) (2017) 21, https://doi.org/10.3390/polym9010021.
[258] Z. Dong, R. Li, Y. Gong, Antibacterial and freshness-preserving mechanisms of chitosan-nano-TiO_2-nano-Ag composite materials, Coatings 11 (8) (2021) 914, https://doi.org/10.3390/coatings11080914.
[259] S. Natarajan, D.S. Lakshmi, V. Thiagarajan, P. Mrudula, N. Chandrasekaran, A. Mukherjee, Antifouling and anti-algal effects of chitosan nanocomposite (TiO_2/Ag) and pristine (TiO_2 and Ag) films on marine microalgae Dunaliella salina, J. Environ. Chem. Eng. 6 (6) (2018) 6870–6880, https://doi.org/10.1016/j.jece.2018.10.050.
[260] P. Bansal, A. Verma, S. Talwar, Detoxification of real pharmaceutical wastewater by integrating photocatalysis and photo-Fenton in fixed-mode, Chem. Eng. J. 349 (2018) 838–848, https://doi.org/10.1016/j.cej.2018.05.140.
[261] N. Kaur, A. Verma, I. Thakur, S. Basu, In-situ dual effect of Ag-Fe-TiO_2 composite for the photocatalytic degradation of Ciprofloxacin in aqueous solution, Chemosphere 276 (2021), 130180, https://doi.org/10.1016/j.chemosphere.2021.130180.
[262] H.P. Shivaraju, H. Egumbo, P. Madhusudan, K. Anil Kumar, G. Midhun, Preparation of affordable and multifunctional clay-based ceramic filter matrix for treatment of drinking water, Environ. Technol. 40 (13) (2019) 1633–1643, https://doi.org/10.1080/09593330.2018.1430853.
[263] A. Hebeish, E. Allam, A. El-Thalouth, A. Ragheb, A. Shahin, H. Shaban, Multifunctional smart nanocolorants for simultaneous printing and antibacterial finishing of cotton fabrics, Egypt. J. Chem. 62 (4) (2019) 621–637, https://doi.org/10.21608/ejchem.2018.5740.1496.
[264] K.S. Yoo, D. Pak, Effect of IONIC LIQUIDS ON SYNTHESIS of Ag/TiO_2 catalyst in water electrolysis, J. Nanosci. Nanotechnol. 15 (8) (2015) 6137–6140, https://doi.org/10.1166/jnn.2015.10473.
[265] R. Zafar, K.M. Zia, S. Tabasum, F. Jabeen, A. Noreen, M. Zuber, Polysaccharide based bionanocomposites, properties and applications: a review, Int. J. Biol. Macromol. 92 (2016) 1012–1024, https://doi.org/10.1016/j.ijbiomac.2016.07.102.
[266] J. Yang, X. Luo, Ag-doped TiO_2 immobilized cellulose-derived carbon beads: one-Pot preparation, photocatalytic degradation performance and mechanism of ceftriaxone sodium, Appl. Surf. Sci. 542 (2021), 148724, https://doi.org/10.1016/j.apsusc.2020.148724.
[267] A. Snyder, Z. Bo, R. Moon, J.-.C. Rochet, L. Stanciu, Reusable photocatalytic titanium dioxide–cellulose nanofiber films, J. Colloid Interface Sci. 399 (2013) 92–98, https://doi.org/10.1016/j.jcis.2013.02.035.
[268] A.A. Omrani, N. Taghavinia, Photo-induced growth of silver nanoparticles using UV sensitivity of cellulose fibers, Appl. Surf. Sci. 258 (7) (2012) 2373–2377, https://doi.org/10.1016/j.apsusc.2011.10.038.
[269] E. Fortunati, I. Armentano, Q. Zhou, A. Iannoni, E. Saino, L. Visai, L.A. Berglund, J. Kenny, Multifunctional bionanocomposite films of poly (lactic acid), cellulose nanocrystals and silver nanoparticles, Carbohydr. Polym. 87 (2) (2012) 1596–1605, https://doi.org/10.1016/j.carbpol.2011.09.066.
[270] J. Virkutyte, V. Jegatheesan, R.S. Varma, Visible light activated TiO_2/microcrystalline cellulose nanocatalyst to destroy organic contaminants in water, Bioresour. Technol. 113 (2012) 288–293, https://doi.org/10.1016/j.biortech.2011.12.090.
[271] J. Zeng, S. Liu, J. Cai, L. Zhang, TiO_2 immobilized in cellulose matrix for photocatalytic degradation of phenol under weak UV light irradiation, J. Phys. Chem. C 114 (17) (2010) 7806–7811, https://doi.org/10.1021/jp1005617.
[272] K.A. Gebru, C. Das, Removal of Pb (II) and Cu (II) ions from wastewater using composite electrospun cellulose acetate/titanium oxide (TiO_2) adsorbent, J. Water Process Eng. 16 (2017) 1–13, https://doi.org/10.1016/j.jwpe.2016.11.008.
[273] S. Abbasizadeh, A.R. Keshtkar, M.A. Mousavian, Preparation of a novel electrospun polyvinyl alcohol/titanium oxide nanofiber adsorbent modified with mercapto groups for uranium (VI) and thorium (IV) removal from aqueous solution, Chem. Eng. J. 220 (2013) 161–171, https://doi.org/10.1016/j.cej.2013.01.029.
[274] X. Jin, J. Xu, X. Wang, Z. Xie, Z. Liu, B. Liang, D. Chen, G. Shen, Flexible TiO_2/cellulose acetate hybrid film as a recyclable photocatalyst, RSC Adv 2 (25) (2014) 12640–12648, https://doi.org/10.1039/C3RA47710J.
[275] S. Bagheri, K. Shameli, S.B. Abd Hamid, Synthesis and characterization of anatase titanium dioxide nanoparticles using egg white solution via Sol-Gel method, J. Chem. (2013) 2013, https://doi.org/10.1155/2013/848205.
[276] J.C. Colmenares, R.S. Varma, P. Lisowski, Sustainable hybrid photocatalysts: titania immobilized on carbon materials derived from renewable and biodegradable resources, Green Chem 18 (21) (2016) 5736–5750, https://doi.org/10.1039/C6GC02477G.
[277] B. Baruah, situ and facile synthesis of silver nanoparticles on baby wipes and their applications in catalysis and SERS, RSC Adv 6 (6) (2016) 5016–5023, https://doi.org/10.1039/C5RA20059H.
[278] A. Mironenko, E. Modin, A. Sergeev, S. Voznesenskiy, S. Bratskaya, Fabrication and optical properties of chitosan/Ag nanoparticles thin film composites, Chem. Eng. J. 244 (2014) 457–463, https://doi.org/10.1016/j.cej.2014.01.094.
[279] C. Aguzzi, P. Capra, C. Bonferoni, P. Cerezo, I. Salcedo, R. Sánchez, C. Caramella, C. Viseras, Chitosan–silicate biocomposites to be used in modified drug release of 5-aminosalicylic acid (5-ASA), Appl. Clay Sci. 50 (1) (2010) 106–111, https://doi.org/10.1016/j.clay.2010.07.011.
[280] N. Bleiman, Y.G. Mishael, Selenium removal from drinking water by adsorption to chitosan–clay composites and oxides: batch and columns tests, J. Hazard. Mater. 183 (1–3) (2010) 590–595, https://doi.org/10.1016/j.jhazmat.2010.07.065.
[281] A. Wang, Q. Zhu, Z. Xing, Design and synthesis of a calcium modified quaternized chitosan hollow sphere for efficient adsorption of SDBS, J. Hazard. Mater. 369 (2019) 342–352, https://doi.org/10.1016/j.jhazmat.2019.02.047.
[282] G. Xiao, Y. Zhao, L. Li, J.O. Pratt, H. Su, T. Tan, Facile synthesis of dispersed Ag nanoparticles on chitosan-TiO_2 composites as recyclable nanocatalysts for 4-nitrophenol reduction, Nanotechnology 29 (15) (2018), 155601, https://doi.org/10.1088/1361-6528/aaac74.
[283] A. Wang, Q. Zhu, Z. Xing, Multifunctional quaternized chitosan@ surface plasmon resonance Ag/N-TiO_2 core-shell microsphere for synergistic adsorption-photothermal catalysis degradation of low-temperature wastewater and bacteriostasis under visible light, Chem. Eng. J. 393 (2020), 124781, https://doi.org/10.1016/j.cej.2020.124781.
[284] D. Geetha, S. Kavitha, P. Ramesh, A novel bio-degradable polymer stabilized Ag/TiO_2 nanocomposites and their catalytic activity on reduction of methylene blue under natural sun light, Ecotoxicol. Environ. Saf. 121 (2015) 126–134, https://doi.org/10.1016/j.ecoenv.2015.04.042.
[285] L. Cordero-Arias, S. Cabanas-Polo, H. Gao, J. Gilabert, E. Sanchez, J. Roether, D. Schubert, S. Virtanen, A.R. Boccaccini, Electrophoretic deposition of nanostructured-TiO_2/chitosan composite coatings on stainless steel, RSC Adv 3 (28) (2013) 11247–11254, https://doi.org/10.1039/C3RA40535D.
[286] G. Xiao, H. Su, T. Tan, Synthesis of core–shell bioaffinity chitosan–TiO_2 composite and its environmental applications, J. Hazard. Mater. 283 (2015) 888–896, https://doi.org/10.1016/j.jhazmat.2014.10.047.
[287] E.M. Ahmed, Hydrogel: preparation, characterization, and applications: a review, J. Adv. Res. 6 (2) (2015) 105–121, https://doi.org/10.1016/j.jare.2013.07.006.
[288] J. Dai, Q. Tian, Q. Sun, W. Wei, J. Zhuang, M. Liu, Z. Cao, W. Xie, M. Fan, TiO_2-alginate composite aerogels as novel oil/water separation and wastewater remediation filters, Compos. B 160 (2019) 480–487, https://doi.org/10.1016/j.compositesb.2018.12.097.
[289] D. González-Ramírez, P. Ávila-Pérez, L. Torres-Bustillos, R. Aguilar-López, F. Esparza-García, R. Rodríguez-Vázquez, Removal of Phenanthrene in an Aqueous Matrix by Entrapped Crude Enzymes on Alginate Beads Combined with TiO_2-C-Ag Coated Fiberglass, Int. J. Environ. Sci. Dev. 8 (9) (2017) 635–641, https://doi.org/10.18178/ijesd.2017.8.9.1030.
[290] I. Hasan, C. Shekhar, W. Alharbi, M. Abu Khanjer, R.A. Khan, A. Alsalme, A highly efficient Ag nanoparticle-immobilized alginate-g-polyacrylonitrile hybrid photocatalyst for the degradation of nitrophenols, Polymers 12 (12) (2020) 3049, https://doi.org/10.3390/polym12123049.
[291] J. Jana, M. Ganguly, T. Pal, Enlightening surface plasmon resonance effect of metal nanoparticles for practical spectroscopic application, RSC Adv 6 (89) (2016) 86174–86211, https://doi.org/10.1039/C6RA14173K.
[292] A.K. Mishra, S. Allauddin, R. Narayan, T.M. Aminabhavi, K. Raju, Characterization of surface-modified montmorillonite nanocomposites, Ceram. Int. 38 (2) (2012) 929–934, https://doi.org/10.1016/j.ceramint.2011.08.012.
[293] P. Daraei, S.S. Madaeni, E. Salehi, N. Ghaemi, H.S. Ghari, M.A. Khadivi, E. Rostami, Novel thin film composite membrane fabricated by mixed matrix nanoclay/chitosan on PVDF microfiltration support: preparation, characterization and performance in dye removal, J. Membr. Sci. 436 (2013) 97–108, https://doi.org/10.1016/j.memsci.2013.02.031.
[294] E. Manova, P. Aranda, M.A. Martín-Luengo, S. Letaïef, E. Ruiz-Hitzky, New titania-clay nanostructured porous materials, Microporous Mesoporous Mater 131 (1–3) (2010) 252–260, https://doi.org/10.1016/j.micromeso.2009.12.031.
[295] R. Koyilapu, S. Singha, B. Sana, T. Jana, Proton exchange membrane prepared by blending polybenzimidazole with poly (aminophosphonate ester), Polym. Test. 85 (2020), 106414, https://doi.org/10.1016/j.polymertesting.2020.106414.
[296] A. Sraw, T. Kaur, Y. Pandey, A. Sobti, R.K. Wanchoo, A.P. Toor, Fixed bed recirculation type photocatalytic reactor with TiO_2 immobilized clay beads for the degradation of pesticide polluted water, J. Environ. Chem. Eng. 6 (6) (2018) 7035–7043, https://doi.org/10.1016/j.jece.2018.10.062.
[297] C. Ju, Photocatalytic degradation of TOC by Ag/TiO_2 coated on light ceramic, Procedia Manuf. 37 (2019) 267–272, https://doi.org/10.1016/j.promfg.2019.12.046.
[298] E. Ajenifuja, J. Ajao, E. Ajayi, Equilibrium adsorption isotherm studies of Cu (II) and Co (II) in high concentration aqueous solutions on Ag-TiO_2-modified kaolinite ceramic adsorbents, Appl. Water Sci. 7 (5) (2017) 2279–2286, https://doi.org/10.1007/s13201-016-0403-6.

[299] X. Li, K. Peng, H. Chen, Z. Wang, TiO_2 nanoparticles assembled on kaolinites with different morphologies for efficient photocatalytic performance, Sci. Rep. 8 (1) (2018) 1–11, https://doi.org/10.1038/s41598-018-29563-8.
[300] E. Rossetto, D.I. Petkowicz, J.H. dos Santos, S.B. Pergher, F.G. Penha, Bentonites impregnated with TiO_2 for photodegradation of methylene blue, Appl. Clay Sci. 48 (4) (2010) 602–606, https://doi.org/10.1016/j.clay.2010.03.010.
[301] D.B. Nguyen, T.D.C. Nguyen, T.P. Dao, H.T. Tran, D.H. Ahn, Preparation, characterization and evaluation of catalytic activity of titania modified with silver and bentonite, J. Ind. Eng. Chem. 18 (5) (2012) 1764–1767, https://doi.org/10.1016/j.jiec.2012.04.004.
[302] C.R. Bender, P.R. Salbego, K. Wust, C.A. Farias, T.S. Beck, G. Machado, R. A. Vaucher, M.A. Martins, C.P. Frizzo, Interaction of pharmaceutical ionic liquids with TiO_2 in anatase and rutile phase, J. Mol. Liq. 269 (2018) 912–919, https://doi.org/10.1016/j.molliq.2018.08.066.
[303] M. Paszkiewicz, J. Łuczak, W. Lisowski, P. Patyk, A. Zaleska-Medynska, The ILs-assisted solvothermal synthesis of TiO_2 spheres: the effect of ionic liquids on morphology and photoactivity of TiO_2, Appl. Catal. B 184 (2016) 223–237, https://doi.org/10.1016/j.apcatb.2015.11.019.
[304] J. Huang, C. Qin, S. Lei, J. Li, M. Li, J. Zhong, T. Wang, Ionic liquid assisted hydrothermal preparation of TiO_2 with largely enhanced photocatalytic performance originated from effective separation of photoinduced carriers, J. Phys. Chem. Solids 139 (2020), 109323, https://doi.org/10.1016/j.jpcs.2019.109323.
[305] H. Zhang, G. Chen, Potent antibacterial activities of Ag/TiO_2 nanocomposite powders synthesized by a one-pot sol− gel method, Environ. Sci. Technol. 43 (8) (2009) 2905–2910, https://doi.org/10.1021/es803450f.
[306] N. Kaur, V. Singh, Current status and future challenges in ionic liquids, functionalized ionic liquids and deep eutectic solvent-mediated synthesis of nanostructured TiO_2: a review, New J. Chem. 41 (8) (2017) 2844–2868, https://doi.org/10.1039/C6NJ04073J.
[307] B.L. Kuhn, G.C. Paveglio, S. Silvestri, E.I. Muller, M.S. Enders, M.A. Martins, N. Zanatta, H.G. Bonacorso, C. Radke, C.P. Frizzo, TiO_2 nanoparticles coated with deep eutectic solvents: characterization and effect on photodegradation of organic dyes, New J. Chem. 43 (3) (2019) 1415–1423, https://doi.org/10.1039/C8NJ05957H.
[308] D. Van Dao, T.T. Nguyen, H.-.Y. Song, J.-.K. Yang, T.-.W. Kim, Y.-.T. Yu, I.-.H. Lee, Ionic liquid-assisted preparation of Ag-CeO_2 nanocomposites and their improved photocatalytic activity, Mater. Des. 159 (2018) 186–194, https://doi.org/10.1016/j.matdes.2018.08.042.
[309] H. Liu, M. Wang, Y. Wang, Y. Liang, W. Cao, Y. Su, Ionic liquid-templated synthesis of mesoporous CeO_2–TiO_2 nanoparticles and their enhanced photocatalytic activities under UV or visible light, J. Photochem. Photobiol. A 223 (2–3) (2011) 157–164, https://doi.org/10.1016/j.jphotochem.2011.06.014.
[310] H. Daupor, S. Wongnawa, Urchinlike Ag/AgCl photocatalyst: synthesis, characterization, and activity, Appl. Catal. A 473 (2014) 59–69, https://doi.org/10.1016/j.apcata.2013.12.036.
[311] X. Zhang, L. Zhang, Y. Li, L. Di, Atmospheric-pressure cold plasma for fabrication of anatase–rutile mixed TiO_2 with the assistance of ionic liquid, Catal. Today 256 (2015) 215–220, https://doi.org/10.1016/j.cattod.2015.04.033.
[312] Y. Zhang, W. Liu, S. Chen, Q. Gao, Q. Li, X. Zhu, Ionic liquids for the controllable preparation of functional TiO_2 nanostructures: a review, Ionics 26 (12) (2020) 1–25, https://doi.org/10.1007/s11581-020-03719-x.
[313] A. Bera, H. Belhaj, Ionic liquids as alternatives of surfactants in enhanced oil recovery—a state-of-the-art review, J. Mol. Liq. 224 (2016) 177–188, https://doi.org/10.1016/j.molliq.2016.09.105.
[314] S.K. Singh, A.W. Savoy, Ionic liquids synthesis and applications: an overview, J. Mol. Liq. 297 (2020), 112038, https://doi.org/10.1016/j.molliq.2019.112038.